NASA TECHNICAL NOTE

NASA TN D-3990

NASA TN D-3990

TRANSPORT STUDY OF THE REAL AND ADJOINT FLUX FOR NASA ZERO POWER REACTOR (ZPR-1)

by Daniel Fieno

Lewis Research Center

Cleveland, Ohio

NATIONAL AERONAUTICS AND SPACE ADMINISTRATION • WASHINGTON, D. C. • MAY 1967

NASA TN D-3990

TRANSPORT STUDY OF THE REAL AND ADJOINT FLUX FOR NASA ZERO POWER REACTOR (ZPR-1)

By Daniel Fieno

Lewis Research Center
Cleveland, Ohio

NATIONAL AERONAUTICS AND SPACE ADMINISTRATION

For sale by the Clearinghouse for Federal Scientific and Technical Information
Springfield, Virginia 22151 – CFSTI price $3.00

TRANSPORT STUDY OF THE REAL AND ADJOINT FLUX FOR NASA ZERO POWER REACTOR (ZPR-1)

by Daniel Fieno

Lewis Research Center

SUMMARY

A one-dimensional, multigroup, multiregion S_n transport program has been developed for the IBM 7094 computer. This program has been used to calculate the real and adjoint fluxes for the NASA Zero Power Reactor (ZPR-1). In particular, the effect on the fluxes of a small spherical shell of cadmium located at the center of the reactor was determined. These calculated real and adjoint fluxes can be used to correct experimental reactivity determinations for materials within the cadmium shell.

The effect of S_n order (n = 2, 4, 6, or 8), elastic scattering order (P_0 or P_1), the number of spatial mesh intervals, and angular flux model representation (diamond or step) on the real and the adjoint fluxes at the center of the reactor and with the cadmium shell in place was determined. The S_4 transport calculations using a diamond model representation of the angular fluxes and using P_1 order elastic scattering were found to be adequate.

INTRODUCTION

The NASA Zero Power Reactor (ZPR-1) consists of uranyl fluoride salt (UO_2F_2) dissolved in water and contained in a cylindrical aluminum tank. For a given concentration of uranyl fluoride salt in water, criticality is achieved by varying the height of the solution in the tank. No control rods are inserted into the solution while the reactor is critical. Criticality calculations for this reactor are given in reference 1. Good experimental conditions exist for obtaining criticality data and for performing reactivity measurements by measuring changes in solution height due to insertions in reactor. Descriptions of the reactor and the reactivity measurements that employ the real and the adjoint fluxes reported herein are found in reference 2.

Activation and reactivity measurements are made on samples in the center of the reactor. These samples are measured with or without a 0.0889-centimeter-thick (35-mil) cadmium cover. Values of the real and adjoint fluxes in the cadmium-covered samples must be known precisely as a function of energy in order to interpret activation and reactivity measurements of various absorber materials in terms of the resonance integral of the material. Since the real and the adjoint fluxes as a function of energy are difficult to determine experimentally, the use of computer calculations is required to make the necessary corrections to the experimental data.

Since the gradient of the real and the adjoint fluxes changes quite drastically in traversing the thin cadmium cover, a transport calculation was assumed necessary to obtain sufficiently accurate values of these fluxes as a function of energy. These transport calculations were made using the S_n method developed by Bengt Carlson of Los Alamos Scientific Laboratory (ref. 3). A description of the mathematical model used in the development of the one-dimensional, multigroup, multiregion S_n transport program for the IBM 7094 II computer is given. Appendix A is a list of the symbols used and appendix B describes the equations used.

This S_n transport program has been used to calculate the real and the adjoint fluxes in the NASA Zero Power Reactor (ZPR-1) having an atom ratio of hydrogen to uranium 235 of 500. The effect of a 35-mil cadmium cover on these fluxes at the center of the reactor is calculated. In addition, the effects of S_n order (n = 2, 4, 6, or 8), elastic scattering order (P_0 or P_1), the number of spatial mesh intervals, and angular flux model representation (diamond or step) on the calculated real and adjoint fluxes are determined.

PROBLEM FORMULATION

Although ZPR-1 is a cylindrical system with pill-box-shaped cadmium-covered samples placed at the center for the reactivity measurements, the calculations are based on a one-dimensional spherical model. Table I presents the size, composition, and atom densities for each region. The low-density aluminum at the center of the system is used to represent a void. The thickness of the cadmium shell is 0.0889 centimeter (35 mil), and its outer diameter is so chosen that the cadmium surface area is 47.74 square centimeters (7.40 sq in.) the same as for the actual cadmium pill boxes. The atom ratio of hydrogen to uranium 235 of the fuel solution is 500.

The outer radius of the spherical system was determined in the following manner. The critical cylindrical ZPR-1 system for an atom ratio of hydrogen to uranium 235 of 500 for the fuel solution was related through the material buckling (ref. 1) to an equivalent spherical system. Then, with the voided spherical cadmium shell located at the

TABLE I. - SIZE AND COMPOSITION OF ZPR-1 REGIONS

Region	Radius		Composition	Element	Atom density, atoms/b-cm
	Inner, cm	Outer, cm			
1	0	1.86024	Al	Al	0.01
2	1.86024	1.9491	Cd	Cd	.0464
3	1.9491	19.1081	$UO_2F_2 + H_2O$ solution	H	.06629
				O	.033429
				F	.00028436
				U^{235}	.00013252
				U^{238}	.00000965

center of the system, the outer radius of the fuel solution was adjusted slightly until the standard calculation gave an eigenvalue of unity.

Thirty energy groups were used to describe the reactor spectra. Two different group spacings were chosen to provide detailed representation of the fast neutron leakage as well as the real and the adjoint fluxes in the resonance energy range. The details of the group structure are presented in table II. The thermal group extends from 0.001 to 0.414 electron volts for both of the group splits. Most of the results obtained in this study used group split A of table II and will be shown in tables III and IV.

Two computer programs were used to provide the necessary group-averaged microscopic cross sections. These programs are GAM II (ref. 4) and GATHER II (ref. 5). GAM II is a B_3 multigroup code for the calculation of fast neutron spectra and was used to calculate cross sections for the 29 fast groups. For this study, the code was used to integrate the B_1 equations over 99 energy groups covering the energy range from 14.92 million electron volts to 0.414 electron volts. The desired cross sections for the 29 fast groups are then obtained by averaging over the 99 group spectrum. GATHER II was used to obtain thermal, or 30th group, cross sections. This program is a P_1 code for the calculation of thermal spectra over 101 energy points covering the energy range from 2.38 to 0.001 electron volts. The scattering kernel for hydrogen bound in a water molecule was based on a model devised by Nelkin (ref. 6). This thermal spectrum was calculated for a temperature of 293° K.

Both these codes generated group-averaged macroscopic cross sections for the uranyl fluoride - water solution having an atom ratio of hydrogen to uranium 235 of 500. Aluminum (Al), cadmium (Cd), and boron 10 (B^{10}) microscopic cross sections were averages over the spectra obtained for this fuel solution. From the GAM II and GATHER II output, both P_0 transport corrected and P_1 cross-section sets were constructed. The various cross-section sets used included a one-group upscattering component for the fuel

TABLE II. - GROUP SPLIT

Group	Group split A			Group split B		
	Group boundary energy, eV	Group boundary, lethargy	Group width, lethargy	Group boundary energy, eV	Group boundary, lethargy	Group width, lethargy
1	1.492×10^{7}	-0.4	0.4	1.492×10^{7}	-0.4	0.9
2	1.000	.0	.3	6.065×10^{6}	.5	.5
3	7.408×10^{6}	.3		3.679	1.0	
4	5.488	.6		2.231	1.5	
5	4.066	.9		1.353	2.0	
6	3.012	1.2		8.209×10^{5}	2.5	
7	2.231	1.5		4.979	3.0	1.0
8	1.653	1.8		1.832	4.0	
9	1.225	2.1		6.738×10^{4}	5.0	
10	9.072×10^{5}	2.4		2.479	6.0	
11	6.721	2.7		9.119×10^{3}	7.0	
12	4.979	3.0		3.355	8.0	
13	3.688	3.3		1.234	9.0	
14	2.732	3.6		4.540×10^{2}	10.0	.75
15	2.024	3.9		2.145	10.75	
16	1.500	4.2		1.013	11.50	
17	1.111	4.5	.5	.47851	12.25	
18	6.738×10^{4}	5.0	1.0	.22603	13.0	.5
19	2.479	6.0		.13710	13.5	
20	9.119×10^{3}	7.0		.08315	14.0	
21	3.355	8.0		.05043	14.5	
22	1.234	9.0		.03059	15.0	.25
23	4.540×10^{2}	10.0		.02382	15.25	
24	1.670	11.0		.01855	15.50	
25	.61442	12.0		.01445	15.75	
26	.22603	13.0		.01125	16.00	
27	.08315	14.0		.00876	16.25	
28	.03059	15.0		.00683	16.50	
29	.01125	16.0		.00532	16.75	
30	.00414	17.0	---	.00414	17.00	-----

solution. The P_1 cross-section sets obtained for group splits A and B are given in computer table V. The P_0 transport corrected cross-section sets are not listed as they may be derived from the P_1 sets in the following manner. Eliminate the P_1 transfer cross sections, replace the total cross section by the transport cross section, and redefine the within group P_0 transfer cross section in accordance with equation (B33) of appendix B. The symbols used on the listings are computer terminology and are mostly self-explanatory. However, these symbols are defined in the symbol table (appendix A). It should be noted that three times the P_1 transfer cross sections are listed.

Since the gradient of the real and the adjoint fluxes changes quite drastically in traversing the thin cadmium cover, diffusion theory calculations would be inaccurate. Thus, transport calculations were necessary to obtain sufficiently accurate values of these fluxes as a function of energy. These transport calculations were made using the S_n quadrature method developed by Bengt Carlson of Los Alamos Scientific Laboratory (ref. 3). A complete description of the mathematical model used in the development of a one-dimensional, multigroup, multiregion S_n transport program for the IBM 7094 II Computer is given in appendix B.

RESULTS AND DISCUSSION

The one-dimensional, multigroup, multiregion S_n transport program used for this study had considerable flexibility and was used to determine an adequate calculational model. The effect of S_n order (n = 2, 4, 6, or 8), of elastic scattering order (P_0 or P_1), of the number of spatial mesh intervals, and of angular flux model representation (diamond or step) on the real and the adjoint fluxes at the center of ZPR-1 both with and without the cadmium shell in place was determined. The standard case chosen for this study was an S_4 calculation using the P_1 elastic scattering transfer cross sections with a total of 65 mesh intervals chosen to represent the spatial variation of the fluxes. Of these mesh intervals, 10 were in the aluminum (void) region, 5 were in the cadmium region, and 50 were used in the fuel solution region. The cross-section data were based on group split A of table II.

The static criticality factor K_{eff} for this case was 0.999951 for the real flux solution and 1.000058 for the adjoint flux solution. The relative real fluxes are plotted as a function of radius in figure 1. The relative adjoint fluxes are plotted as a function of radius in figure 2. For this standard calculation, the relative real fluxes at the center of ZPR-1 are shown for all the neutron groups as case 1 in table III(a). The relative adjoint fluxes as a function of lethargy are similarly shown as case 1 in table III(b). For the real flux calculation, the normalization corresponds to 1000 source neutrons. The adjoint fluxes are normalized so that equation (B41) of appendix B integrated over the

TABLE III. - COMPARISON OF SPECTRUM AT CENTER OF CADMIUM SHELL IN ZPR-1 FOR VARIOUS CALCULATIONS[a]

[D, diamond model; S, step model; P_1, P_1 elastic scattering; P_0, P_0 elastic scattering.]

(a) Relative real flux spectrum

Group	Case											
	1 S_4, P_1, D standard	2 S_2, P_1, D	3 S_6, P_1, D	4 S_8, P_1, D	5 S_4, P_1, S	6 S_4, P_0, D	7 S_4, P_1, D aluminum density, 0.06 barn-cm	8 S_4, P_1, D aluminum region, 2.36 cm	9 S_4, P_1, D aluminum shell	10 S_4, P_1, D cadmium shell, 20 mil	11 S_4, P_1, D boron 10 shell, 0.025 in.	12 S_4, P_1, D boron 10 in cadmium shell
1	5.4899×10^{-4}	5.6095×10^{-4}	5.5101×10^{-4}	5.5176×10^{-4}	5.8792×10^{-4}	5.0717×10^{-4}	5.0397×10^{-4}	5.2182×10^{-4}	6.0540×10^{-4}	5.5219×10^{-4}	5.1827×10^{-4}	4.9150×10^{-4}
2	3.8325×10^{-3}	3.9214×10^{-3}	3.8467×10^{-3}	3.8521×10^{-3}	4.1067×10^{-3}	3.4794×10^{-3}	3.5179×10^{-3}	3.6454×10^{-3}	4.2271×10^{-3}	3.8547×10^{-3}	3.6314×10^{-3}	3.4691×10^{-3}
3	1.3933×10^{-2}	1.4290×10^{-2}	1.3988×10^{-2}	1.4010×10^{-2}	1.4949×10^{-2}	1.2694×10^{-2}	1.2785×10^{-2}	1.3269×10^{-2}	1.5387×10^{-2}	1.4006×10^{-2}	1.3215×10^{-2}	1.2721×10^{-2}
4	3.1320	3.2129	3.1456	3.1510	3.3425	2.8735	2.8884	2.9874	3.4767	3.1489	2.9583	2.8372
5	4.8982	5.0291	4.9299	4.9327	5.1937	4.6101	4.5806	4.6843	5.4778	4.9249	4.5900	4.3699
6	7.0302	7.2181	7.0641	7.0774	7.4593	6.3235	6.7786	6.7314	7.8124	7.0649	6.5496	6.1588
7	6.4796	6.6652	6.5147	6.5288	6.8773	6.1239	6.4621	6.2225	7.2425	6.5052	6.1291	5.9749
8	6.4873	6.6836	6.5263	6.5421	6.8654	6.2125	6.4429	6.2367	7.2425	6.5061	6.1032	5.9661
9	5.5959	5.7707	5.6319	5.6465	5.9124	5.4625	5.7615	5.3936	6.2484	5.6049	5.2437	5.1477
10	5.9453	6.1370	5.9832	5.9985	6.2718	5.6688	6.0454	5.7295	6.5611	5.9518	5.4653	5.1841
11	4.6785	4.8399	4.7096	4.7222	4.9404	4.4682	4.8424	4.5171	5.1037	4.6776	4.3534	4.2045
12	3.4488	3.5718	3.4734	3.4833	3.6408	3.3711	3.5976	3.3321	3.7706	3.4454	3.2246	3.1673
13	3.5731	3.7004	3.5978	3.6079	3.7670	3.4655	3.5840	3.4461	3.8800	3.5703	3.2506	3.0568
14	2.9678	3.0773	2.9885	2.9969	3.1266	2.8757	3.0530	2.8684	3.2032	2.9664	2.7191	2.5560
15	2.5514	2.6468	2.5694	2.5767	2.6878	2.4753	2.4074	2.4553	2.7326	2.5507	2.3482	2.2138
16	2.3095	2.3989	2.3259	2.3326	2.4291	2.2397	2.6330	2.2475	2.4911	2.3113	2.0852	1.8787
17	3.2475	3.3752	3.2707	3.2801	3.4166	3.1594	3.4449	3.1449	3.4815	3.2509	2.8623	2.4574
18	5.2912	5.5021	5.3292	5.3445	5.5628	5.1603	5.3724	5.1184	5.6471	5.2996	4.4429	3.4395
19	4.5403	4.7227	4.5726	4.5856	4.7674	4.4333	4.5335	4.3914	4.8324	4.5521	3.4437	2.1732
20	4.2433	4.4148	4.2733	4.2852	4.4474	4.1468	4.2436	4.1062	4.5258	4.2642	2.7379	1.2759
21	4.1461	4.3147	4.1751	4.1866	4.3409	4.0503	4.1565	4.0140	4.4140	4.1685	2.0691	6.0579×10^{-3}
22	4.0529	4.2188	4.0807	4.0917	4.2396	3.9598	4.0621	3.9247	4.3079	4.0766	1.3228	1.7960
23	3.9863	4.1504	4.0132	4.0237	4.1684	3.8954	3.9942	3.8610	4.2218	4.0073	6.5019×10^{-3}	2.4739×10^{-4}
24	3.7956	3.9542	3.8210	3.8308	3.9422	3.7226	3.8002	3.6760	4.1512	3.8739	2.0626	8.8056×10^{-6}
25	3.8259	3.9835	3.8517	3.8616	3.9858	3.7205	3.8292	3.7054	4.0540	3.8532	3.0510×10^{-4}	9.5635×10^{-8}
26	3.7661	3.9220	3.7906	3.8001	3.9311	3.6724	3.7700	3.6481	3.9554	3.7810	1.1225×10^{-5}	4.6926×10^{-10}
27	3.6551	3.8078	3.6782	3.6870	3.8133	3.5786	3.6565	3.5412	3.8461	3.6751	2.7907×10^{-8}	1.0926×10^{-12}
28	3.5274	3.6761	3.5493	3.5577	3.6671	3.4634	3.5237	3.4175	3.7611	3.5693	4.5203×10^{-11}	1.8841×10^{-15}
29	2.5776	2.6847	2.5963	2.6033	2.5790	2.5467	2.5638	2.4937	3.6389	2.9500	7.7816×10^{-14}	1.9498×10^{-18}
30	4.5035×10^{-5}	4.6735×10^{-5}	4.5260×10^{-5}	4.5340×10^{-5}	4.6219×10^{-4}	4.4604×10^{-5}	2.7494	5.5065×10^{-5}	5.7748×10^{-1}	8.6031	1.1517×10^{-16}	6.2215×10^{-22}

(b) Relative adjoint flux spectrum

1	2.2560×10^{-2}	2.4165×10^{-2}	2.2549×10^{-2}	2.2565×10^{-2}	2.6447×10^{-2}	2.5621×10^{-2}	2.4258×10^{-2}	2.1530×10^{-2}	2.2005×10^{-2}	2.2119×10^{-2}	2.1573×10^{-2}	2.3429×10^{-2}
2	2.6407	2.8285	2.6405	2.6429	3.0878	2.9855	2.8559	2.5199	2.6281	2.6111	2.5472	2.6628
3	3.4917	3.7174	3.4965	3.5011	3.9768	3.7685	3.7396	3.3360	3.5400	3.4783	3.3932	3.4441
4	4.4970	4.7447	4.5100	4.5177	4.9535	4.6422	4.7391	4.3035	4.5850	4.4868	4.3530	4.3684
5	5.6696	5.9449	5.6937	5.7055	6.0619	5.6781	5.8489	5.4403	5.8088	5.6644	5.4604	5.4326
6	6.1124	6.3683	6.1400	6.1522	6.4667	5.9462	6.2445	5.8513	6.2716	6.1090	5.9022	5.8855
7	7.2539	7.5217	7.2926	7.3083	7.4848	7.0000	7.3488	6.9656	7.4903	7.2568	6.9017	6.7679
8	8.0842	8.3617	8.1318	8.1503	8.2295	7.8138	8.1655	7.7791	8.3971	8.0926	7.6700	7.5637
9	8.7049	8.9828	8.7590	8.7795	8.7865	8.4459	8.7406	8.3838	9.0971	8.7186	8.1784	8.0416
10	8.9096	9.1826	8.9650	8.9857	8.9829	8.5334	8.9448	8.5761	9.3271	8.9245	8.3388	8.1193
11	9.2853	9.5550	9.3446	9.3665	9.3251	8.8780	9.3227	8.9397	9.7708	9.3041	8.5413	8.1480
12	9.7084	9.9745	9.7742	9.7983	9.7165	9.4655	9.7212	9.3472	1.0317×10^{-1}	9.7348	8.6747	8.1468
13	9.7752	1.0035×10^{-1}	9.8406	9.8645	9.7829	9.4708	9.7961	9.4067	1.0401	9.8019	8.6857	8.0232
14	9.9110	1.0166	9.9785	1.0003	9.9148	9.5906	9.9283	9.5333	1.0589	9.9402	8.6787	7.8539
15	1.0023×10^{-1}	1.0273	1.0093×10^{-1}	1.0118×10^{-1}	1.0024×10^{-1}	9.6999	1.0043×10^{-1}	9.6366	1.0758	1.0055×10^{-1}	8.6104	7.5942
16	1.0114	1.0359	1.0186	1.0212	1.0115	9.7967	1.0121	9.7182	1.0906	1.0150	8.5053	7.2742
17	1.0193	1.0430	1.0266	1.0293	1.0194	9.8789	1.0196	9.7859	1.1053	1.0232	8.3286	6.8251
18	1.0269	1.0495	1.0345	1.0373	1.0272	9.9534	1.0262	9.8466	1.1235	1.0315	7.9860	6.0344
19	1.0313	1.0525	1.0391	1.0420	1.0315	9.9765	1.0311	9.8747	1.1415	1.0373	7.3093	4.5880
20	1.0291	1.0492	1.0372	1.0401	1.0287	9.9419	1.0282	9.8417	1.1550	1.0376	6.1624	2.7732
21	1.0298	1.0489	1.0381	1.0411	1.0296	9.9271	1.0295	9.8384	1.1667	1.0389	4.7922	1.3236
22	1.0301	1.0482	1.0385	1.0416	1.0301	9.8969	1.0297	9.8295	1.1780	1.0391	3.1777	3.9856×10^{-3}
23	1.0312	1.0483	1.0399	1.0431	1.0309	9.8459	1.0301	9.8284	1.1890	1.0389	1.6196	5.4171×10^{-4}
24	.99208	1.0084	1.0005	1.0036	.98798	9.5287	.99075	9.4433	1.1997	1.0148	5.3089×10^{-3}	1.5080×10^{-5}
25	1.0134	1.0289	1.0221	1.0253	1.0160	9.6855	1.0122	9.6347	1.2079	1.0231	8.1089×10^{-4}	1.8293×10^{-8}
26	1.0114	1.0258	1.0204	1.0238	1.0172	9.5916	1.0098	9.6004	1.2216	1.0167	2.9860×10^{-5}	(b)
27	.99270	1.0053	1.0020	1.0055	.99974	9.3104	.98994	9.4025	1.2345	.99778	3.6051×10^{-8}	(b)
28	.96169	.97086	.97138	.97515	.96918	8.8755	.95458	9.0886	1.2498	.96983	(b)	(b)
29	.68845	.69106	.69551	.69838	.68562	6.6280	.67420	6.4852	1.2623	.78717	(b)	(b)
30	(b)	(b)	(b)	(b)	9.5185×10^{-5}	(b)	(b)	(b)	1.2703	6.7494×10^{-6}	(b)	(b)

[a]Calculations used 65-mesh intervals and group split A of table II.

[b]Zero value was computed by program.

TABLE IV. - COMPARISON OF STATIC CRITICALITY FACTOR K_{eff} OF ZPR-1 WITH CADMIUM SHELL AT CENTER FOR VARIOUS CALCULATIONS[a]

[D, diamond model; S, step model; P_1, P_1 elastic scattering; P_0, P_0 elastic scattering.]

Case	Remarks	Static criticality factor, K_{eff}	
		Flux solution	Adjoint solution
1	S_4, P_1, D standard	0.9999508	1.0000582
2	S_2, P_1, D	1.0109144	1.0114419
3	S_6, P_1, D	.9979524	.9980232
4	S_8, P_1, D	.9974600	.9974964
5	S_4, P_1, S	.9835186	.9835383
6	S_4, P_0, D	.9819350	.9820091
7	S_4, P_1, D aluminum density, 0.06 barn-cm	1.0000674	1.0001739
8	S_4, P_1, D aluminum region, 2.36-cm	.9930746	.9932324
9	S_4, P_1, D aluminum shell	1.0109665	1.0109960
10	S_4, P_1, D cadmium shell, 20-mil	1.0002964	1.0003930
11	S_4, P_1, D boron-10 shell, 0.25-in	.9903159	.9903664
12	S_4, P_1, D boron 10 in cadmium shell	.9903693	.9904238

[a]All calculations used 65 mesh intervals and group split A of table II.

volume is equal to 1000.0. This standard case was also calculated using the cross section set based on group split B as given in table II. The K_{eff} for this case was 1.000446 for the real flux solution and 1.000559 for the adjoint flux solution.

For each group of the calculations using group splits A and B, the flux per unit lethargy at the center of ZPR-1 was obtained. These results are plotted as one curve in figure 3(a) as a function of the midpoint lethargy of the groups. Group split A tends to emphasize the high-energy end of the spectrum while group split B emphasizes resonance energies of the spectrum. Thus, the curve in figure 3(a) gives the detailed real flux spectrum at the center of a cadmium shell placed in ZPR-1. Figure 3(b) is a detailed plot of the adjoint flux spectrum at the center of a cadmium shell placed in ZPR-1 and represents calculations performed with both group splits A and B.

The effect of mesh point spacing was determined by doubling the number of mesh intervals in each region. The K_{eff} for this calculation was nearly identical for both the real and the adjoint flux solutions to those obtained for the standard case with group split A. In addition, the real and the adjoint fluxes at the center of the system differed but slightly from those obtained for the standard case. Therefore, the number of mesh intervals used for the standard case was adequate for the remaining calculations.

The effect of the order of the S_n approximation on the relative flux and adjoint spectrum at the center of ZPR-1 as well as on the reactor eigenvalue is shown in tables III and IV. Cases 2, 3, and 4 of table III(a) list the values of the real flux for each group for the S_2, S_6, and S_8 approximations, respectively. The S_4 approximation listed in case 1 for the flux does not differ appreciably from the S_6 and the S_8 approximations. Similar conclusions may be reached for the adjoint flux spectrum shown in table III(b). Table IV indicates that the S_2 approximation predicts a value for K_{eff} that is higher than the S_4, S_6, and S_8 approximations by about 1 percent. The tables show that the real and adjoint fluxes obtained from the S_2 calculation differ, in general, from the corresponding S_6 and S_8 fluxes more than the S_4 solution. The S_2 calculation is the lowest order S_n calculation and corresponds to a diffusion type of calculation. In general, S_2 transport calculations are somewhat more accurate than diffusion theory calculations. Thus, the assumption that diffusion theory calculations would not give accurate values of the real and adjoint fluxes at the center of the cadmium shell is confirmed.

The effect of replacing the diamond model representation of the angular fluxes by the step model (eqs. (B64) and (B67) of appendix B) is shown as case 5 in tables III and IV. The step model predicts considerably lower values of K_{eff} by about 1.6 percent than the diamond model. In addition, the real and the adjoint fluxes in the fission spectrum energy range differ considerably.

The effect of scattering order on the relative flux and the adjoint spectrum at the center of ZPR-1 is shown as case 6 in table III. Table III(a) shows that the P_0 fluxes differ the most from the P_1 fluxes in the high-energy groups. However, the adjoint

fluxes in table III(b) show that the P_0 fluxes are 3 to 4 percent lower than the P_1 fluxes in the groups representing the resonance energy range. Table IV indicates that the P_0 calculation underestimates the eigenvalue obtained by the P_1 calculation by nearly 2 percent.

The reduced-density aluminum at the center of the cadmium shell was used to represent void. A value of 0.01 barn-centimeter was chosen for the aluminum atom density for the standard calculation. Case 7 in tables III and IV shows the effect of increasing the aluminum atom density to 0.06 barn-centimeter. These calculations indicate very little effect on the fluxes and eigenvalue due to the increased aluminum density. Thus, the void region at the center of ZPR-1 is adequately simulated by reduced-density aluminum.

The radius of the void was increased by 0.5 centimeter to indicate the effect of cavity size on the fluxes and the eigenvalue at the center of ZPR-1. The radius of the fuel solution was so reduced a corresponding amount (0.5 cm) that the overall reactor size remained the same. Case 8 in tables III(a) and (b) compares the real and the adjoint flux spectra at the center of ZPR-1. There are differences in both the real and the adjoint fluxes as a function of energy. Table IV gives the eigenvalues for the calculations with two different void regions.

The effect of reducing the thickness of the cadmium shell is shown as case 10 in tables III and IV. The outer radius of the cadmium shell remained fixed, and the inner radius was varied. The results in the tables indicate very little difference for the 0.0889-centimeter (35-mil) and 0.0508-centimeter (20-mil) thick cadmium shells. The greatest differences in the fluxes occur in groups 29 and 30. The eigenvalues for these two calculations are essentially the same.

Replacement of the cadmium shell in the standard calculation by void would indicate the magnitude of the effect of the cadmium on the real and the adjoint fluxes at the center of ZPR-1. This effect is demonstrated as case 9 in table III where aluminum has replaced cadmium, but the atom density of the region remains unchanged. As expected, results given in table III show a considerable difference for the real and the adjoint fluxes in the resonance energy range from those shown for case 1. Table IV indicates that the cadmium shell has a worth of nearly 1 percent in reactivity compared with an aluminum shell.

The cadmium shell has the effect of eliminating the thermal real and adjoint fluxes at the center of ZPR-1. Thus, reactivity effects caused by an absorber are due only to resonance absorption and can be accurately measured in ZPR-1. If the cadmium shell is replaced by boron 10, different flux and adjoint spectra will be obtained at the center of ZPR-1. The boron 10 eliminates the real and the adjoint thermal flux and considerably reduces the fluxes in the resonance energy range. The result will be a real and an adjoint flux spectra that enhance the relative effect due to fast neutron reactions. Thus, with a boron 10 shell it may be possible to measure in ZPR-1 reactivity effects due to,

say, inelastic scattering. Case 11 in tables III and IV compares the results of a calculation replacing a 0.0889-centimeter (35-mil) cadmium shell with a 0.635-centimeter (0.25-in.) boron 10 shell with an atom density of 0.0682 barn-centimeter. The outer radius of the shells was the same, but the sizes of the voids differed. The resonance and thermal fluxes are considerably reduced for the boron 10 shell as compared to the cadmium shell. Table IV indicates that the boron 10 reduces the reactor K_{eff} by nearly 1 percent.

Case 12 of tables III and IV shows the result of replacing the aluminum within the cadmium shell by boron 10 with an atom density of 0.0682 barn-centimeter. Since boron 10 is essentially a 1/v absorber (i.e., the absorption cross section varies as the reciprocal of the neutron velocity) with a thermally averaged absorption cross section of 2745 barns, it drastically changes the real and the adjoint flux spectra at the center of ZPR-1 (table III). Note that table IV shows that the boron 10 reduces the eigenvalue of the system by about 1 percent.

CONCLUSIONS

An S_4 calculation, in which the scattering is treated through the P_1 order and in which the diamond model is used to interrelate the angular fluxes, was found to be adequate for determining the real and the adjoint fluxes at the center of a cadmium shell placed in ZPR-1. The various calculations indicated the sensitivity of the results to the S_n order used, to the scattering order used (P_0 or P_1), to the angular flux model representation (diamond or step), to the number of mesh intervals used, to the size of the cavity, to the thickness of the cadmium shell, and to the density of the aluminum used to simulate the void. Additional results are obtained for a 0.25-inch-thick boron 10 shell. Finally, the effect of a 1/v absorber (boron 10) on the flux and adjoint spectra at the center of ZPR-1 is indicated.

These calculations, therefore, indicate the techniques to be used to compute real and adjoint flux spectra at the center of a cadmium shell placed in ZPR-1. These spectra can then be used to correct experimental reactivity data for materials within the cadmium shell.

Lewis Research Center,
National Aeronautics and Space Administration,
Cleveland, Ohio,
129-02-04-03-22.

APPENDIX A

SYMBOLS

A	element of area, cm^2
B^2	transverse geometric buckling, cm^{-2}
C	constant (eq. (B38))
D_g	diffusion coefficient for energy group g, cm
$d\vec{r}$	differential volume element, cm^3
E	neutron energy, eV
E_g	high-energy limit of group g, eV
E_{g-1}	low-energy limit of group g, eV
f_g	fraction of fission neutrons produced in energy group g (eq. (B26))
H	cylindrical height, cm
$\hat{i}$	unit vector along X-axis of Cartesian coordinate system
$\vec{J}_g^+(\vec{r})$	net neutron adjoint current vector (eq. (B44))
$\vec{J}_g(\vec{r})$	vector such that its dot product with unit vector $\vec{\Omega}$ gives net number of neutrons per unit time crossing unit area perpendicular to position vector $\vec{r}$ (eq. (B16))
$\hat{j}$	unit vector along Y-axis of Cartesian coordinate system
K	temperature, ^oK
K_{eff}	static criticality factor
$\hat{k}$	unit vector along Z-axis of Cartesian coordinate system
NG	total number of neutron energy groups
$N_g(r, \mu)$	angular flux for group g for one-dimensional spherical geometry (eq. (B54b))
$N_g(r, \theta, \varphi)$	angular flux for group g for one-dimensional cylindrical geometry (eq. (B55b))
$N_g(x, \mu)$	angular flux for group g for one-dimensional slab geometry (eq. (B53b))
$N_{i,\overline{m}}$	value of angular flux at left-hand edge of spatial volume element for m^{th} angular interval

$N_{\bar{i},m}$	value of angular flux at left-hand edge of angular volume element for i^{th} spatial volume element
$N_{\bar{i},\bar{m}}$	average value of angular flux in i^{th} spatial volume element and m^{th} angular interval
$N_{\bar{i},m+1}$	value of angular flux at right-hand edge of angular volume element for i^{th} spatial volume element
$N_{i+1,\bar{m}}$	value of angular flux at right-hand edge of spatial volume element for m^{th} angular interval
$n_g(\vec{r},\vec{\Omega})d\vec{r}\,d\vec{\Omega}$	probable number of neutrons belonging to energy group g in space volume element $d\vec{r}$ about position $\vec{r}$ and in element of solid angle $d\vec{\Omega}$ about $\vec{\Omega}$
$P(E'\rightarrow E;\mu_L)dE$	probability that neutron at energy E' will, after elastic scattering collision, be in energy range dE about energy E and with scattering angle being through angle cosine μ_L in laboratory coordinate system (eqs. (B23) and (B24))
$P_l(\mu)$	Legendre polynomial of index l and argument μ (eq. (B9))
$P_l^m(\mu)$	associated Legendre polynomial of index l, m and argument μ (eq. (B8))
$P_{l,m}(\vec{\Omega})$	surface spherical harmonic of index l, m and argument $\vec{\Omega}$ (eqs. (B7a) and (B7b))
$\langle P_l(\mu_L)\Sigma_{es}\rangle_g$	average for group g of elastic scattering cross section times l^{th} Legendre polynomial of cosine of laboratory scattering angle (eq. (B30e))
$Q_g(\vec{r})$	number of neutrons produced in group g by external source at position $\vec{r}$ per unit volume per unit time, number/cm^3/sec
R	radius of cylinder, cm
$\vec{R}$	vector indicating outer boundary of reactor system
$\vec{r}$	position vector
$S_g(r,\theta,\varphi)$	angular source term for group g for one-dimensional cylindrical geometry (eq. (B55c))
$S_g(r,\mu)$	angular source term for group g for one-dimensional spherical geometry (eq. (B54c))

$S_g(\vec{r},\vec{\Omega})$	angular source term giving number of neutrons produced in group g and moving in direction $\vec{\Omega}$ at position $\vec{r}$ per unit solid angle, per unit volume, and per unit time, number/cm^3/sr/sec (eq. (B2))
$S_g^+(\vec{r},\vec{\Omega})$	angular adjoint source term (eq. (B39))
$S_g(\vec{r},\vec{\Omega})\Big\|_{P_1}$	P_1 approximation to angular source $S_g(\vec{r},\vec{\Omega})$ (eq. (B31))
$S_g(\vec{r},\vec{\Omega})\Big\|_{P_0(\Sigma_{tr})}$	P_0 transport corrected approximation to angular source $S_g(\vec{r},\vec{\Omega})$ (eq. (B32))
$S_g^+(\vec{r},\vec{\Omega})\Big\|_{P_0(\Sigma_{tr})}$	P_0 transport corrected approximation to angular adjoint source $S_g^+(\vec{r},\vec{\Omega})$ (eq. (B49))
$S_g^+(\vec{r},\vec{\Omega})\Big\|_{P_1}$	P_1 approximation to angular adjoint source $S_g^+(\vec{r},\vec{\Omega})$ (eq. (B48))
$S_g(x,\mu)$	angular source term for group g for one-dimensional slab geometry (eq. (B53c))
$S_{\bar{i},\bar{m}}$	average value of angular source in i^{th} spatial volume element and m^{th} angular interval
$S_{l,g}(\vec{r})$	l^{th} moment component of angular source $S_g(\vec{r},\vec{\Omega})$ (eq. (B5))
$S_{l,g}^+(\vec{r})$	l^{th} moment component of angular adjoint source term $S_g^+(\vec{r},\vec{\Omega})$ (eq. (B40c))
S_n	refers to quadrature scheme developed by Carlson for solution of neutron transport equation where n is order of quadrature
$S_{0,g}(\vec{r})$	isotropic component of angular source $S_g(\vec{r},\vec{\Omega})$ that includes contributions from external sources, fission, downscattering, and upscattering of neutrons, number/cm^3/sec (eq. (B3))
$S_{0,g}^+(\vec{r})$	isotropic component of angular adjoint source term $S_g^+(\vec{r},\vec{\Omega})$ (eq. (B40a))
$S_{1,g}(\vec{r})$	first moment component of angular source $S_g(\vec{r},\vec{\Omega})$ (eq. (B4))
$S_{1,g}^+(\vec{r})$	first moment component of angular adjoint source term $S_g^+(\vec{r},\vec{\Omega})$ (eq. (B40b))
$T_g^l(\vec{r},\vec{\Omega})$	variable related to surface spherical harmonic components of angular flux for neutron group g (eq. (B19))

$T_g^{l+}(\vec{r},\vec{\Omega})$ variable related to surface spherical harmonic components of angular adjoint flux for group g (eq. (B43b))

$T^l(\vec{r},E,\vec{\Omega})$ variable related to surface spherical harmonic components of energy dependent angular flux (eq. (B18))

v_g average neutron speed for group g, cm/sec

V element of volume, cm^3

W quadrature weight

X X-axis in Cartesian coordinate system

Y Y-axis in Cartesian coordinate system

Z Z-axis in Cartesian coordinate system

α parameter arising from angular redistribution term in spherical and cylindrical geometry (eqs. (B58), (B61), and (B62))

$(\alpha/W)_m$ parameter defined by equation (B65a)

δ Kronecker delta (eq. (B13))

η $\equiv \sin\theta \sin\varphi$ (eq. (B56b))

θ polar angle between $\vec{\Omega}$ and z-axis

μ $\equiv \cos\theta$ (eq. (B11))

or cosine of angle between $\vec{\Omega}$ and x-axis in slab geometry (eq. (B53a))

or cosine of angle between $\vec{\Omega}$ and radius in spherical geometry (eq. (B54a))

or $\equiv \sin\theta \cos\varphi$ for cylindrical geometry (eq. (B56a))

μ_L cosine of angle in laboratory coordinate system between initial and final direction of motion of elastically scattered neutron

$\langle \mu_L \Sigma_{es} \rangle_g$ average for group g of elastic scattering cross section times cosine of scattering angle in laboratory coordinate system (eq. (B30d))

$\mu_{\overline{m}}$ S_n quadrature coefficient for m^{th} angular interval

μ_0 value of $\mu_{\overline{m}}$ for spherical or cylindrical geometry used in starting equation of recursion relation for computing angular flux

ν_g number of neutrons produced per fission in group g

$\Sigma_{a,g}$ macroscopic neutron absorption cross section for group g, cm^{-1}

$\Sigma_{es,g}$ macroscopic neutron elastic scattering cross section for group g, cm^{-1}

$\Sigma^{l}_{es}(E' \rightarrow E)$	l^{th} moment coefficient in expansion of elastic scattering kernel in Legendre polynomial series (eqs. (B23) and (B24))
$\Sigma^{l}_{es}(g' \rightarrow g)$	l^{th} moment neutron cross section for transfer of neutrons from group g' to group g, cm^{-1} times l^{th} Legendre polynomial of cosine of scattering angle in laboratory coordinate system (eqs. (B22) and (B30e))
$\Sigma^{0}_{es}(g' \rightarrow g)$	probability per unit path length for transfer of neutrons from group g' to group g by elastic scattering, cm^{-1} (eqs. (B22), (B29), and (B30a))
$\Sigma^{1}_{es}(g' \rightarrow g)$	first moment neutron cross section for transfer of neutrons from group g' to group g, cm^{-1} times cosine of scattering angle in laboratory coordinate system (eqs. (B22) and (B30d))
$\Sigma_{f,g}$	macroscopic neutron fission cross section for group g, cm^{-1}
$\Sigma_{in,g}$	macroscopic neutron inelastic scattering cross section for group g, cm^{-1}
$\Sigma_{in}(g' \rightarrow g)$	probability per unit path length for transfer of neutrons from group g' to group g by inelastic scattering, cm^{-1} (eqs. (B22) and (B30b))
$\Sigma_{N2N,g}$	macroscopic neutron (N, 2N) reaction cross section for group g, cm^{-1}
$\Sigma_{N2N}(g' \rightarrow g)$	probability per unit path length for transfer of neutrons from group g' to group g by N, 2N reaction, cm^{-1} (eqs. (B22) and (B30c))
$\Sigma_{t,g}$	macroscopic neutron total cross section for group g ($\equiv \sigma_g$), cm^{-1}
$\Sigma_{tr,g}$	macroscopic neutron transport cross section for group g $\left(\equiv \frac{1}{3D_g}$ or $\Sigma_{t,g} - \langle \mu \Sigma_{es} \rangle_g\right)$, cm^{-1} (eq. (B34))
$\sigma(g' \rightarrow g)$	macroscopic neutron cross section for transfer of neutrons from group g' to group g (may include elastic scattering, inelastic scattering, and N, 2N reactions), cm^{-1} (eq. (B29))
$\sigma_{eff}(g \rightarrow g)$	effective within group scattering cross section used in P_0 transport corrected calculation, cm^{-1} (eq. (B33))
σ_g	macroscopic neutron total cross section for energy group g ($\equiv \Sigma_{t,g}$), cm^{-1} (eq. (B28a))
$\sigma_g\big\|_{P_0(\Sigma_{tr})}$	$\equiv \Sigma_{tr,g}$ (eq. (B34))
$\sigma_{\overline{i}}$	average value of σ_g for i^{th} spatial volume element
$\Phi_g(\vec{r})$	scalar neutron flux for group g $\left[\equiv \varphi^{g}_{0,0}(\vec{r})\right]$, neutrons/$cm^2$/sec (eq. (B15))

$\Phi_g^+(\vec{r})$	scalar adjoint flux for group g $\left[\equiv \varphi_{0,0}^{g+}(\vec{r})\right]$ (eqs. (B43a) and (B46a))
φ	azimuthal angle between projection of $\vec{\Omega}$ on X-Y plane and X-axis
$\phi_g(\vec{r},\vec{\Omega})$	total angular flux for group g $\left[\equiv n_g(\vec{r},\vec{\Omega})v_g\right]$, neutrons/cm^2/sr/sec
$\phi_g^+(\vec{r},\vec{\Omega})$	angular adjoint flux or neutron importance. It is proportional to (after sufficiently long time) power level due to neutron belonging to energy group g and having direction of motion $\vec{\Omega}$ being injected into reactor system at position $\vec{r}$. (See eqs. (B37) and (B38).)
$\phi_{l,m}(\vec{r},E)$	l,m^{th} coefficient of expansion of energy-dependent angular flux in surface spherical harmonic series
$\phi_{l,m}^g(\vec{r})$	l,m^{th} coefficient of expansion of angular flux for group g in surface spherical harmonic series (eqs. (B6) and (B15))
$\phi_{l,m}^{g+}(\vec{r})$	l,m^{th} coefficient of expansion of angular adjoint flux for group g in surface spherical harmonic series (eqs. (B42) and (B43a))
$\chi(\vec{r})$	total number of neutrons produced by fission at position $\vec{r}$ per unit volume and per unit time, number/cm^3/sec (eq. (B25))
$\chi^+(\vec{r})$	fission spectrum weighted neutron importance (eq. (B41d))
Ω_x	x-component in Cartesian coordinates of $\vec{\Omega}$
Ω_y	y-component in Cartesian coordinates of $\vec{\Omega}$
Ω_z	z-component in Cartesian coordinates of $\vec{\Omega}$
$\vec{\Omega}$	unit vector in direction of motion of neutron travel
$\vec{\Omega}^+$	designates vector $\vec{\Omega}$ directed out of reactor system
$\vec{\Omega}^-$	designates vector $\vec{\Omega}$ directed into reactor system
$\vec{\omega}$	$\equiv -\vec{\Omega}$(eq. (B52))

Subscripts:

g	neutron energy group
i	left-hand edge of spatial mesh interval
i+1	right-hand edge of spatial mesh interval
$\bar{i}$	midpoint of spatial mesh interval
l	index of either surface spherical harmonic, associated Legendre polynomial, or Legendre polynomial

m index for surface spherical harmonics or left-hand "edge" of angular mesh interval

m+1 right-hand "edge" of angular mesh interval

$\overline{m}$ midpoint of angular mesh interval

n order of S_n approximation

r radial direction of cylinder

z Z-direction of cylinder or if slab, Y-direction

Superscripts:

g neutron energy group

m index for associated Legendre polynomials

+ adjoint quantity

Computer listing terminology:

ALPHA	f
ANUSIG	$\nu\Sigma_f$
SIG	Σ_t
SIGA	Σ_a
SIGSO(G-G)	$\sigma(g \rightarrow g)$
SIGSI(G-G)	$3\Sigma^1_{es}(g \rightarrow g)$
SIGTR	Σ_{tr}

P(0) TRANSFER MATRIX = $\sigma(g' \rightarrow g)$

P(1) TRANSFER MATRIX = $3\Sigma^1_{es}(g' \rightarrow g)$

APPENDIX B

DESCRIPTION OF S_n EQUATIONS

Equations for the Real Flux

The basis for the development of a one-dimensional, multigroup, multiregion S_n transport program for the IBM 7094 computer is the multigroup form of the time-independent Boltzmann transport equation for neutrons

$$\vec{\Omega} \cdot \vec{\nabla}\phi_g(\vec{r},\vec{\Omega}) + \sigma_g(\vec{r})\phi_g(\vec{r},\vec{\Omega}) = S_g(\vec{r},\vec{\Omega}) \qquad g = 1,2, \ldots, NG \tag{B1}$$

In the previous equation, $\vec{\Omega}$ is a unit vector along the direction of motion of neutron travel, $\phi_g(\vec{r},\vec{\Omega}) \equiv n_g(\vec{r},\vec{\Omega})v_g$ is the total angular flux for group g where $n_g(\vec{r},\vec{\Omega})$ is the total number of neutrons in group g per unit volume at position $\vec{r}$ and per unit solid angle about $\vec{\Omega}$ per unit time while v_g is the average neutron speed for group g, $\sigma_g(\vec{r})$ is the total macroscopic cross section at position $\vec{r}$ for group g, and $S_g(\vec{r},\vec{\Omega})$ is the angular source term giving the number of neutrons produced in group g per unit time and moving in the direction $\vec{\Omega}$ at position $\vec{r}$ per unit solid angle and per unit volume. Thus, equation (B1) represents a time-independent transport equation for group g where neutron losses per unit volume at position $\vec{r}$ and per unit solid angle about direction $\vec{\Omega}$ due to collisions and streaming are balanced by gains due to fission sources, external sources, downscattering of neutrons from neutron groups with higher neutron speeds, and upscattering of neutrons from groups that have lower neutron speeds.

The source term $S_g(\vec{r},\vec{\Omega})$ for equation (B1) can be written explicitly as

$$4\pi S_g(\vec{r},\vec{\Omega}) = S_{0,g}(\vec{r}) + \sigma(\vec{r};g \to g)\Phi_g(\vec{r}) + 3\left[S_{1,g}(\vec{r}) + \Sigma^1_{es}(\vec{r},g \to g)\vec{\Omega} \cdot \vec{J}_g(\vec{r})\right]$$

$$+ \sum_{l=2}^{\infty} (2l+1)\left[S_{l,g}(\vec{r}) + \Sigma^l_{es}(\vec{r},g \to g)T^l_g(\vec{r},\vec{\Omega})\right] \tag{B2}$$

where

$$S_{0,g}(\vec{r}) = Q_g(\vec{r}) + \frac{f_g\chi(\vec{r})}{K_{eff}} + \sum_{\substack{g' \\ (g' \neq g)}} \sigma(\vec{r},g' \to g)\Phi_{g'}(\vec{r}) \tag{B3}$$

$$S_{1,g}(\vec{r}) = \sum_{\substack{g' \\ (g' \neq g)}} \Sigma^{1}_{es}(\vec{r}, g' \rightarrow g)\vec{\Omega} \cdot \vec{J}_{g'}(\vec{r}) \tag{B4}$$

$$S_{l,g}(\vec{r}) = \sum_{\substack{g' \\ (g' \neq g)}} \Sigma^{l}_{es}(\vec{r}, g' \rightarrow g)T^{l}_{g'}(\vec{r}, \vec{\Omega}) \tag{B5}$$

The terms $S_{0,g}(\vec{r})$, $S_{1,g}(\vec{r})$, and $S_{l,g}(\vec{r})$ are the zeroth, first, and l^{th} components of the angular source $S_g(\vec{r}, \vec{\Omega})$ and are obtained from the expansion of the angular flux in surface spherical harmonics.

The expansion of the angular flux in surface spherical harmonics is given by

$$\phi_g(\vec{r}, \vec{\Omega}) = \sum_{l=0}^{\infty} \sum_{m=-l}^{l} \frac{2l+1}{4\pi} \phi^{g}_{l,m}(\vec{r}) P_{l,m}(\vec{\Omega}) \tag{B6}$$

The surface spherical harmonics $P_{l,m}(\vec{\Omega})$ are defined as

$$P_{l,m}(\vec{\Omega}) = \left[\frac{2(l-m)!}{(l+m)!}\right]^{1/2} P^{m}_{l}(\mu)\cos(m\varphi) \qquad l \geq 0,\ 0 < m \leq l \tag{B7a}$$

$$P_{l,-m}(\vec{\Omega}) = \left[\frac{2(l-m)!}{(l+m)!}\right]^{1/2} P^{m}_{l}(\mu)\sin(m\varphi) \qquad l \geq 0,\ 0 < m \leq l \tag{B7b}$$

The $P^{m}_{l}(\mu)$ are the associated Legendre polynomials given by

$$P^{m}_{l}(\mu) = \frac{(1-\mu^2)^{m/2}}{2^l l!} \frac{d^{l+m}}{d\mu^{l+m}} (\mu^2 - 1)^l \tag{B8}$$

For $P_{l,0}(\vec{\Omega})$, the Legendre polynomials are used, and these are defined by the following expression:

$$P_{l,0}(\vec{\Omega}) \equiv P_l(\mu) = \frac{1}{2^l l!} \frac{d^l}{d\mu^l}(\mu^2 - 1)^l \qquad l \geq 0 \tag{B9}$$

The unit vector $\vec{\Omega}$ is given in terms of the polar angle θ between $\vec{\Omega}$ and the Z-axis and the azimuthal angle φ between the projection of $\vec{\Omega}$ on the X-Y plane and the X-axis as

$$\begin{aligned}\vec{\Omega} &= \hat{i}\Omega_x + \hat{j}\Omega_y + \hat{k}\Omega_z \\ &= \hat{i}\sin\theta\cos\varphi + \hat{j}\sin\theta\sin\varphi + \hat{k}\cos\theta \\ &= \hat{i}P_{1,1}(\vec{\Omega}) + \hat{j}P_{1,-1}(\vec{\Omega}) + \hat{k}P_{1,0}(\vec{\Omega})\end{aligned} \tag{B10}$$

where $\hat{i}$, $\hat{j}$, and $\hat{k}$ are unit vectors along the X-, Y-, and Z-coordinate axes, respectively. The quantity μ is given by

$$\mu = \cos\theta \tag{B11}$$

These surface spherical harmonics have the orthogonality property

$$\int P_{l,m}(\vec{\Omega})P_{l',m'}(\vec{\Omega})d\vec{\Omega} = \frac{4\pi}{2l+1}\delta_{ll'}\delta_{mm'} \tag{B12}$$

where δ is here the Kronecker delta defined as

$$\left.\begin{aligned}\delta_{kk'} &= 1 \qquad k' = k \\ &= 0 \qquad k' \neq k\end{aligned}\right\} \tag{B13}$$

The addition theorem for these spherical harmonics is expressed by the equation

$$P_l(\vec{\Omega}\cdot\vec{\Omega}') = \sum_{m=-l}^{l} P_{l,m}(\vec{\Omega})P_{l,m}(\vec{\Omega}') \tag{B14}$$

By the orthogonality property of these harmonics, the $\phi^g_{l,m}(\vec{r})$ of equation (B6) may be determined:

$$\phi^g_{l,m}(\vec{r}) = \int \phi_g(\vec{r},\vec{\Omega})P_{l,m}(\vec{\Omega})d\vec{\Omega} \tag{B15}$$

The quantity $\phi^g_{0,0}(\vec{r})$ is the scalar neutron flux and will be represented more simply as $\Phi_g(\vec{r})$. The net neutron current vector $\vec{J}_g(\vec{r})$ is given by the equation

$$\vec{J}_g(\vec{r}) = \int \phi_g(\vec{r},\vec{\Omega})\vec{\Omega}\, d\vec{\Omega}$$

$$= \hat{i}\phi^g_{1,1}(\vec{r}) + \hat{j}\phi^g_{1,-1}(\vec{r}) + \hat{k}\phi^g_{1,0}(\vec{r}) \tag{B16}$$

Equations (B10) and (B16) yield the dot product of $\vec{\Omega}$ and $\vec{J}_g(\vec{r})$. This is

$$\vec{\Omega} \cdot \vec{J}_g(\vec{r}) = \sum_{m=-1}^{1} \phi^g_{1,m}(\vec{r}) P_{1,m}(\vec{\Omega}) \tag{B17}$$

For values of $l \geq 2$, there are no such simple identifications for the $\phi^g_{l,m}(\vec{r})$ as these quantities have a tensor aspect.

If we define $T^l(\vec{r},E,\vec{\Omega})$ by the relation

$$T^l(\vec{r},E,\vec{\Omega}) = \sum_{m=-l}^{l} \phi_{l,m}(\vec{r},E) P_{l,m}(\vec{\Omega}) \tag{B18}$$

then, the quantity $T^l_g(\vec{r},\vec{\Omega})$ in equation (B2) is the integral over group g of $T^l(\vec{r},E,\vec{\Omega})$, that is,

$$T^l_g(\vec{r},\vec{\Omega}) = \int_{E=E_{g-1}}^{E_g} T^l(\vec{r},E,\vec{\Omega})\, dE$$

$$= \sum_{m=-l}^{l} \phi^g_{l,m}(\vec{r}) P_{l,m}(\vec{\Omega}) \tag{B19}$$

where

$$\phi^g_{l,m}(\vec{r}) = \int_{E=E_{g-1}}^{E_g} \phi_{l,m}(\vec{r},E)dE \tag{B20}$$

and where E_{g-1} and E_g are the lower and the upper energy limits, respectively, of group g. From equation (B19), $T^0_g(\vec{r},\vec{\Omega})$ and $T^1_g(\vec{r},\vec{\Omega})$ are specifically given by

$$T_g^0(\vec{r},\vec{\Omega}) = \Phi_g(\vec{r}) \tag{B21a}$$

$$T_g^1(\vec{r},\vec{\Omega}) = \vec{\Omega} \cdot \vec{J}_g(r) \tag{B21b}$$

The l^{th} order transfer cross section from group g' to group g, $\Sigma_{es}^l(\vec{r}, g' \to g)$, can now be defined in terms of the $T_g^l(\vec{r},\vec{\Omega})$. These $\Sigma_{es}^l(\vec{r}, g' \to g)$ are defined by the equation

$$\Sigma_{es}^l(\vec{r}, g' \to g) = \frac{\displaystyle\int_{E=E_{g-1}}^{E_g} dE \int_{E'=E_{g'-1}}^{E_{g'}} \Sigma_{es}^l(\vec{r}, E' \to E) \sum_{m=-l}^{l} P_{l,m}(\vec{\Omega})\phi_{l,m}(\vec{r}, E')dE'}{\displaystyle\int_{E'=E_{g'-1}}^{E_{g'}} \sum_{m=-l}^{l} P_{l,m}(\vec{\Omega})\phi_{l,m}(\vec{r}, E')dE'}$$

$$= \frac{1}{T_{g'}^l(\vec{r},\vec{\Omega})} \int_{E=E_{g-1}}^{E_g} dE \int_{E'=E_{g'-1}}^{E_{g'}} \Sigma_{es}^l(\vec{r}, E' \to E) T^l(\vec{r}, E', \vec{\Omega})dE' \tag{B22}$$

The quantity $\Sigma_{es}^l(\vec{r}, E' \to E)$ arises from the expansion of the elastic scattering kernel in a series of Legendre polynomials:

$$\Sigma_{es}(\vec{r}, E')P(E' \to E; \mu_L) = \sum_{l=0}^{\infty} \frac{2l+1}{4\pi} \Sigma_{es}^l(\vec{r}, E' \to E)P_l(\mu_L) \tag{B23}$$

where $\Sigma_{es}(r, E')$ is the elastic scattering cross section at energy E' and position $\vec{r}$, and $P(E' \to E; \mu_L)dE$ is the probability that a neutron at energy E' will, after an elastic scattering collision, be in the energy range dE about E with the scattering angle in the laboratory coordinate system being angle cosine μ_L. By the orthogonality property of the Legendre polynomials, $\Sigma_{es}^l(\vec{r}, E' \to E)$ is given as

$$\Sigma_{es}^l(\vec{r}; E' \to E) = 2\pi \int \Sigma_{es}(\vec{r}, E')P(E' \to E; \mu_L)P_l(\mu_L)d\mu_L \tag{B24}$$

This equation is evaluated in terms of experimentally determined differential cross-section data.

The quantity $Q_g(\vec{r})$ in equation (B3) represents an isotropic fixed source at position $\vec{r}$ while $\chi(\vec{r})$ is the source of neutrons due to fissions. This term is given by

$$\chi(\vec{r}) = \sum_{g'} \left[\nu(\vec{r})\Sigma_f(\vec{r})\right]_{g'} \Phi_{g'}(\vec{r}) \tag{B25}$$

where $\nu_g(\vec{r})$ is the average number of neutrons per fission event in group g at position $\vec{r}$ while $\Sigma_{f,g}(\vec{r})$ is the probability per unit path length of a fission at position $\vec{r}$ in group g.

In equation (B3), f_g represents the fraction of fission neutrons produced in group g and is so normalized that

$$\sum_g f_g = 1.0 \tag{B26}$$

The quantity K_{eff} is the static criticality factor of the system. In the absence of the external source $Q_g(\vec{r})$, K_{eff} is an eigenvalue of the system and can take on a range of values. If the system includes an external source, the system must be subcritical to maintain a time-independent condition. This static criticality factor is given in terms of the function $\chi(\vec{r})$ as an integral over the entire reactor system:

$$K_{eff} = \int \chi(\vec{r})d\vec{r} \tag{B27}$$

where $d\vec{r}$ is the element of volume.

The total macroscopic cross section $\sigma_g(\vec{r})$ of equation (B1) is the probability per unit path length of a collision, whether scattering or absorption, occurring in group g at position $\vec{r}$. This probability is given by

$$\sigma_g(\vec{r}) = \Sigma_{a,g}(\vec{r}) + \Sigma_{es,g}(\vec{r}) + \Sigma_{in,g}(\vec{r}) + \Sigma_{N2N,g}(\vec{r}) \tag{B28a}$$

$$= \Sigma_{t,g}(\vec{r})$$

where $\Sigma_{a,g}(\vec{r})$, $\Sigma_{es,g}(\vec{r})$, $\Sigma_{in,g}(\vec{r})$, and $\Sigma_{N2N,g}(\vec{r})$ are the probabilities per unit path length for absorption, elastic scattering, inelastic scattering, and for the N, 2N reaction, respectively, at position $\vec{r}$ in group g. If more than one nuclear species is present, then $\sigma_g(\vec{r})$ represents a summation over all elements in the volume element at $\vec{r}$.

The total cross section $\sigma_g(\vec{r})$ may also include transverse leakage effects. Transverse leakage for cylindrical or planar geometry may be approximated by adding an absorption-like cross section to equation (B28). This cross section $D_g B_z^2$ is given by

$$D_g B_z^2 = \frac{\pi^2 \Sigma_{tr,g}}{3\left(H\Sigma_{tr,g} + 1.42\right)^2} \tag{B28b}$$

where H is the height of the cylindrical system and $\Sigma_{tr,g}$ is the group transport cross section. Equation (B28b) includes an extrapolation distance of $0.71/\Sigma_{tr,g}$ for each end of the cylinder. For a two-dimensional slab, the height H is interpreted as the y-direction with the x-dimension being the direction of solution. For a three-dimensional slab system, transverse leakage in the z-direction is approximated by adding a term similar to that given by equation (B28b). For a cylindrical system being solved along the z-axis, the radial leakage cross section is approximated by

$$D_g B_r^2 = \frac{(2.4048)^2 \Sigma_{tr,g}}{3\left(R\Sigma_{tr,g} + 0.71\right)^2} \tag{B28c}$$

where R is the radius of the cylinder. This equation includes an extrapolation distance of $0.71/\Sigma_{tr,g}$ for the radial direction.

Inelastic scattering and the $N,2N$ reaction are considered to be isotropic and hence do not contribute to the anisotropic part of $S_g(\vec{r},\vec{\Omega})$. Elastic scattering is considered to be anisotropic, and the number of terms retained in equation (B2) is determined by degree of anisotropy exhibited by a given nuclear specie, availability of nuclear data, and computer time and size limitations.

The source of neutrons due to scattering into a group g by isotropic elastic scattering, inelastic scattering, or by the $N,2N$ reaction is given by the third term of equation (B3). Here, the quantity $\sigma(\vec{r},g' \rightarrow g)$ is given by

$$\sigma(\vec{r},g' \rightarrow g) = \Sigma_{es}^{0}(\vec{r},g' \rightarrow g) + \Sigma_{in}(\vec{r},g' \rightarrow g) + \Sigma_{N2N}(\vec{r},g' \rightarrow g) \tag{B29}$$

The quantity $\Sigma_{es}^{0}(\vec{r},g' \rightarrow g)$ is defined by equation (B22) for $l = 0$ while $\Sigma_{in}(\vec{r},g' \rightarrow g)$ and $\Sigma_{N2N}(\vec{r},g' \rightarrow g)$ are averaged in a similar manner. Thus $\Sigma_{es}^{0}(\vec{r},g' \rightarrow g)$, $\Sigma_{in}(\vec{r},g' \rightarrow g)$, and $\Sigma_{N2N}(\vec{r},g' \rightarrow g)$ represent the probability per unit path length for the transfer of neutrons from group g' to group g by elastic scattering, inelastic scattering, and the $N,2N$ reaction, respectively, at position $\vec{r}$.

If more than one nuclear species is present in a volume element at position $\vec{r}$, then $\sigma(r, g' \rightarrow g)$ should be a summation over all elements that are present. Similar comments apply to the anisotropic scattering source terms in equation (B2). Upscattering is formally included in the formulations indicated by equations (B2) and (B4); the index g' in the summations then includes all groups except $g' = g$. For convenience in performing the numerical calculations, the terms for $g = g$ are indicated separately in equation(B2).

The various scattering out cross sections are assumed to have the following normalizations:

$$\Sigma_{es,g} = \sum_{g'} \Sigma^0_{es}(g \rightarrow g') \tag{B30a}$$

$$\Sigma_{in,g} = \sum_{g'} \Sigma_{in}(g \rightarrow g') \tag{B30b}$$

$$2\Sigma_{N2N,g} = \sum_{g'} \Sigma_{N2N}(g \rightarrow g') \tag{B30c}$$

$$\langle \mu_L \Sigma_{es} \rangle_g = \sum_{g'} \Sigma^1_{es}(g \rightarrow g') \tag{B30d}$$

and, in general, for the l^{th} term

$$\langle P_L(\mu_L)\Sigma_{es} \rangle_g = \sum_{g'} \Sigma^l_{es}(g \rightarrow g') \tag{B30e}$$

Two common approximations can be obtained from equation (B2). These are the P_1 and the P_0 transport corrected approximations. The P_1 approximation is obtained from equation (B2) by setting all terms for $l \geq 2$ to 0, then

$$4\pi S_g(\vec{r}, \vec{\Omega})\Big|_{P_1} = S_{0,g}(\vec{r}) + \sigma(\vec{r}, g \rightarrow g)\Phi_g(\vec{r}) + 3\left[S_{1,g}(\vec{r}) + \Sigma^1_{es}(\vec{r}, g \rightarrow g)\vec{\Omega} \cdot \vec{J}_g(\vec{r})\right] \tag{B31}$$

The development given for equation (B1) applies for any geometry. Considerable simplifications can be obtained for the three one-dimensional geometries. In particular, for the spherical and planar geometries, only the $m = 0$ terms of equation (B6) are retained. This simplification corresponds to an expansion of the angular flux in a series of Legendre polynomials. For the one-dimensional cylinder, azimuthal symmetry condition permits the dropping of the $\sin(m\varphi)$ terms (eqs. (B6) and (B7b)) while polar angle symmetry reduces the number of flux component terms still further since only those terms are retained for which $l + m$ is even. Thus, for any l, the number of terms retained for one-dimensional cylindrical geometry is the integer part of $l/2 + 1$.

Equations for Adjoint Flux

The equation that is adjoint to equation (B1) is given by

$$-\vec{\Omega} \cdot \vec{\nabla}\phi_g^+(\vec{r},\vec{\Omega}) + \sigma_g(\vec{r})\phi_g^+(\vec{r},\vec{\Omega}) = S_g^+(\vec{r},\vec{\Omega}) \qquad g = 1, 2, \ldots, NG \tag{B37}$$

The quantity $\phi_g^+(\vec{r},\vec{\Omega})$ is termed the adjoint flux or neutron importance. The physical interpretation of $\phi_g^+(\vec{r},\vec{\Omega})$ can be determined from the following considerations. Suppose there are no neutrons in a just critical reactor at the beginning (time $t = 0$), that is, its power is equal to zero. If at some position $\vec{r}$, N neutrons of energy group g and direction of motion $\vec{\Omega}$ are injected, then the neutrons will be distributed in the reactor after some sufficiently long time according to their eigenfunctions, and a definite level of power will be established. This level evidently depends on the position $\vec{r}$, energy group g, and direction of motion $\vec{\Omega}$ and its proportional to the number of neutrons N injected into the reactor. Thus, the adjoint flux or neutron importance is then a quantity proportional to this power level related to one neutron:

$$\phi_g^+(r,\Omega) = C\,\frac{\text{Power level as } t \to \infty \text{ if N neutrons of group g and direction } \vec{\Omega} \text{ are injected at point } \vec{r}}{N} \tag{B38}$$

Neutron importance is determined with an accuracy up to the multiplication constant C.

The source term for equation (B37) can be written as

$$4\pi S_g^+(\vec{r},\vec{\Omega}) = S_{0,g}^+(\vec{r}) + \sigma(\vec{r};g \to g)\Phi_g^+(\vec{r}) + 3\left[S_{1,g}^+(\vec{r}) + \Sigma_{es}^1(\vec{r},g \to g)\vec{\Omega} \cdot \vec{J}_g^+(\vec{r})\right]$$

$$+ \sum_{l=2}^{\infty}(2l+1)\left[S_{l,g}^+(\vec{r}) + \Sigma_{es}^l(\vec{r},g \to g)T_g^{l+}(\vec{r},\vec{\Omega})\right] \tag{B39}$$

where

$$S^{+}_{0,g}(\vec{r}) = \frac{\left[\nu(\vec{r})\Sigma_f(\vec{r})\right]_g \chi^{+}(\vec{r})}{K_{eff}} + \sum_{\substack{g' \\ (g' \neq g)}} \sigma(\vec{r}, g \rightarrow g')\Phi^{+}_{g'}(\vec{r}) \tag{B40a}$$

$$S^{+}_{1,g}(\vec{r}) = \sum_{\substack{g' \\ (g' \neq g)}} \Sigma^{1}_{es}(\vec{r}, g \rightarrow g')\vec{\Omega} \cdot \vec{J}^{+}_{g'}(\vec{r}) \tag{B40b}$$

$$S^{+}_{l,g}(\vec{r}) = \sum_{\substack{g' \\ (g' \neq g)}} \Sigma^{l}_{es}(\vec{r}, g \rightarrow g')T^{l+}_{g'}(\vec{r}, \vec{\Omega}) \tag{B40c}$$

and where

$$\chi^{+}(\vec{r}) = \sum_{g'} f_{g'}\Phi^{+}_{g'}(\vec{r}) \tag{B41}$$

In considering the source term as given by equation (B40), the fixed adjoint source $Q^{+}_{g}(\vec{r})$ is arbitrarily assumed to be zero.

The expansion for the angular adjoint flux is similar to that for the real flux and is given by

$$\phi^{+}_{g}(\vec{r}, \vec{\Omega}) = \sum_{l=0}^{\infty} \sum_{m=-l}^{l} \frac{2l+1}{4\pi} \phi^{g+}_{l,m}(\vec{r})P_{l,m}(\vec{\Omega})$$

$$= \sum_{l=0}^{\infty} \frac{2l+1}{4\pi} T^{l+}_{g}(\vec{r}, \vec{\Omega}) \tag{B42}$$

where

$$\phi^{g+}_{l,m}(\vec{r}) = \int \phi^{+}_{g}(\vec{r}, \vec{\Omega})P_{l,m}(\vec{\Omega})d\vec{\Omega} \tag{B43a}$$

$$T_g^{l+}(\vec{r},\vec{\Omega}) = \sum_{m=-l}^{l} \phi_{l,m}^{g+}(\vec{r}) P_{l,m}(\vec{\Omega}) \tag{B43b}$$

As for the real flux, the net neutron current vector $\vec{J}_g^+(\vec{r})$ for the adjoint equation is given by

$$\vec{J}_g^+(\vec{r}) = \int \phi_g^+(\vec{r},\vec{\Omega})\vec{\Omega}\, d\vec{\Omega}$$

$$= \hat{i}\phi_{1,1}^{g+}(\vec{r}) + \hat{j}\phi_{1,-1}^{g+}(\vec{r}) + \hat{k}\phi_{1,0}^{g+}(\vec{r}) \tag{B44}$$

Equations (B10) and (B44) yield the dot product of $\vec{\Omega}$ and $\vec{J}_g^+(\vec{r})$, that is,

$$\vec{\Omega} \cdot \vec{J}^+(r) = \sum_{m=-1}^{1} \phi_{1,m}^{g+}(\vec{r}) P_{1,m}(\vec{\Omega}) \tag{B45}$$

The scalar adjoint flux $\Phi_g^+(\vec{r})$ as well as the term $\vec{\Omega} \cdot \vec{J}_g^+(\vec{r})$ may be simply expressed in terms of the $T_g^{l+}(\vec{r},\vec{\Omega})$. These relations are

$$T_g^{0+}(\vec{r},\vec{\Omega}) = \phi_{0,0}^{g+}(\vec{r})$$

$$= \Phi_g^+(\vec{r}) \tag{B46a}$$

$$T_g^{1+}(\vec{r},\vec{\Omega}) = \vec{\Omega} \cdot \vec{J}^+(\vec{r}) \tag{B46b}$$

The static criticality factor K_{eff} for this adjoint equation is given by

$$K_{eff} = \int \chi^+(\vec{r})d\vec{r} \tag{B47}$$

For the P_1 approximation to the source term of the adjoint equation,

$$4\pi S_g^+(\vec{r},\vec{\Omega})\Big|_{P_1} = S_{0,g}^+(\vec{r}) + \sigma(\vec{r}, g \to g)\Phi_g^+(\vec{r}) + 3\left[S_{1,g}^+(\vec{r}) + \Sigma_{es}^1(\vec{r}, g \to g)\vec{\Omega} \cdot \vec{J}_g^+(\vec{r})\right] \tag{B48}$$

The P_0 transport corrected approximation to the source term of the adjoint equation is given by

$$4\pi S_g^+(\vec{r},\vec{\Omega})\Big|_{P_0(\Sigma_{tr})} = S_{0,g}^+(\vec{r}) + \sigma_{eff}(\vec{r}, g \to g)\Phi_g^+(\vec{\Omega}) \tag{B49}$$

where $\sigma_{eff}(\vec{r}, g \rightarrow g)$ is defined by equation (B33). In addition, $\sigma_g(\vec{r})$ must be replaced by the transport cross section defined in equation (B34).

Again, two types of boundary conditions will be considered at the external boundary of a system. For one type of condition at R on the external surface, the angular adjoint flux is taken as

$$\phi_g^+(\vec{R}, \vec{\Omega}^+) = 0 \tag{B50}$$

Here $\vec{\Omega}^+$ designates the vector $\vec{\Omega}$ directed out of the system. Thus, equation (B50) states that neutrons that leave the system do not contribute to the neutron importance. The mirror reflection condition at the surface of the system takes the form

$$\phi_g^+(\vec{R}, \vec{\Omega}^+) = \phi_g^+(\vec{R}, \vec{\Omega}^-) \tag{B51}$$

As for the flux equation, a Lambert reflection condition as well as mixed boundary conditions are also possible. In addition, for planar systems, periodic boundary conditions may also be applied.

Equation (B37) can be cast into the form of equation (B1) if

$$\vec{\omega} = -\vec{\Omega} \tag{B52}$$

Then equation (B37) can be written as

$$\vec{\omega} \cdot \vec{\nabla}\phi_g^+(\vec{r}, -\vec{\omega}) + \sigma_g(\vec{r})\phi_g^+(\vec{r}, -\vec{\omega}) = S_g^+(\vec{r}, -\vec{\omega}) \qquad g = NG, NG-1, \ldots, 1$$

This equation now has the same structure as equation (B1). Also, note that the order in which the groups are solved is now reversed from thermal to fast rather than from fast to thermal as for the flux case. This substitution is now made in all the adjoint equations which involve an $\vec{\Omega}$. The important conclusion is reached that finite difference equations need be obtained for equation (B1) only. The adjoint fluxes may be solved for by the same difference equations if the following differences are noted: (1) the groups are solved in reverse order, (2) the source term is computed according to equation (B39), and (3) the angular fluxes will be given in inverted order with respect to $\vec{\Omega}$.

Discrete S_n Finite Difference Equations

Equation (B1) can be specialized for the three one-dimensional geometries. For slab geometry, this equation becomes

$$\mu \frac{\partial N_g(x,\mu)}{\partial x} + \sigma_g(x) N_g(x,\mu) = S_g(x,\mu) \qquad -1 \leq \mu \leq 1 \tag{B53a}$$

where

$$N_g(x,\mu) = 4\pi\phi_g(\vec{r},\vec{\Omega}) \tag{B53b}$$

$$S_g(x,\mu) = 4\pi S_g(\vec{r},\vec{\Omega}) \tag{B53c}$$

$$\sigma_g(x) = \sigma_g(\vec{r}) \tag{B53d}$$

Here x is the spatial coordinate, and μ is the cosine of the angle between $\vec{\Omega}$ and the x-axis. For spherical geometry, equation (B1) becomes

$$\frac{\mu}{r^2}\frac{\partial}{\partial r}\left[r^2 N_g(r,\mu)\right] + \frac{1}{r}\frac{\partial}{\partial \mu}\left[(1-\mu^2)N_g(r,\mu)\right]$$

$$+ \sigma_g(r) N_g(r,\mu) = S_g(r,\mu) \qquad -1 \leq \mu \leq 1 \tag{B54a}$$

where

$$N_g(r,\mu) = 4\pi\phi_g(\vec{r},\vec{\Omega}) \tag{B54b}$$

$$S_g(r,\mu) = 4\pi S_g(\vec{r},\vec{\Omega}) \tag{B54c}$$

$$\sigma_g(r) = \sigma_g(\vec{r}) \tag{B54d}$$

Here r is the spatial coordinate, and μ is the cosine of the angle between $\vec{\Omega}$ and the r-axis. For cylindrical geometry, equation (B1) reduces to

$$\frac{\sin\theta\cos\varphi}{r}\frac{\partial}{\partial r}\left[r N_g(r,\theta,\varphi)\right] - \frac{1}{r}\frac{\partial}{\partial \varphi}\left[\sin\theta\sin\varphi N_g(r,\theta,\varphi)\right]$$

$$+ \sigma_g(r) N_g(r,\theta,\varphi) = S_g(r,\theta,\varphi) \qquad 0 \leq \theta \leq \frac{\pi}{2};\ 0 \leq \varphi \leq \pi \tag{B55a}$$

where

$$N_g(r,\theta,\varphi) = 4\pi\phi_g(\vec{r},\vec{\Omega}) \tag{B55b}$$

$$S_g(r,\theta,\varphi) = 4\pi S_g(\vec{r},\vec{\Omega}) \tag{B55c}$$

$$\sigma_g(r) = \sigma_g(\vec{r}) \tag{B55d}$$

Here θ is the polar angle between $\vec{\Omega}$ and the Z-axis, φ is the azimuthal angle between the projection of Ω on the X-Y plane and the X-axis, r is the spatial position coordinate in a plane perpendicular to the Z-axis. If we so define the quantities μ and η that

$$\mu = \sin\theta\cos\varphi \tag{B56a}$$

$$\eta = \sin\theta\sin\varphi \tag{B56b}$$

then equation (B55a) may be put into the following convenient form:

$$\frac{\mu}{r}\frac{\partial}{\partial r}\left[rN_g(r,\mu)\right] - \frac{1}{r}\frac{\partial}{\partial\varphi}\left[\eta N_g(r,\mu)\right] + \sigma_g(r)N_g(r,\mu) = S_g(r,\mu) \qquad -1 \le \mu \le 1 \tag{B57a}$$

where

$$N_g(r,\mu) \equiv N_g(r,\theta,\varphi) \tag{B57b}$$

$$S_g(r,\mu) \equiv S_g(r,\theta,\varphi) \tag{B57c}$$

If the techniques described by Carlson (ref 4) are followed, it can be shown that the finite difference form of equations (B53a), (B54a), and (B57a) is given, with a proper definition of terms, by

$$\mu_{\bar{m}}\left(A_{i+1}N_{i+1,\bar{m}} - A_iN_{i,\bar{m}}\right) + \frac{A_{i+1} - A_i}{2W_m}\left(\alpha_{m+1}N_{\bar{i},m+1} - \alpha_mN_{\bar{i},m}\right)$$

$$+ \sigma_{\bar{i}}N_{\bar{i},\bar{m}}V_i = S_{\bar{i},\bar{m}}V_i \tag{B58}$$

This equation is essentially the conservation equation for the phase space volume element. Indexes i and i + 1 refer to the edges of the spatial volume element while $\bar{i}$ refers to the midpoint value; similarly, indexes m and m + 1 refer to the edges of the angular volume element while $\bar{m}$ refers to the midpoint value. These relations are shown in sketch (a). The A_{i+1} and A_i are area elements while V_i is the volume element. For the three one-dimensional geometries, these quantities are given in the following table:

Geometry	Coordinate	Area		Volume element, V_i
		A_{i+1}	A_i	
Slab	x	1.0	1.0	$x_{i+1} - x_i$
Cylinder	r	$2\pi r_{i+1}$	$2\pi r_i$	$\pi\left(r_{i+1}^2 - r_i^2\right)$
Sphere	r	$4\pi r_{i+1}^2$	$4\pi r_i^2$	$\frac{4\pi}{3}\left(r_{i+1}^3 - r_i^3\right)$

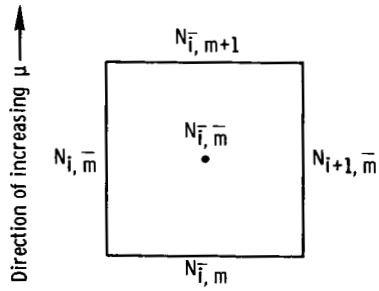

(a) μ-x (or r) phase volume element.

The $\mu_{\bar{m}}$ are essentially S_n quadrature coefficients with the W_m being the associated weights. The quantities α_{m+1} and α_m are related to the $\mu_{\bar{m}}$ and W_m as will be shown. Also $\sigma_{\bar{i}}$ is the total cross section for the i^{th} spatial interval while $S_{\bar{i}, \bar{m}}$ is the angular source for the i^{th} spatial interval and m^{th} angular interval.

The S_n quadrature coefficients in the Gaussian set satisfy a number of conditions, the most important ones are (ref. 4)

$$\sum_m W_m = 1.0 \tag{B59a}$$

$$\sum_m W_m \mu_{\bar{m}} = 0 \tag{B59b}$$

$$\sum_m W_m \mu_{\bar{m}}^2 = \frac{1}{3} \tag{B59c}$$

The first relation, equation (B59a), represents solid angle normalization. The second relation given by equation (B59b) indicates symmetry about $\mu = 0$ and with $\mu = 0$ specifically excluded. The third relation is the so-called diffusion theory condition. Various quadrature sets may be constructed that satisfy the three given conditions. If a double-P quadrature set is used, then an additional condition is satisfied:

$$\sum_m W_m \left|\mu_{\bar{m}}\right| = \frac{1}{2} \tag{B60}$$

In reference 4, Carlson gives considerable detail concerning the construction of quadrature sets for the discrete S_n method.

For a given S_n order n, there will be n equations for slab geometry, n + 1 equations for spherical geometry, and n(n + 4)/4 equations for cylindrical geometry. For

the sphere, there will be n directions with weight while for the cylinder $n(n+2)/4$ directions have weight. The directions without weight are called starting directions and are obtained for the sphere and cylinder by zeroing the angular redistribution terms in the nonconservative forms of equations (B54a) and (B55a). The finite difference form of these starting equations is imbedded in equation (B58).

The coefficients α_{m+1} and α_m may be determined if a configuration is so specified that the neutron flow is uniform. This configuration implies that all N are equal to some constant, and that, for each separate cell and angular interval, the net flow is zero. Equation (B58) must correctly describe this particular situation; this can be accomplished if, for this situation, the first term of equation (B58) and the associated curvature term are zero. Therefore,

$$\alpha_{m+1} - \alpha_m = -2W_m\mu_{\overline{m}} \tag{B61}$$

The first and last α in any sequence must be equal to zero because the outer edges of the first and last angular intervals coincide with the singular loci on the unit sphere that do not contribute or remove neutrons in the angular redistribution process. From equation (B61),

$$\alpha_{m+1} = -2(W_m\mu_{\overline{m}} + W_{m-1}\mu_{\overline{m-1}} + \ldots) \tag{B62}$$

where the terms extend back to the starting point ($\alpha_1 = W_1 = 0$).

A recursion relation relating the value of the angular flux at the midpoint of the phase cell to the value of the fluxes at two adjacent edges of the cell can be obtained using various model representation of the five fluxes in equation (B58). One of these representations is the diamond-spatial - diamond-angular model where for $\mu_{\overline{m}}$ positive

$$N_{i+1,\overline{m}} = 2N_{\overline{i},\overline{m}} - N_{i,\overline{m}} \tag{B63a}$$

$$N_{\overline{i},m+1} = 2N_{\overline{i},\overline{m}} - N_{\overline{i},m} \tag{B63b}$$

Substitution of these two equations into equation (B58) yields the desired diamond-spatial - diamond-angular model recursion relation:

$$N_{\overline{i},\overline{m}} = \frac{2|\mu_{\overline{m}}|AN_{i,\overline{m}} + 2\left(\frac{\alpha}{W}\right)_m N_{\overline{i},m} + S_{\overline{i},\overline{m}}V_i}{2|\mu_{\overline{m}}|A + 2\left(\frac{\alpha}{W}\right)_m + \sigma_{\overline{i}}V_i} \tag{B64}$$

The quantity A is simply the average of A_{i+1} and A_i for the i^{th} spatial interval. The parameter $(\alpha/W)_m$ is related to α_{m+1} and α_m by the expression

$$\left(\frac{\alpha}{W}\right)_m = \frac{A_{i+1} - A_i}{4W_m}(\alpha_{m+1} + \alpha_m) \tag{B65a}$$

the parameter $(\alpha/W)_m$ is conveniently computed by

$$\left.\begin{aligned} 2\left(\frac{\alpha}{W}\right)_m &= \frac{1}{W_m}\left\{\left[(W\mu)_m + (W\mu)_{m-1}\right](A_i - A_{i+1}) + W_{m-1}\left[2\left(\frac{\alpha}{W}\right)_{m-1}\right]\right\} \quad \text{for } W_m \neq 0 \\ \text{and} \\ 2\left(\frac{\alpha}{W}\right)_m &= 0 \quad \text{for } W_m = 0 \end{aligned}\right\} \tag{B65b}$$

From equation (B64), the fact is deduced that $N_{\bar{i},\bar{m}}$ will always be positive provided that the source term $S_{\bar{i},\bar{m}}$ and the total cross section $\sigma_{\bar{i}}$ for the given phase cell are positive. However, use of equation (B63a) and/or equation (B63b) may lead to negative values for the angular fluxes used as input to the next phase space cell. Flux fix-up rules to prevent negative values of the angular flux will be presented later.

Equation (B64) is used for sweeps from i to $i + 1$ and m to $m + 1$ that occur for positive values of $\mu_{\bar{m}}$. For negative values of $\mu_{\bar{m}}$, the sweeps will be from $i + 1$ to i and m to $m + 1$. However, equation (B64) will still apply if $N_{i+1,\bar{m}}$ is replaced by $N_{i,\bar{m}}$ and $N_{i,\bar{m}}$ is replaced by $N_{i+1,\bar{m}}$. The same considerations apply for equation (B63a). The starting equation for spherical or cylindrical geometry is properly imbedded in equation (B64); setting $(\alpha/W)_m$ equal to zero accomplishes this. For the starting equation, $N_{\bar{i},m+1}$ is set equal to $N_{\bar{i},\bar{m}}$ instead of using equation (B63b).

For the step-spatial - step-angular model, the values of $N_{i+1,\bar{m}}$ and $N_{\bar{i},m+1}$ are given by

$$N_{i+1,\bar{m}} = N_{\bar{i},\bar{m}} \tag{B66a}$$

$$N_{\bar{i},m+1} = N_{\bar{i},\bar{m}} \tag{B66b}$$

when $\mu_{\bar{m}}$ is positive. Substitution of these two equations into equation (B58) yields the desired step-spatial - step-angular model recursion relation:

$$N_{\bar{i},\bar{m}} = \frac{|\mu_{\bar{m}}|A_i N_{i,\bar{m}} + \left[\left(\frac{\alpha}{W}\right)_m + \frac{(A_{i+1} - A_i)}{2}|\mu_{\bar{m}}|\right] N_{\bar{i},m} + S_{\bar{i},\bar{m}} V_i}{|\mu_{\bar{m}}|A_i + \left[\left(\frac{\alpha}{W}\right)_m + \frac{(A_{i+1} - A_i)}{2}|\mu_{\bar{m}}|\right] + \sigma_{\bar{i}} V_i} \tag{B67}$$

From equations (B66a), (B66b), and (B67), $N_{\bar{i},\bar{m}}$, $N_{i+1,\bar{m}}$, and $N_{\bar{i},m+1}$ will always be positive if $S_{\bar{i},\bar{m}}$ and $\sigma_{\bar{i}}$ do not change the intrinsic positiveness of the numerator and the denominator of equation (B67).

Equation (B67) is used for sweeps from i to i + 1 and from m to m + 1 that occur when $\mu_{\bar{m}}$ is positive. For negative values of $\mu_{\bar{m}}$, the sweeps will be from i + 1 to i and from m to m + 1. However, equation (B67) applies if $N_{i,\bar{m}}$, $N_{i+1,\bar{m}}$, A_{i+1}, and A_i are replaced by $N_{i+1,\bar{m}}$, $N_{i,\bar{m}}$, A_i, and A_{i+1}, respectively. If $(\alpha/W)_m$ is set equal to zero, the step model starting equation for spherical and cylindrical geometries is properly imbedded in equation (B67).

In addition to the diamond and step models previously discussed, mixed models may be constructed. One of these models uses a diamond spatial and a step angular representation. For this model, the values of $N_{i+1,\bar{m}}$ and $N_{\bar{i},m+1}$ are given by

$$N_{i+1,\bar{m}} = 2N_{\bar{i},\bar{m}} - N_{i,\bar{m}} \tag{B68a}$$

$$N_{\bar{i},m+1} = N_{\bar{i},\bar{m}} \tag{B68b}$$

for $\mu_{\bar{m}}$ positive. Substitution of these two equations into equation (B58) yields the diamond-spatial - step-angular model:

$$N_{\bar{i},\bar{m}} = \frac{2|\mu_{\bar{m}}|AN_{i,\bar{m}} + \left[\left(\frac{\alpha}{W}\right)_m + \frac{(A_{i+1} - A_i)}{2}|\mu_{\bar{m}}|\right] N_{\bar{i},m} + S_{\bar{i},\bar{m}} V_i}{2|\mu_{\bar{m}}|A + \left[\left(\frac{\alpha}{W}\right)_m + \frac{(A_{i+1} - A_i)}{2}|\mu_{\bar{m}}|\right] + \sigma_{\bar{i}} V_i} \tag{B69}$$

Equation (B69) will always be positive if $S_{\bar{i},\bar{m}}$ and $\sigma_{\bar{i}}$ do not become negatively large and thus change the inherent positiveness of the numerator and the denominator of equation (B69). However, $N_{i+1,\bar{m}}$ in equation (B68a) may give a negative value for use in the next phase space cell.

Equation (B69) is used for sweeps from i to i + 1 and from m to m + 1 that occur when $\mu_{\bar{m}}$ is positive. For negative values of $\mu_{\bar{m}}$, the sweeps will be from i + 1

to i and from m to m + 1. However, equation (B69) applies if $N_{i,\overline{m}}$, $N_{i+1,\overline{m}}$, A_{i+1}, and A_i are replaced by $N_{i+1,\overline{m}}$, $N_{i,\overline{m}}$, A_i, and A_{i+1}, respectively. The starting equation is obtained from equation (B69) if the second term of both the numerator and the denominator are set to zero.

Another type of mixed model has also been considered. This type uses a step-spatial and a diamond-angular representation. For this model the values of $N_{i+1,\overline{m}}$ and $N_{\overline{i},m+1}$ are given by

$$N_{i+1,\overline{m}} = N_{\overline{i},\overline{m}} \tag{B70a}$$

$$N_{\overline{i},m+1} = 2N_{\overline{i},\overline{m}} - N_{\overline{i},m} \tag{B70b}$$

for $\mu_{\overline{m}}$ positive. Substitution of these two equations into equation (B58) yields the step-spatial - diamond-angular model:

$$N_{\overline{i},\overline{m}} = \frac{|\mu_{\overline{m}}|A_i N_{i,\overline{m}} + 2\left(\frac{\alpha}{W}\right)_m N_{\overline{i},m} + S_{\overline{i},\overline{m}} V_i}{|\mu_{\overline{m}}|A_i + 2\left(\frac{\alpha}{W}\right)_m + \sigma_{\overline{i}} V_i} \tag{B71}$$

Equation (B71) will always be positive if $S_{\overline{i},\overline{m}}$ and $\sigma_{\overline{i}}$ do not become negatively large and thus change the inherent positiveness of the numerator and the denominator. Equation (B70b), however, may give a negative value for $N_{\overline{i},m+1}$ for use in the next phase cell.

Equation (B71) is used for sweeps from i to i + 1 and from m to m + 1 for $\mu_{\overline{m}}$ positive. For negative values of $\mu_{\overline{m}}$, the sweeps will be from i + 1 to i and from m to m + 1. Equation (B71) applies, however, if $N_{i,\overline{m}}$, $N_{i+1,\overline{m}}$, A_{i+1}, and A_i are replaced by $N_{i+1,\overline{m}}$, $N_{i,\overline{m}}$, A_i, and A_{i+1}, respectively. The starting equation for this step-spatial - diamond-angular model is given by

$$N_{\overline{i},0} = \frac{|\mu_0|AN_{i+1,0} + S_{\overline{i},0} V_i}{|\mu_0|A + \sigma_{\overline{i}} V_i} \tag{B72}$$

where μ_0 is the initial unweighted direction. For this starting equation, $N_{i,0} = N_{\overline{i},0}$, and $N_{\overline{i},m} = N_{\overline{i},0}$.

Of the four recursion relations discussed, the diamond-spatial and diamond-angular representation appears to be the most accurate and useful. Since negative values of

$N_{i+1,\bar{m}}$, $N_{i,\bar{m}}$, and $N_{\bar{i},m+1}$ can be generated by equation (B63) used in conjunction with equation (B64), provisions must be made to eliminate these negative values. The negative value is zeroed, and equation (B58) is adjusted to preserve the neutron balance. Flux fix-up equations can be derived on this basis.

If $N_{\bar{i},m+1}$ is negative by equation (B63b), then it is set equal to zero. With this quantity equal to zero, equation (B58) will now yield the following result for $N_{\bar{i},\bar{m}}$ to preserve the neutron balance:

$$N_{\bar{i},\bar{m}} = \frac{2|\mu_{\bar{m}}|AN_{i,\bar{m}} + \left[\left(\frac{\alpha}{W}\right)_m + \frac{(A_{i+1} - A_i)}{2}|\mu_{\bar{m}}|\right]N_{\bar{i},m} + S_{\bar{i},\bar{m}}V_i}{2|\mu_{\bar{m}}|A_{i+1} + \sigma_{\bar{i}}V_i} \tag{B73a}$$

also,

$$N_{i+1,\bar{m}} = 2N_{\bar{i},\bar{m}} - N_{i,\bar{m}} \tag{B73b}$$

$$N_{\bar{i},m+1} = 0 \tag{B73c}$$

Equation (B73a) applies for $\mu_{\bar{m}}$ positive. If $\mu_{\bar{m}}$ is negative, then $N_{i,\bar{m}}$, $N_{i+1,\bar{m}}$, A_i, and A_{i+1} are replaced by $N_{i+1,\bar{m}}$, $N_{i,\bar{m}}$, A_{i+1}, and A_i, respectively.

If $\mu_{\bar{m}}$ is positive and $N_{i+1,\bar{m}}$, as computed by equation (B63a), is negative, then $N_{i+1,\bar{m}}$ is set to zero. With this quantity equal to zero, equation (B58) will now yield the following result for $N_{\bar{i},\bar{m}}$ to preserve the neutron balance:

$$N_{\bar{i},\bar{m}} = \frac{\mu_{\bar{m}}A_iN_{i,\bar{m}} + 2\left(\frac{\alpha}{W}\right)_m N_{\bar{i},m} + S_{\bar{i},\bar{m}}V_i}{\mu_{\bar{m}}A_i - \mu_{\bar{m}}A_{i+1} + 2\left(\frac{\alpha}{W}\right)_m + \sigma_{\bar{i}}V_i} \tag{B74a}$$

also,

$$N_{i+1,\bar{m}} = 0 \tag{B74b}$$

$$N_{\bar{i},m+1} = 2N_{\bar{i},\bar{m}} - N_{\bar{i},m} \tag{B74c}$$

If $\mu_{\bar{m}}$ is negative and $N_{i,\bar{m}}$ computed by an extrapolation formula similar to equation (B63a) is negative, then $N_{i,\bar{m}}$ is set to zero. With this quantity equal to zero,

equation (B58) will now yield the following result for $N_{\bar{i},\bar{m}}$ to preserve the neutron balance:

$$N_{\bar{i},\bar{m}} = \frac{-\mu_{\bar{m}} A_{i+1} N_{i+1,\bar{m}} + 2\left(\frac{\alpha}{W}\right)_m N_{\bar{i},m} + S_{\bar{i},\bar{m}} V_i}{-\mu_{\bar{m}} A_{i+1} + \mu_{\bar{m}} A_i + 2\left(\frac{\alpha}{W}\right)_m + \sigma_{\bar{i}} V_i} \tag{B75a}$$

also,

$$N_{i,\bar{m}} = 0 \tag{B75b}$$

$$N_{\bar{i},m+1} = 2N_{\bar{i},\bar{m}} - N_{\bar{i},m} \tag{B75c}$$

If $\mu_{\bar{m}}$ is positive and both $N_{\bar{i},m+1}$ and $N_{i+1,\bar{m}}$ are negative as computed by equations (B63a) and (B63b), then $N_{\bar{i},m+1}$ and $N_{i+1,\bar{m}}$ are set equal to zero. With both of these quantities zeroed, equation (B58) will now yield the following result for $N_{\bar{i},\bar{m}}$ to preserve the neutron balance:

$$N_{\bar{i},\bar{m}} = \frac{\mu_{\bar{m}} A_i N_{i,\bar{m}} + \left[\left(\frac{\alpha}{W}\right)_m + \frac{(A_{i+1} - A_i)}{2}\mu_{\bar{m}}\right] N_{\bar{i},m} + S_{\bar{i},\bar{m}} V_i}{\sigma_{\bar{i}} V_i} \tag{B76a}$$

also,

$$N_{i+1,\bar{m}} = 0 \tag{B76b}$$

$$N_{\bar{i},m+1} = 0 \tag{B76c}$$

Note that in equation (B76a) $\sigma_{\bar{i}}$ must not be zero.

If $\mu_{\bar{m}}$ is negative and both $N_{\bar{i},m+1}$ and $N_{i,\bar{m}}$ are negative as computed by equations (B63a) and (B63b), then both $N_{\bar{i},m+1}$ and $N_{i,\bar{m}}$ are set equal to zero. With both of these quantities zeroed, equation (B58) will now yield the following result for $N_{\bar{i},\bar{m}}$ to preserve the neutron balance:

$$N_{\bar{i},\bar{m}} = \frac{-\mu_{\bar{m}} A_{i+1} N_{i+1,\bar{m}} + \left[\left(\frac{\alpha}{W}\right)_m + \frac{(A_{i+1} - A_i)}{2}\mu_{\bar{m}}\right] N_{\bar{i},m} + S_{\bar{i},\bar{m}} V_i}{\sigma_{\bar{i}} V_i} \qquad \text{(B77a)}$$

also,

$$N_{i,\bar{m}} = 0 \qquad \text{(B77b)}$$

$$N_{\bar{i},m+1} = 0 \qquad \text{(B77c)}$$

Note that in equation (B77a) $\sigma_{\bar{i}}$ must not be zero.

Solution Techniques for S_n Equations

The finite difference form of equation (B1) and either equation (B64) or (B67) is solved for the real flux starting with the highest energy group (group 1). If no fixed source is present, a fission neutron distribution is assumed (eq. (B25)). This fission distribution is normalized to a given number of neutrons. The source for the group is computed, and the scalar flux is obtained as the solution to an inhomogeneous problem. The solution proceeds to the next group in a similar manner. Finally, when all groups have been computed for the scalar flux, a new fission neutron distribution is computed. The process is repeated until the input fission neutron distribution satisfy a convergence criterion. Each cycle of the calculation is referred to as an outer iteration.

The techniques of overrelaxation may be applied to accelerate the convergence of the fission neutron distribution. If upscattering is present, scaling of the fluxes in those groups to which neutrons upscatter improves the convergence of the fission neutron distribution. This scaling of the fluxes ensures that the neutron conservation criterion is satisfied.

The static criticality factor K_{eff} can be determined after each outer iteration. After convergence has been reached for a given set of system parameters, a parameter may be so varied that a specified condition may be achieved. This parameter may be the thickness of a region, the atoms per cubic centimeter of an element in a given region, the height of a cylindrical system, or some other variable chosen as the eigenvalue of the given system.

The solution for a given group g of equation (B64), or the other equations that correspond to various model representations, for the scalar flux and higher moments of the surface spherical harmonics representation of the group angular flux is obtained by per-

forming inner iterations. The equations corresponding to a given S_n order and geometry are solved in a follow-the-neutron scheme. Boundary conditions are applied at the right boundary of the system, and the equations are solved recursively for negative values of μ_m^- and for decreasing values of x (or r) until the origin is reached. After solutions for all the negative values of μ_m^- are completed, boundary conditions are applied at the origin, and the equations are solved recursively for positive values of μ_m^- for increasing values of x (or r). A complete cycle of calculation for all values of μ_m^- is called an inner iteration.

After a complete inner iteration, the within group part of the source is updated, and the calculation is repeated. Both acceleration and scaling techniques are employed to speed the convergence process. Inner iterations are continued until the pointwise scalar fluxes for the group are converged to specified criteria.

REFERENCES

1. Fieno, Daniel: Consistent P1 Analysis of Aqueous Uranium-235 Critical Assemblies. NASA TN D-1102, 1961.

2. Shook, Donald F.; and Bogart, Donald: Effective Resonance Integrals of Separated Tungsten Isotopes. NASA TN D-3957, 1967.

3. Carlson, Bengt G.: The Numerical Theory of Neutron Transport, in Methods in Computational Physics (Alder, Berni; Fernbach, Sidney; and Rotenberg, Manuel, eds.), Academic Press, 1963, pp. 1-42.

4. Joanou, G. D.; and Dudek, J. S.: GAM-II. A B_3 Code for the Calculation of Fast-Neutron Spectra and Associated Multigroup Constants. Rep. No. GA-4265, General Atomic Div., General Dynamics Corp., Sept. 16, 1963.

5. Joanou, G. D.; Smith, C. V.; and Vieweg, H. A.: Gather-II - An IBM-7090 Fortran-II Program for the Computation of Thermal-Neutron Spectra and Associated Multigroup Cross Sections. Rep. No. GA-4132, General Dynamics Corp., July 8, 1963.

6. Nelkin, Mark: Scattering of Slow Neutrons by Water. Phys. Rev., vol. 119, no. 2, July 15, 1960, pp. 741-746.

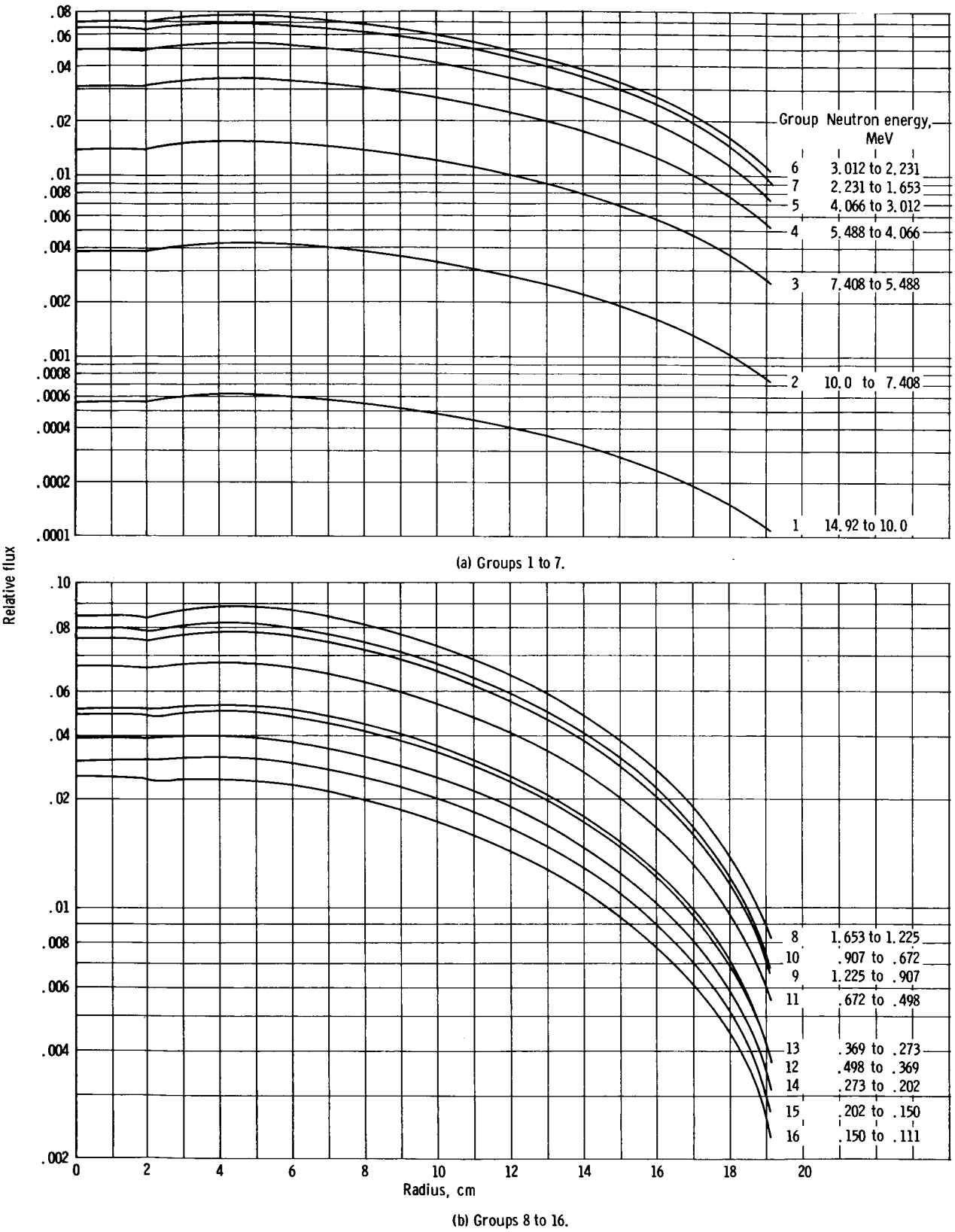

Figure 1. - Relative real flux for ZPR-1 with 0.0889 centimeter (35 mil) cadmium shell between 1.86024 to 1.9491 centimeter from the center. S_4 calculation using the diamond model, P_1 elastic scattering, and 65 mesh intervals.

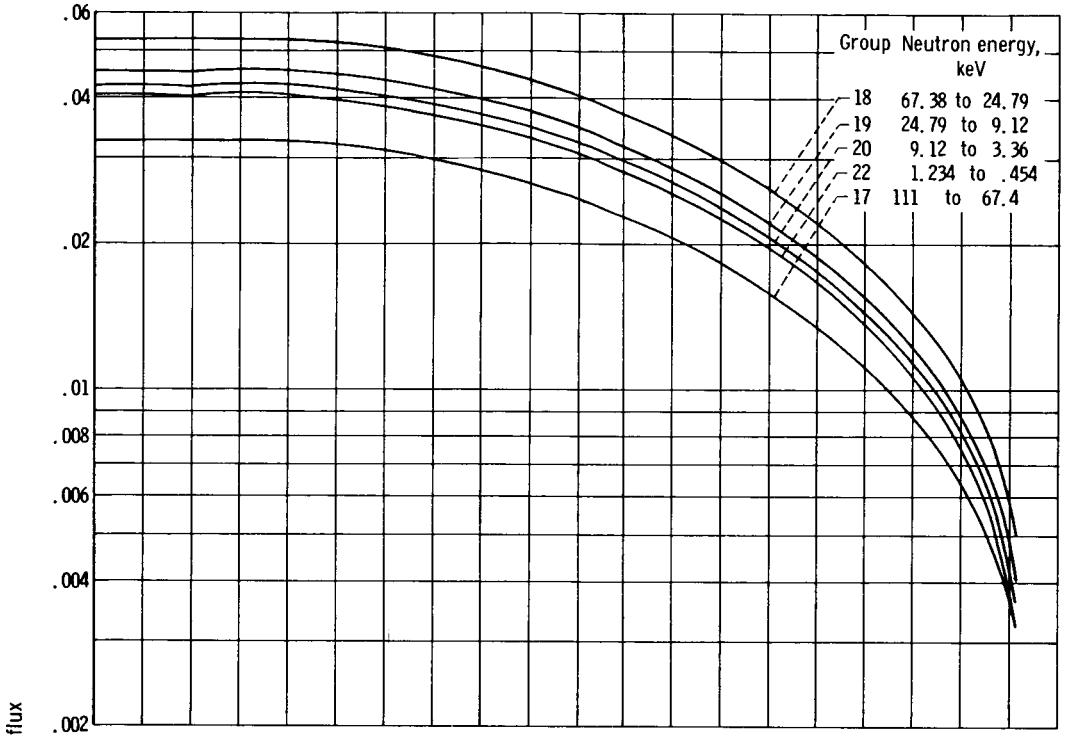

(c) Groups 17 to 20 and 22.

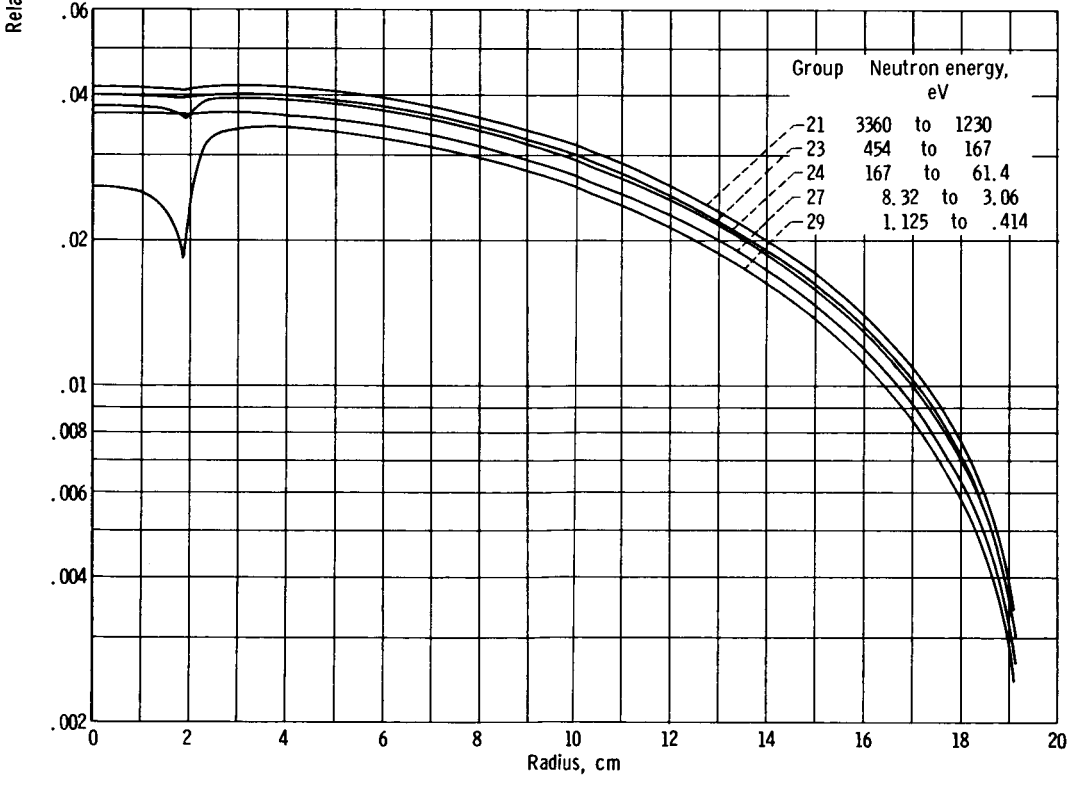

(d) Groups 21, 23, 24, 27, and 29.

Figure 1. - Continued.

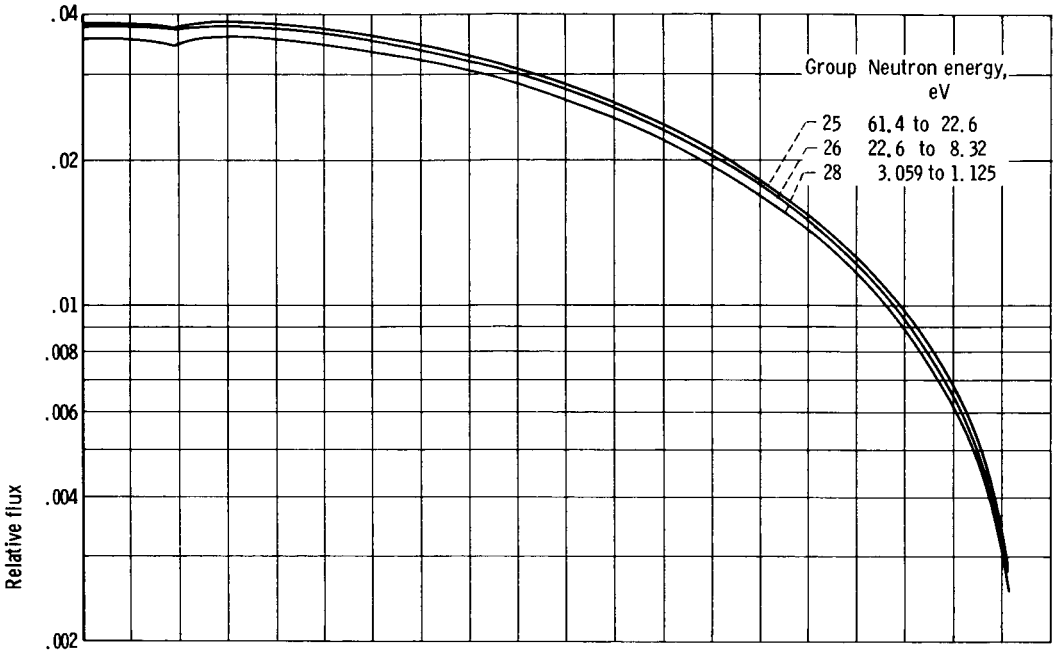

(e) Groups 25, 26, and 28.

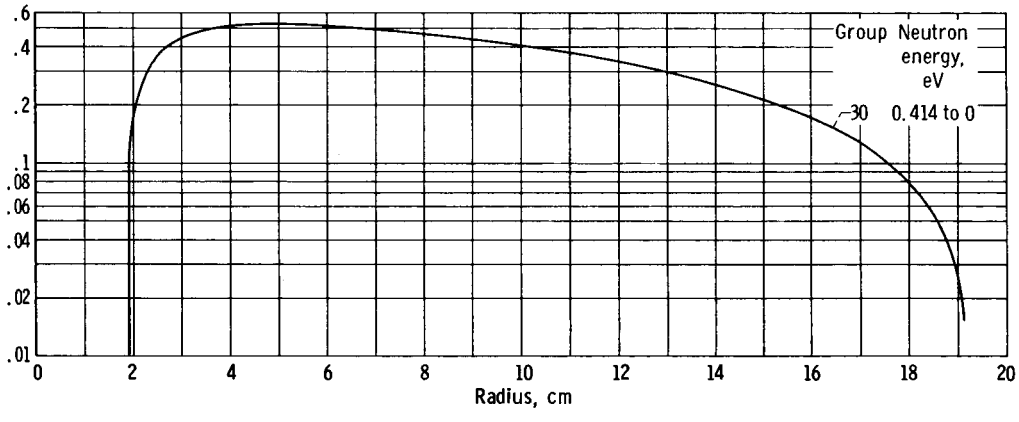

(f) Group 30.

Figure 1. - Concluded.

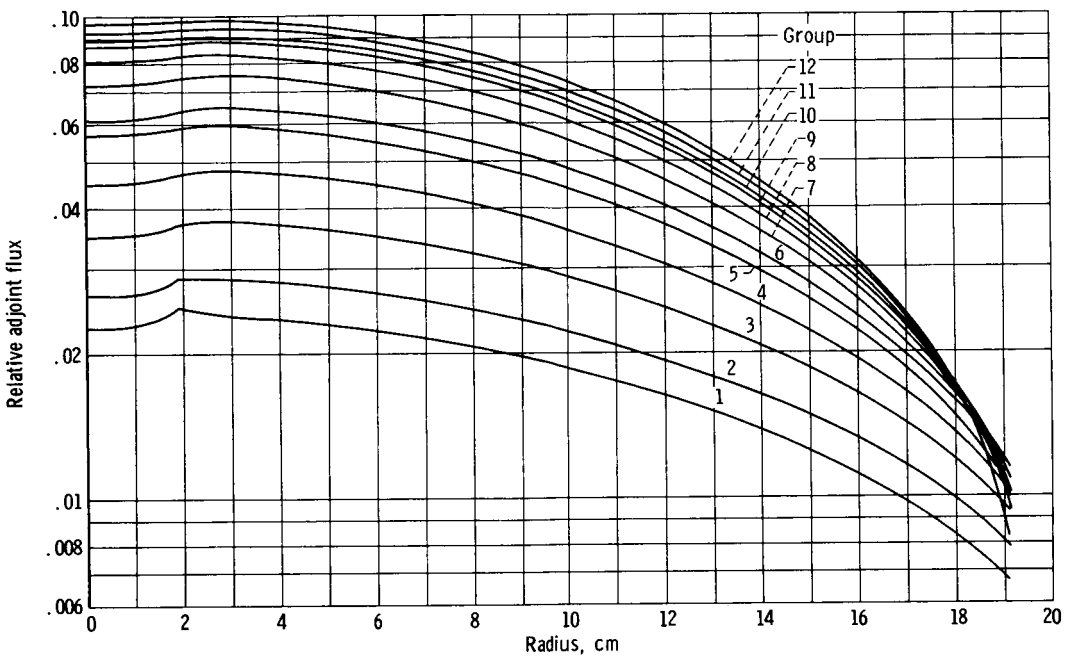

(a) Groups 1 to 12.

Figure 2. - Relative adjoint flux for ZPR-1 with 0.0889-centimeter (35 mil) cadmium shell from 1.86024 to 1.9491 centimeters from center. S_4 calculation using diamond model, P_1 elastic scattering, and 65 mesh intervals.

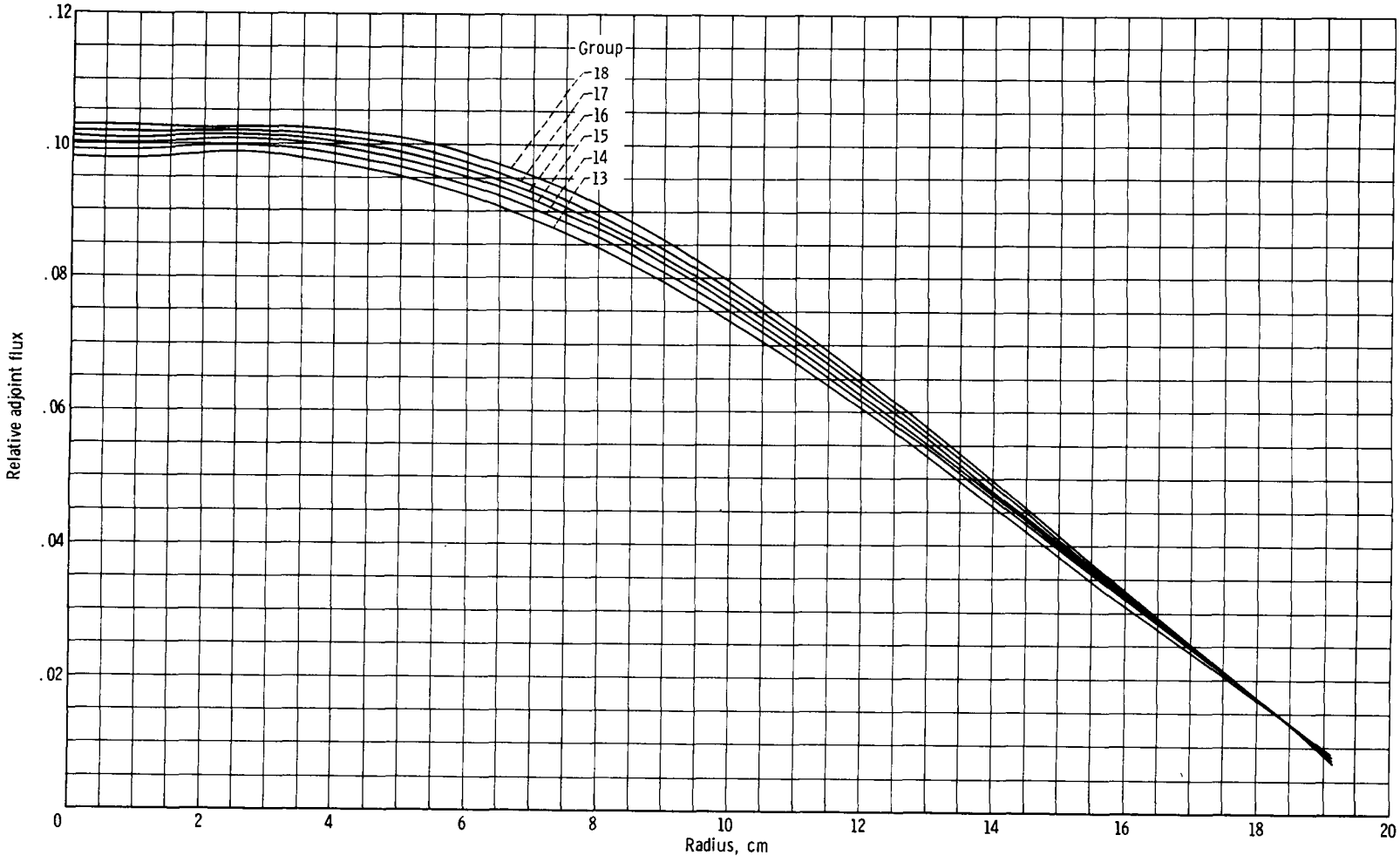

(b) Groups 13 to 18.

Figure 2. - Continued.

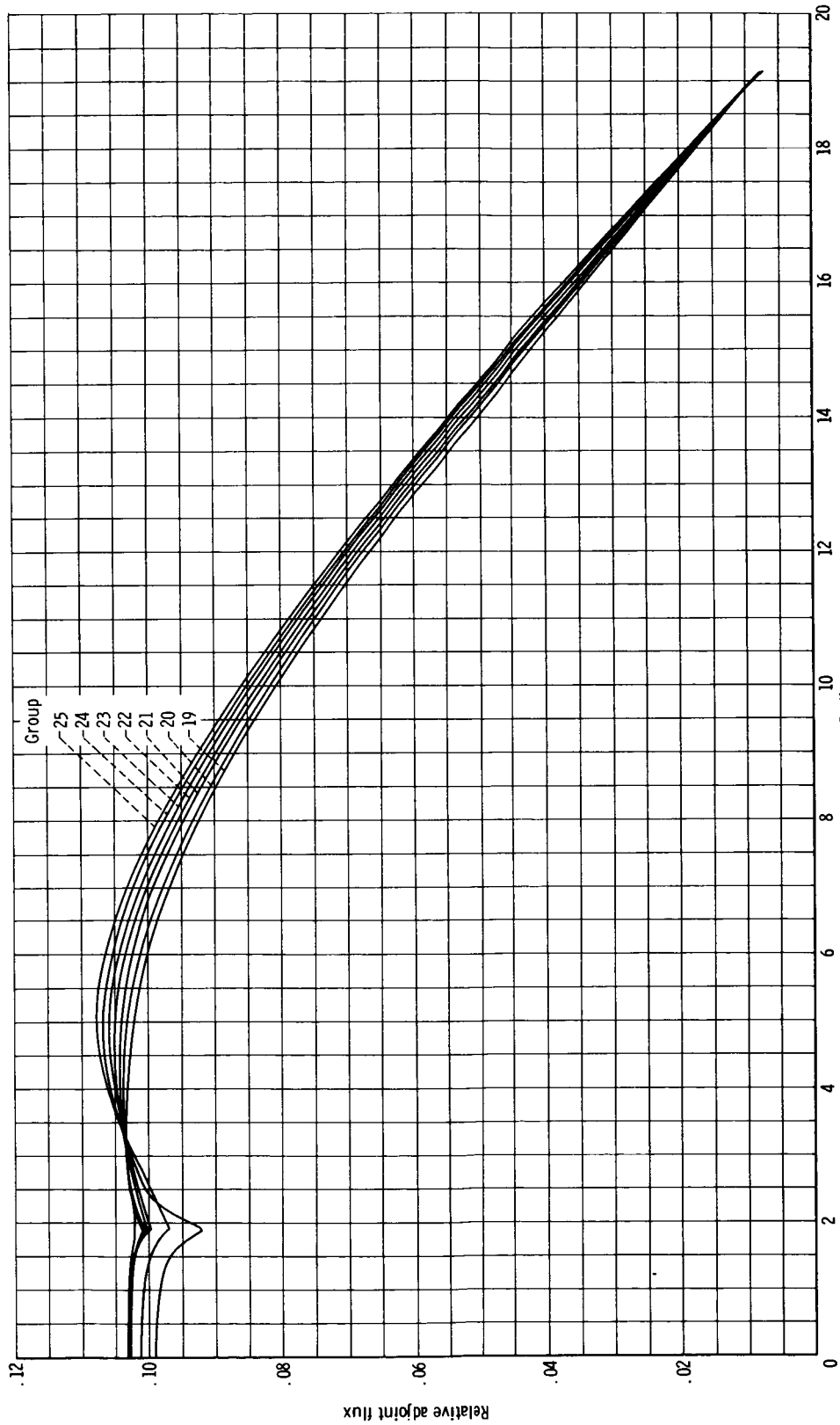

(c) Groups 19 to 25.

Figure 2. - Continued.

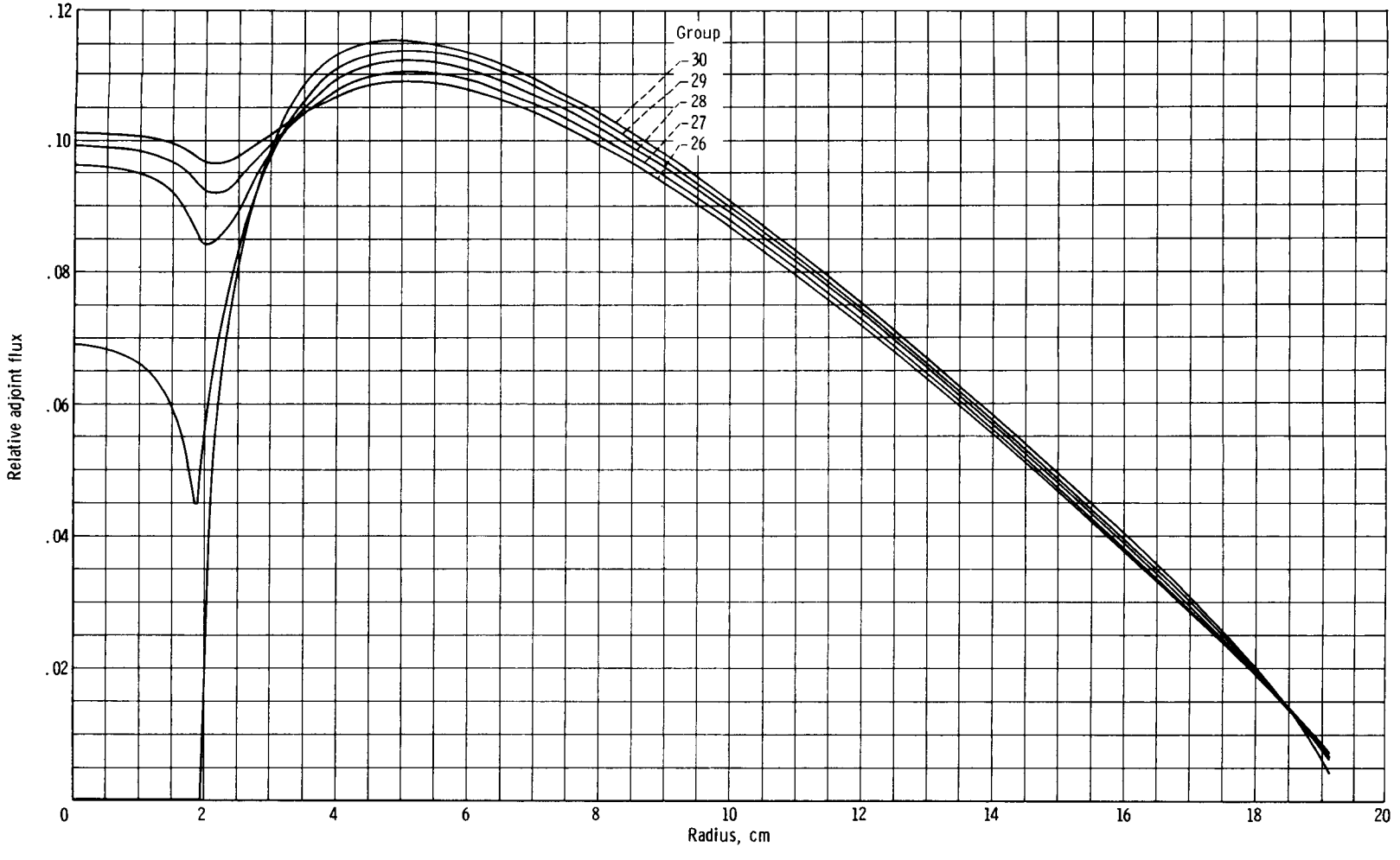

(d) Groups 26 to 30.

Figure 2. - Concluded.

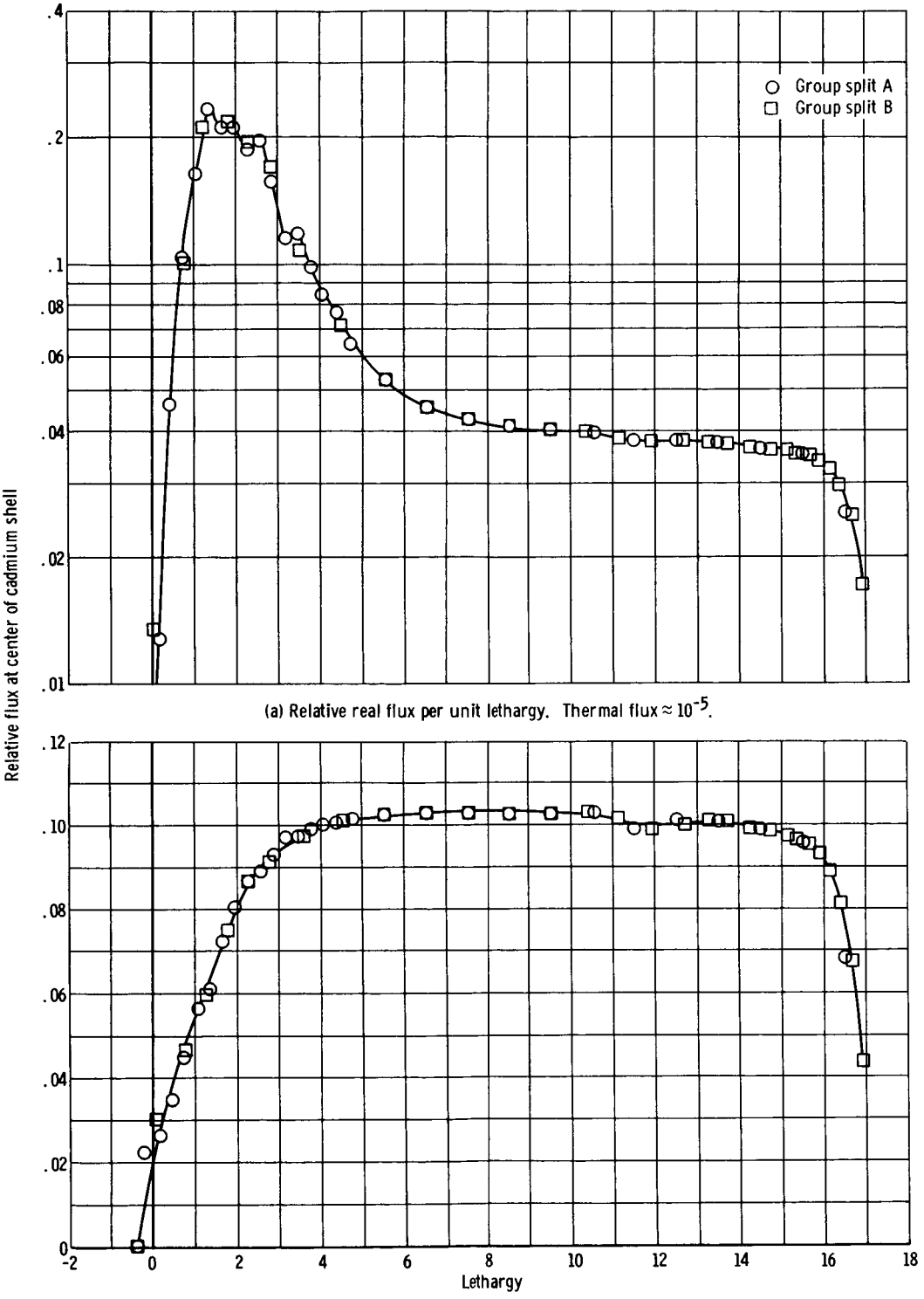

(a) Relative real flux per unit lethargy. Thermal flux $\approx 10^{-5}$.

(b) Relative adjoint flux spectrum. Thermal adjoint flux ≈ 0.

Figure 3. - Relative flux at center of cadmium shell in ZPR-1. S_4 calculation using diamond model, P_1 elastic scattering, and 65 mesh intervals.

TABLE V. - CROSS-SECTION DATA FOR ALUMINUM, CADMIUM, BORON 10, AND URANYL FLUORIDE SALT IN WATER FUEL SOLUTION

[Atom ratio of hydrogen to uranium 235; 500.]

(a) Group split A

ELEMENT 1 AL NGDS 21 NGE 10 NGDST 1 NGDSPI 1 NGUS 1 NSTART 29

GROUP	SIG	SIGSO(G-G)	SIGSI(G-G)	SIGA	ANUSIG	ALPHA	SIGTR
1	1.7087170	0.7394730	1.5818880	0.2081940	0.	-0.	1.1481710
2	1.7934610	0.8023250	1.6769740	0.1377770	0.	-0.	1.2344840
3	2.0184490	0.9841650	1.8156990	0.0565390	0.	-0.	1.4148670
4	2.2548380	1.2108670	2.0780820	0.0180710	0.	-0.	1.5692620
5	2.4911560	1.4771840	2.4109400	0.0056920	0.	-0.	1.6982990
6	2.8676670	2.1030670	3.0698420	0.0011260	0.	-0.	1.8580720
7	3.0613010	2.3130870	3.0541330	0.0005010	0.	-0.	2.1050800
8	3.0624850	2.2645300	2.7180910	0.0003360	0.	-0.	2.2311650
9	3.0713620	2.4557490	2.5861750	0.0003690	0.	-0.	2.3414950
10	4.0374260	3.4428560	3.1031220	0.0005700	0.	-0.	3.0624980
11	3.7616650	3.0598350	2.6184020	0.0006670	0.	-0.	3.0551510
12	3.9920270	3.1555650	2.2919370	0.0010150	0.	-0.	3.5070340
13	4.1943820	3.1747260	2.2346820	0.0010380	0.	-0.	3.6749210
14	3.4719340	2.3913440	1.4372370	0.0013750	0.	-0.	3.3618210
15	5.4150840	3.3666160	2.2466710	0.0032050	0.	-0.	4.9711930
16	4.9770460	4.1368900	1.2974810	0.0046570	0.	-0.	5.2689460
17	6.6909790	6.4499630	0.7518550	0.0022360	0.	-0.	6.6972450
18	5.5118000	5.4677730	0.4398210	0.0070780	0.	-0.	5.3564660
19	0.8633550	0.7827630	0.1331620	0.0030380	0.	-0.	0.8293250
20	2.1692990	2.0628290	0.2536580	0.0052620	0.	-0.	2.1163510
21	1.4110220	1.3085820	0.1985690	0.0009980	0.	-0.	1.3783430
22	1.4113900	1.3085110	0.1991850	0.0013670	0.	-0.	1.3781940
23	1.4122810	1.3082850	0.1998010	0.0022570	0.	-0.	1.3784880
24	1.4137500	1.3083520	0.1999790	0.0037260	0.	-0.	1.3796800
25	1.4161610	1.3083710	0.2001200	0.0061370	0.	-0.	1.3822460
26	1.4201410	1.3090310	0.1993650	0.0101170	0.	-0.	1.3864530
27	1.4267070	1.3087170	0.1997680	0.0166830	0.	-0.	1.3927030
28	1.4375320	1.3086460	0.1998460	0.0275080	0.	-0.	1.4033930
29	1.4552700	1.3109890	0.1967300	0.0452460	0.	-0.	1.4233880
30	1.5946260	1.4100000	0.2041380	0.1846260	-0.	-0.	1.5265800

ELEMENT 2 CD NGDS 22 NGE 15 NGDST 1 NGDSPI 1 NGUS 1 NSTART 29

GROUP	SIG	SIGSO(G-G)	SIGSI(G-G)	SIGA	ANUSIG	ALPHA	SIGTR
1	5.0784820	2.5947130	6.6696210	0.0133990	0.	-0.	2.8552610
2	4.8005270	2.3438830	5.5677520	0.0126740	0.	-0.	2.9456360
3	4.2004560	2.0622520	4.3005490	0.0141460	0.	-0.	2.7649850
4	4.1551190	1.9780250	3.6298450	0.0151690	0.	-0.	2.9450090
5	4.3949870	2.2742630	3.4139520	0.0176780	0.	-0.	3.2598560
6	4.9813020	3.0328780	4.1389340	0.0219960	0.	-0.	3.6142730
7	5.7370550	4.0325600	5.3409260	0.0303030	0.	-0.	3.9625310
8	6.4121950	4.9867980	6.4591000	0.0415160	0.	-0.	4.2698460
9	6.6686280	5.5154420	6.8357210	0.0575780	0.	-0.	4.4167400
10	6.8903070	5.8447920	6.6960760	0.0783030	0.	-0.	4.6823230
11	7.1491190	6.3175020	6.3222480	0.0960430	0.	-0.	5.0752410
12	6.9924200	6.2893100	5.7201090	0.1076960	0.	-0.	5.1419880
13	7.0554640	6.4747960	4.6877310	0.1137080	0.	-0.	5.5423340
14	7.0461430	6.5311180	3.6310350	0.1150000	0.	-0.	5.9136790
15	7.0217340	6.5322800	2.7874590	0.1173620	0.	-0.	6.1888700
16	6.9991740	6.5086170	2.0448620	0.1257460	0.	-0.	6.4330160
17	6.9986920	6.6129810	1.0950320	0.1578460	0.	-0.	6.7124940
18	7.0107100	6.6110390	0.3221830	0.2917460	0.	-0.	6.9497210
19	6.9455700	5.9805990	0.1864480	0.8804170	0.	-0.	6.9339410
20	6.4421660	4.1409120	0.1502980	2.2202350	0.	-0.	6.4137000
21	6.5519190	3.9918970	0.1284360	2.5000000	0.	-0.	6.5419420
22	7.5672790	4.8976890	0.2499010	2.5000000	0.	-0.	7.4873800
23	6.8482510	4.5356810	0.1643060	2.2258140	0.	-0.	6.8455450
24	19.1536319	8.9068331	0.2320480	10.1707180	0.	-0.	19.1037340
25	7.5639880	4.4231990	0.1523670	3.0647220	0.	-0.	7.5288830
26	4.6745080	3.9297260	0.1379150	0.6744800	0.	-0.	4.6531210
27	5.2236890	3.9295070	0.1382090	1.2236620	0.	-0.	5.1999220
28	9.3497180	4.4218580	0.1649580	4.8387670	0.	-0.	9.3107680
29	80.8530941	7.6189880	0.2841480	73.0789948	0.	-0.	80.2500563
30	3055.5466003	17.2365999	-259.9602890	3038.3099976	-0.	-0.	3142.2000122

TABLE V. - Continued. CROSS-SECTION DATA FOR ALUMINUM, CADMIUM, BORON 10, AND URANYL FLUORIDE SALT IN WATER FUEL SOLUTION

[Atom ratio of hydrogen to uranium 235; 500.]

(a) Continued. Group split A

ELEMENT 3 UO2F2 NGDS 29 NGF 30 NGDST 0 NGDSPI 29 NGUS 1 NSTART 29

GROUP	SIG	SIGSO(G-G)	SIGSI(G-G)	SIGA	ANUSIG	ALPHA	SIGTR
1	0.1028220	0.0239230	0.0588920	0.0107940	0.0009930	0.0010407	0.0856900
2	0.1141170	0.0307430	0.0664750	0.0071420	0.0008650	0.0072417	0.0921690
3	0.1414650	0.0436410	0.1012700	0.0035780	0.0005860	0.0274920	0.1036770
4	0.1673600	0.0492390	0.1053990	0.0025170	0.0004790	0.0645644	0.1215240
5	0.2238270	0.0741150	0.1376800	0.0004720	0.0004800	0.1063810	0.1553510
6	0.1985210	0.0460590	0.0910210	0.0001840	0.0004860	0.1352093	0.1477770
7	0.2618340	0.0619550	0.1214780	0.0001860	0.0004680	0.1422628	0.1606040
8	0.3462130	0.1044880	0.1716870	0.0001780	0.0004290	0.1305248	0.2003220
9	0.4309870	0.1216740	0.2127470	0.0001770	0.0004110	0.1084575	0.2251450
10	0.4243410	0.1129320	0.1828090	0.0001750	0.0003900	0.0838867	0.2488040
11	0.4955380	0.1333270	0.2551090	0.0001820	0.0003910	0.0615982	0.2314610
12	0.7371570	0.2504050	0.4464120	0.0001960	0.0004170	0.0435572	0.2738330
13	0.6388330	0.1404880	0.2058090	0.0002090	0.0004340	0.0299650	0.3129310
14	0.7089180	0.1487270	0.2601750	0.0002230	0.0004500	0.0202047	0.3011580
15	0.7806910	0.1600480	0.3014090	0.0002460	0.0004830	0.0134247	0.3089490
16	0.8779750	0.1748240	0.3458030	0.0002750	0.0005280	0.0088240	0.3247530
17	0.9930370	0.2782150	0.5514970	0.0003160	0.0005880	0.0084168	0.3464850
18	1.1771330	0.4954560	1.0566000	0.0003970	0.0007120	0.0060194	0.3880960
19	1.3374690	0.5536730	1.2139830	0.0005360	0.0009140	0.0009289	0.4420850
20	1.4099930	0.5813810	1.2793190	0.0008430	0.0013350	-0.	0.4849630
21	1.4331240	0.5911970	1.2956770	0.0013020	0.0020720	-0.	0.5150930
22	1.4529680	0.5988590	1.3110660	0.0022750	0.0034910	-0.	0.5362640
23	1.4653210	0.6030580	1.3200960	0.0037870	0.0056780	-0.	0.5504180
24	1.4716370	0.6050330	1.3238990	0.0047380	0.0067410	-0.	0.5594720
25	1.4849120	0.6083640	1.3320070	0.0100680	0.0122370	-0.	0.5671240
26	1.4942690	0.6102280	1.3372290	0.0154690	0.0186400	-0.	0.5730710
27	1.5079290	0.6166860	1.3547020	0.0083860	0.0061560	-0.	0.5784710
28	1.5209230	0.6228700	1.3702500	0.0064650	0.0069110	-0.	0.5828800
29	1.5685390	0.6376170	1.4111490	0.0150640	0.0228280	-0.	0.5935950
30	2.9997590	2.9120210	2.0854400	0.0868270	0.1434560	-0.	1.9185340

ELEMENT 4 B-10 NGDS 20 NGF 9 NGDST 2 NGDSPI 2 NGUS 1 NSTART 29

GROUP	SIG	SIGSO(G-G)	SIGSI(G-G)	SIGA	ANUSIG	ALPHA	SIGTR
1	1.4505830	0.7265280	1.7667170	0.1015670	0.	-0.	0.8616760
2	1.4497860	0.7725030	1.8710560	0.0797450	0.	-0.	0.8123230
3	1.4786570	0.8282830	1.9788260	0.0902450	0.	-0.	0.7930910
4	1.6959890	0.9300480	2.1917060	0.1457950	0.	-0.	0.9413550
5	1.8107500	0.8153850	1.8563780	0.1625260	0.	-0.	1.2217900
6	2.1644800	0.8828990	1.8501910	0.2153440	0.	-0.	1.6436660
7	2.0933500	0.7501190	1.3956510	0.3567120	0.	-0.	2.1266410
8	2.0478450	0.7431900	1.3304280	0.2300500	0.	-0.	2.0100020
9	2.4705300	1.0199610	1.8462060	0.2043470	0.	-0.	2.2970510
10	3.2361270	1.3313020	2.2530740	0.3066890	0.	-0.	2.8607610
11	4.1799640	1.7854800	3.0540420	0.5258960	0.	-0.	3.5137430
12	4.7339400	2.0030040	3.5164620	0.6492490	0.	-0.	4.0673110
13	4.7249570	1.8105140	3.0739250	0.8202770	0.	-0.	4.1503500
14	5.0128070	1.8024030	2.9790500	1.0116070	0.	-0.	4.6038150
15	4.9831670	1.6382520	2.6456990	1.3008190	0.	-0.	4.7714540
16	4.7909220	1.3865140	2.2048960	1.6701690	0.	-0.	4.7301590
17	4.7737670	1.6747850	1.3851130	2.2181970	0.	-0.	4.7405480
18	5.2833690	1.7106240	0.6918390	3.2615380	0.	-0.	5.2205580
19	7.6387080	1.7861400	0.9571100	5.2419150	0.	-0.	7.3942750
20	12.6616091	3.2353840	1.4415770	8.6643341	0.	-0.	12.3398030
21	18.3887119	3.3363060	1.4693830	14.2886640	0.	-0.	18.1036780
22	27.6613960	3.3358750	1.4726000	23.5613480	0.	-0.	27.3697920
23	42.9556112	3.3343550	1.4758570	38.8555632	0.	-0.	42.6581831
24	68.1613522	3.3346960	1.4772220	64.0613050	0.	-0.	67.8596830
25	109.7107267	3.3351310	1.4767360	105.6106796	0.	-0.	109.3965502
26	178.1736221	3.3391080	1.4747100	174.0735760	0.	-0.	177.8409004
27	291.1191444	3.3370750	1.4765150	287.0191002	0.	-0.	290.7516899
28	477.3599434	3.3365820	1.4769180	473.2598915	0.	-0.	476.9346695
29	782.4773331	3.3528990	1.4596910	778.3772964	0.	-0.	781.2099457
30	2749.0000000	4.0000000	0.7200000	2745.0000000	-0.	-0.	2748.7600098

TABLE V. - Continued. CROSS-SECTION DATA FOR ALUMINUM, CADMIUM, BORON 10, AND URANYL FLUORIDE SALT IN WATER FUEL SOLUTION

[Atom ratio of hydrogen to uranium 235; 500.]

(a) Continued. Group split A

P(0) TRANSFER MATRIX AL

TO \ FROM	1	2	3	4	5	6	7	8
1	0.	0.	0.	0.	0.	0.	0.	0.
2	1.82581E-01	0.	0.	0.	0.	0.	0.	0.
3	8.67240E-02	2.38478E-01	0.	0.	0.	0.	0.	0.
4	1.05163E-01	1.11829E-01	2.94385E-01	0.	0.	0.	0.	0.
5	1.04230E-01	1.21978E-01	1.46978E-01	3.66385E-01	0.	0.	0.	0.
6	8.88160E-02	1.11648E-01	1.45158E-01	1.06470E-01	4.41712E-01	0.	0.	0.
7	6.76040E-02	8.96370E-02	1.23356E-01	1.70016E-01	1.19809E-01	4.96992E-01	0.	0.
8	4.73040E-02	6.52610E-02	9.36990E-02	1.62943E-01	6.15950E-02	1.28518E-01	4.46949E-01	0.
9	3.10910E-02	4.41770E-02	6.54620E-02	1.01418E-01	9.93460E-02	3.54470E-02	1.29970E-01	5.10747E-01
10	1.95050E-02	2.83290E-02	4.29750E-02	3.74560E-02	1.24337E-01	5.54100E-03	1.24106E-01	1.31930E-02
11	1.18210E-02	1.74500E-02	2.69380E-02	2.70090E-02	5.90770E-02	3.20560E-02	4.66550E-02	7.61870E-02
12	6.98300E-03	1.04330E-02	1.63150E-02	1.87670E-02	3.91910E-02	2.45870E-02	3.40000E-05	9.47040E-02
13	4.04700E-03	6.10100E-03	9.63300E-03	1.34140E-02	2.63980E-02	1.38520E-02	0.	5.30490E-02
14	2.31300E-03	3.50900E-03	5.58100E-03	8.92000E-03	1.69570E-02	7.42600E-03	0.	3.04220E-02
15	1.30800E-03	1.99400E-03	3.18800E-03	5.42000E-03	9.32800E-03	5.65900E-03	0.	1.78580E-02
16	7.34000E-04	1.12300E-03	1.80300E-03	3.16600E-03	4.26700E-03	4.60600E-03	0.	1.45900E-03
17	5.75000E-04	8.83000E-04	1.42300E-03	2.53900E-03	3.19600E-03	4.47200E-03	0.	0.
18	2.95000E-04	4.55000E-04	7.35000E-04	1.51200E-03	2.18100E-03	3.09500E-03	0.	0.
19	4.10000E-05	6.30000E-05	1.02000E-04	3.38030E-04	6.21000E-04	8.11000E-04	0.	0.
20	6.00000E-06	9.00000E-06	1.40000E-05	9.70000E-05	1.95000E-04	2.76000E-04	0.	0.
21	1.00000E-06	1.00000E-06	2.00000E-06	2.70000E-05	5.20000E-05	1.17000E-04	0.	0.
22	0.	0.	0.	5.00000E-06	1.60000E-05	1.20000E-05	0.	0.
23	0.	0.	0.	0.	1.00000E-06	4.00000E-06	0.	0.
24	0.	0.	0.	0.	0.	1.00000E-06	0.	0.
25	0.	0.	0.	0.	0.	0.	0.	0.
26	0.	0.	0.	0.	0.	0.	0.	0.
27	0.	0.	0.	0.	0.	0.	0.	0.
28	0.	0.	0.	0.	0.	0.	0.	0.
29	0.	0.	0.	0.	0.	0.	0.	0.
30	0.	0.	0.	0.	0.	0.	0.	0.

TO \ FROM	9	10	11	12	13	14	15	16
1	0.	0.	0.	0.	0.	0.	0.	0.
2	0.	0.	0.	0.	0.	0.	0.	0.
3	0.	0.	0.	0.	0.	0.	0.	0.
4	0.	0.	0.	0.	0.	0.	0.	0.
5	0.	0.	0.	0.	0.	0.	0.	0.
6	0.	0.	0.	0.	0.	0.	0.	0.
7	0.	0.	0.	0.	0.	0.	0.	0.
8	0.	0.	0.	0.	0.	0.	0.	0.
9	0.	0.	0.	0.	0.	0.	0.	0.
10	4.92753E-01	0.	0.	0.	0.	0.	0.	0.
11	0.	5.93487E-01	0.	0.	0.	0.	0.	0.
12	2.90000E-05	0.	7.01163E-01	0.	0.	0.	0.	0.
13	1.42310E-02	0.	0.	8.35446E-01	0.	0.	0.	0.
14	1.85580E-02	0.	0.	0.	1.01862E 00	0.	0.	0.
15	1.81740E-02	0.	0.	0.	0.	1.07922E 00	0.	0.
16	2.64990E-02	0.	0.	0.	0.	0.	2.04526E 00	0.
17	2.88100E-02	0.	0.	0.	0.	0.	0.	8.35498E-01
18	1.37500E-02	2.00000E-04	0.	0.	0.	0.	0.	0.
19	1.82300E-03	2.46000E-04	0.	0.	0.	0.	0.	0.
20	3.99000E-04	5.00000E-05	0.	0.	0.	0.	0.	0.
21	1.60000E-04	1.30000E-05	0.	0.	0.	0.	0.	0.
22	4.50000E-05	3.00000E-06	0.	0.	0.	0.	0.	0.
23	1.30000E-05	1.00000E-06	0.	0.	0.	0.	0.	0.
24	0.	0.	0.	0.	0.	0.	0.	0.
25	0.	0.	0.	0.	0.	0.	0.	0.
26	0.	0.	0.	0.	0.	0.	0.	0.
27	0.	0.	0.	0.	0.	0.	0.	0.
28	0.	0.	0.	0.	0.	0.	0.	0.
29	0.	0.	0.	0.	0.	0.	0.	0.
30	0.	0.	0.	0.	0.	0.	0.	0.

TABLE V. - Continued. CROSS-SECTION DATA FOR ALUMINUM, CADMIUM, BORON 10, AND URANYL FLUORIDE SALT IN WATER FUEL SOLUTION

[Atom ratio of hydrogen to uranium 235; 500.]

(a) Continued. Group split A

TO \ FROM	17	18	19	20	21	22	23	24
1	0.	0.	0.	0.	0.	0.	0.	0.
2	0.	0.	0.	0.	0.	0.	0.	0.
3	0.	0.	0.	0.	0.	0.	0.	0.
4	0.	0.	0.	0.	0.	0.	0.	0.
5	0.	0.	0.	0.	0.	0.	0.	0.
6	0.	0.	0.	0.	0.	0.	0.	0.
7	0.	0.	0.	0.	0.	0.	0.	0.
8	0.	0.	0.	0.	0.	0.	0.	0.
9	0.	0.	0.	0.	0.	0.	0.	0.
10	0.	0.	0.	0.	0.	0.	0.	0.
11	0.	0.	0.	0.	0.	0.	0.	0.
12	0.	0.	0.	0.	0.	0.	0.	0.
13	0.	0.	0.	0.	0.	0.	0.	0.
14	0.	0.	0.	0.	0.	0.	0.	0.
15	0.	0.	0.	0.	0.	0.	0.	0.
16	0.	0.	0.	0.	0.	0.	0.	0.
17	0.	0.	0.	0.	0.	0.	0.	0.
18	2.38780E-01	0.	0.	0.	0.	0.	0.	0.
19	0.	3.69480E-02	0.	0.	0.	0.	0.	0.
20	0.	0.	7.75540E-02	0.	0.	0.	0.	0.
21	0.	0.	0.	1.01208E-01	0.	0.	0.	0.
22	0.	0.	0.	0.	1.01442E-01	0.	0.	0.
23	0.	0.	0.	0.	0.	1.01512E-01	0.	0.
24	0.	0.	0.	0.	0.	0.	1.01739E-01	0.
25	0.	0.	0.	0.	0.	0.	0.	1.01672E-01
26	0.	0.	0.	0.	0.	0.	0.	0.
27	0.	0.	0.	0.	0.	0.	0.	0.
28	0.	0.	0.	0.	0.	0.	0.	0.
29	0.	0.	0.	0.	0.	0.	0.	0.
30	0.	0.	0.	0.	0.	0.	0.	0.

TO \ FROM	25	26	27	28	29	30
1	0.	0.	0.	0.	0.	0.
2	0.	0.	0.	0.	0.	0.
3	0.	0.	0.	0.	0.	0.
4	0.	0.	0.	0.	0.	0.
5	0.	0.	0.	0.	0.	0.
6	0.	0.	0.	0.	0.	0.
7	0.	0.	0.	0.	0.	0.
8	0.	0.	0.	0.	0.	0.
9	0.	0.	0.	0.	0.	0.
10	0.	0.	0.	0.	0.	0.
11	0.	0.	0.	0.	0.	0.
12	0.	0.	0.	0.	0.	0.
13	0.	0.	0.	0.	0.	0.
14	0.	0.	0.	0.	0.	0.
15	0.	0.	0.	0.	0.	0.
16	0.	0.	0.	0.	0.	0.
17	0.	0.	0.	0.	0.	0.
18	0.	0.	0.	0.	0.	0.
19	0.	0.	0.	0.	0.	0.
20	0.	0.	0.	0.	0.	0.
21	0.	0.	0.	0.	0.	0.
22	0.	0.	0.	0.	0.	0.
23	0.	0.	0.	0.	0.	0.
24	0.	0.	0.	0.	0.	0.
25	0.	0.	0.	0.	0.	0.
26	1.01653E-01	0.	0.	0.	0.	0.
27	0.	1.00993E-01	0.	0.	0.	0.
28	0.	0.	1.01307E-01	0.	0.	0.
29	0.	0.	0.	1.01378E-01	0.	-0.
30	0.	0.	0.	0.	9.90350E-02	0.

TABLE V. - Continued. CROSS-SECTION DATA FOR ALUMINUM, CADMIUM, BORON 10, AND URANYL FLUORIDE SALT IN WATER FUEL SOLUTION

[Atom ratio of hydrogen to uranium 235; 500.]

(a) Continued. Group split A

P(0) TRANSFER MATRIX CD

FROM / TO	1	2	3	4	5	6	7	8
1	0.	0.	0.	0.	0.	0.	0.	0.
2	7.29460E-02	0.	0.	0.	0.	0.	0.	0.
3	1.00828E-01	9.70840E-02	0.	0.	0.	0.	0.	0.
4	2.69348E-01	1.33245E-01	1.09644E-01	0.	0.	0.	0.	0.
5	4.84565E-01	2.84540E-01	1.33585E-01	1.55649E-01	0.	0.	0.	0.
6	6.46231E-01	4.31844E-01	2.37941E-01	1.92480E-01	2.38399E-01	0.	0.	0.
7	6.87867E-01	5.06547E-01	3.14887E-01	2.90956E-01	2.37802E-01	2.97284E-01	0.	0.
8	6.18265E-01	4.89629E-01	3.33207E-01	3.40272E-01	3.13412E-01	2.63381E-01	3.54304E-01	0.
9	4.89700E-01	4.09452E-01	2.98164E-01	3.28183E-01	3.30644E-01	3.06713E-01	2.56594E-01	3.75277E-01
10	3.52962E-01	3.07308E-01	2.35377E-01	2.73995E-01	2.95211E-01	2.94878E-01	2.69262E-01	2.26906E-01
11	2.37153E-01	2.12790E-01	1.69231E-01	2.05394E-01	2.32662E-01	2.45610E-01	2.39453E-01	2.17911E-01
12	1.51237E-01	1.38771E-01	1.13495E-01	1.42094E-01	1.67076E-01	1.83794E-01	1.88161E-01	1.81351E-01
13	9.27770E-02	8.65560E-02	7.22770E-02	9.26050E-02	1.11949E-01	1.26986E-01	1.34823E-01	1.35622E-01
14	5.52990E-02	5.22320E-02	4.42940E-02	5.77330E-02	7.12460E-02	8.26790E-02	9.01910E-02	9.36600E-02
15	3.22640E-02	3.07550E-02	2.63810E-02	3.48250E-02	4.36400E-02	5.15080E-02	5.73300E-02	6.09590E-02
16	1.85290E-02	1.77820E-02	1.53830E-02	2.05000E-02	2.59820E-02	3.10550E-02	3.50840E-02	3.79670E-02
17	1.48280E-02	1.43150E-02	1.24780E-02	1.67670E-02	2.14660E-02	2.59430E-02	2.97000E-02	3.26450E-02
18	7.77500E-03	7.55200E-03	6.63400E-03	8.99100E-03	1.16300E-02	1.42180E-02	1.64990E-02	1.84270E-02
19	1.08500E-03	1.05900E-03	9.35000E-04	1.27600E-03	1.66300E-03	2.05100E-03	2.40400E-03	2.71700E-03
20	1.48000E-04	1.45000E-04	1.29000E-04	1.76000E-04	2.30000E-04	2.84000E-04	3.34000E-04	3.80000E-04
21	2.00000E-05	2.00000E-05	1.80000E-05	2.40000E-05	3.10000E-05	3.90000E-05	4.60000E-05	5.20000E-05
22	3.00000E-06	3.00000E-06	2.00000E-06	3.00000E-06	4.00000E-06	5.00000E-06	6.00000E-06	7.00000E-06
23	0.	0.	0.	0.	1.00000E-06	1.00000E-06	1.00000E-06	1.00000E-06
24	0.	0.	0.	0.	0.	0.	0.	0.
25	0.	0.	0.	0.	0.	0.	0.	0.
26	0.	0.	0.	0.	0.	0.	0.	0.
27	0.	0.	0.	0.	0.	0.	0.	0.
28	0.	0.	0.	0.	0.	0.	0.	0.
29	0.	0.	0.	0.	0.	0.	0.	0.
30	0.	0.	0.	0.	0.	0.	0.	0.

FROM / TO	9	10	11	12	13	14	15	16
1	0.	0.	0.	0.	0.	0.	0.	0.
2	0.	0.	0.	0.	0.	0.	0.	0.
3	0.	0.	0.	0.	0.	0.	0.	0.
4	0.	0.	0.	0.	0.	0.	0.	0.
5	0.	0.	0.	0.	0.	0.	0.	0.
6	0.	0.	0.	0.	0.	0.	0.	0.
7	0.	0.	0.	0.	0.	0.	0.	0.
8	0.	0.	0.	0.	0.	0.	0.	0.
9	0.	0.	0.	0.	0.	0.	0.	0.
10	3.54891E-01	0.	0.	0.	0.	0.	0.	0.
11	1.87956E-01	3.94405E-01	0.	0.	0.	0.	0.	0.
12	1.66919E-01	1.59903E-01	3.71114E-01	0.	0.	0.	0.	0.
13	1.31031E-01	1.32942E-01	1.10097E-01	3.85647E-01	0.	0.	0.	0.
14	9.38170E-02	9.93460E-02	8.64030E-02	6.74920E-02	3.53834E-01	0.	0.	0.
15	6.27250E-02	6.85700E-02	6.18510E-02	5.04630E-02	3.84660E-02	3.53441E-01	0.	0.
16	3.98540E-02	4.46110E-02	4.13460E-02	3.48440E-02	2.75130E-02	1.65360E-02	3.60842E-01	0.
17	3.48810E-02	3.98740E-02	3.78600E-02	3.28420E-02	2.67630E-02	1.67250E-02	6.15200E-03	3.64811E-01
18	2.00510E-02	2.34220E-02	2.27960E-02	2.03700E-02	1.71440E-02	1.11490E-02	4.24800E-03	0.
19	2.99600E-03	3.55700E-03	3.52500E-03	3.22000E-03	2.77500E-03	1.85800E-03	7.26000E-04	0.
20	4.21000E-04	5.02000E-04	5.01000E-04	4.62000E-04	4.01000E-04	2.72000E-04	1.07000E-04	0.
21	5.80000E-05	6.90000E-05	6.90000E-05	6.40000E-05	5.60000E-05	3.80000E-05	1.50000E-05	0.
22	8.00000E-06	9.00000E-06	9.00000E-06	9.00000E-06	8.00000E-06	5.00000E-06	0.	0.
23	1.00000E-06	1.00000E-06	1.00000E-06	1.00000E-06	1.00000E-06	1.00000E-06	0.	0.
24	0.	0.	0.	0.	0.	0.	0.	0.
25	0.	0.	0.	0.	0.	0.	0.	0.
26	0.	0.	0.	0.	0.	0.	0.	0.
27	0.	0.	0.	0.	0.	0.	0.	0.
28	0.	0.	0.	0.	0.	0.	0.	0.
29	0.	0.	0.	0.	0.	0.	0.	0.
30	0.	0.	0.	0.	0.	0.	-0.	0.

TABLE V. - Continued. CROSS-SECTION DATA FOR ALUMINUM, CADMIUM, BORON 10, AND URANYL FLUORIDE SALT IN WATER FUEL SOLUTION

[Atom ratio of hydrogen to uranium 235; 500.]

(a) Continued. Group split A

TO \ FROM	17	18	19	20	21	22	23	24
1	0.	0.	0.	0.	0.	0.	0.	0.
2	0.	0.	0.	0.	0.	0.	0.	0.
3	0.	0.	0.	0.	0.	0.	0.	0.
4	0.	0.	0.	0.	0.	0.	0.	0.
5	0.	0.	0.	0.	0.	0.	0.	0.
6	0.	0.	0.	0.	0.	0.	0.	0.
7	0.	0.	0.	0.	0.	0.	0.	0.
8	0.	0.	0.	0.	0.	0.	0.	0.
9	0.	0.	0.	0.	0.	0.	0.	0.
10	0.	0.	0.	0.	0.	0.	0.	0.
11	0.	0.	0.	0.	0.	0.	0.	0.
12	0.	0.	0.	0.	0.	0.	0.	0.
13	0.	0.	0.	0.	0.	0.	0.	0.
14	0.	0.	0.	0.	0.	0.	0.	0.
15	0.	0.	0.	0.	0.	0.	0.	0.
16	0.	0.	0.	0.	0.	0.	0.	0.
17	0.	0.	0.	0.	0.	0.	0.	0.
18	2.27866E-01	0.	0.	0.	0.	0.	0.	0.
19	0.	1.07924E-01	0.	0.	0.	0.	0.	0.
20	0.	0.	8.45540E-02	0.	0.	0.	0.	0.
21	0.	0.	0.	8.10190E-02	0.	0.	0.	0.
22	0.	0.	0.	0.	6.00220E-02	0.	0.	0.
23	0.	0.	0.	0.	0.	1.69590E-01	0.	0.
24	0.	0.	0.	0.	0.	0.	8.67560E-02	0.
25	0.	0.	0.	0.	0.	0.	0.	7.60810E-02
26	0.	0.	0.	0.	0.	0.	0.	0.
27	0.	0.	0.	0.	0.	0.	0.	0.
28	0.	0.	0.	0.	0.	0.	0.	0.
29	0.	0.	0.	0.	0.	0.	0.	0.
30	0.	0.	0.	0.	0.	0.	0.	0.

TO \ FROM	25	26	27	28	29	30
1	0.	0.	0.	0.	0.	0.
2	0.	0.	0.	0.	0.	0.
3	0.	0.	0.	0.	0.	0.
4	0.	0.	0.	0.	0.	0.
5	0.	0.	0.	0.	0.	0.
6	0.	0.	0.	0.	0.	0.
7	0.	0.	0.	0.	0.	0.
8	0.	0.	0.	0.	0.	0.
9	0.	0.	0.	0.	0.	0.
10	0.	0.	0.	0.	0.	0.
11	0.	0.	0.	0.	0.	0.
12	0.	0.	0.	0.	0.	0.
13	0.	0.	0.	0.	0.	0.
14	0.	0.	0.	0.	0.	0.
15	0.	0.	0.	0.	0.	0.
16	0.	0.	0.	0.	0.	0.
17	0.	0.	0.	0.	0.	0.
18	0.	0.	0.	0.	0.	0.
19	0.	0.	0.	0.	0.	0.
20	0.	0.	0.	0.	0.	0.
21	0.	0.	0.	0.	0.	0.
22	0.	0.	0.	0.	0.	0.
23	0.	0.	0.	0.	0.	0.
24	0.	0.	0.	0.	0.	0.
25	0.	0.	0.	0.	0.	0.
26	7.60670E-02	0.	0.	0.	0.	0.
27	0.	7.03010E-02	0.	0.	0.	0.
28	0.	0.	7.05200E-02	0.	0.	0.
29	0.	0.	0.	8.90930E-02	0.	-0.
30	0.	0.	0.	0.	1.55112E-01	0.

TABLE V. - Continued. CROSS-SECTION DATA FOR ALUMINUM, CADMIUM, BORON 10, AND URANYL FLUORIDE SALT IN WATER FUEL SOLUTION

[Atom ratio of hydrogen to uranium 235; 500.]

(a) Continued. Group split A

P(0) TRANSFER MATRIX UO2F2

FROM / TO	1	2	3	4	5	6	7	8
1	0.	0.	0.	0.	0.	0.	0.	0.
2	1.92110E-02	0.	0.	0.	0.	0.	0.	0.
3	1.20440E-02	2.76810E-02	0.	0.	0.	0.	0.	0.
4	9.54700E-03	1.25330E-02	3.40510E-02	0.	0.	0.	0.	0.
5	7.37300E-03	9.30000E-03	1.55410E-02	4.20010E-02	0.	0.	0.	0.
6	5.53900E-03	6.90700E-03	1.15310E-02	1.90200E-02	5.94690E-02	0.	0.	0.
7	4.06800E-03	5.13500E-03	8.56100E-03	1.41100E-02	2.32230E-02	4.57910E-02	0.	0.
8	2.94200E-03	3.81900E-03	6.36000E-03	1.04730E-02	1.72250E-02	2.75780E-02	7.27890E-02	0.
9	2.10800E-03	2.83900E-03	4.72500E-03	7.77400E-03	1.27770E-02	2.04390E-02	3.29070E-02	9.21410E-02
10	1.50400E-03	2.10700E-03	3.50700E-03	5.76800E-03	9.47700E-03	1.51680E-02	2.43920E-02	3.87540E-02
11	1.07300E-03	1.56100E-03	2.59900E-03	4.27600E-03	7.02600E-03	1.12410E-02	1.80540E-02	2.87040E-02
12	7.68000E-04	1.15500E-03	1.92500E-03	3.16700E-03	5.20500E-03	8.32200E-03	1.33730E-02	2.12700E-02
13	5.51000E-04	8.54000E-04	1.42400E-03	2.34400E-03	3.85400E-03	6.16400E-03	9.90400E-03	1.57470E-02
14	3.98000E-04	6.31000E-04	1.05300E-03	1.73500E-03	2.85300E-03	4.56300E-03	7.33400E-03	1.16560E-02
15	2.88000E-04	4.66000E-04	7.79000E-04	1.28300E-03	2.11100E-03	3.37600E-03	5.43300E-03	8.62700E-03
16	2.10000E-04	3.44000E-04	5.76000E-04	9.49300E-04	1.56300E-03	2.50000E-03	4.02200E-03	6.39100E-03
17	2.32000E-04	3.86000E-04	6.46000E-04	1.06600E-03	1.75500E-03	2.80900E-03	4.52100E-03	7.18500E-03
18	2.22000E-04	3.75000E-04	6.28000E-04	1.03700E-03	1.70800E-03	2.73500E-03	4.40300E-03	6.99900E-03
19	8.00000E-05	1.38000E-04	2.31000E-04	3.81000E-04	6.27000E-04	1.00500E-03	1.61900E-03	2.57400E-03
20	2.90000E-05	5.10000E-05	8.50000E-05	1.40000E-04	2.31000E-04	3.70000E-04	5.96000E-04	9.47000E-04
21	1.10000E-05	1.90000E-05	3.10000E-05	5.10000E-05	8.50000E-05	1.36000E-04	2.19000E-04	3.48000E-04
22	4.00000E-06	7.00000E-06	1.10000E-05	1.90000E-05	3.10000E-05	5.00000E-05	8.10000E-05	1.28000E-04
23	1.00000E-06	3.00000E-06	4.00000E-06	7.00000E-06	1.10000E-05	1.80000E-05	3.00000E-05	4.70000E-05
24	1.00000E-06	1.00000E-06	2.00000E-06	3.00000E-06	4.00000E-06	7.00000E-06	1.10000E-05	1.70000E-05
25	0.	0.	1.00000E-06	1.00000E-06	2.00000E-06	2.00000E-06	4.00000E-06	6.00000E-06
26	0.	0.	0.	0.	1.00000E-06	1.00000E-06	1.00000E-06	2.00000E-06
27	0.	0.	0.	0.	0.	0.	1.00000E-06	1.00000E-06
28	0.	0.	0.	0.	0.	0.	0.	0.
29	0.	0.	0.	0.	0.	0.	0.	0.
30	0.	0.	0.	0.	0.	0.	0.	0.

FROM / TO	9	10	11	12	13	14	15	16
1	0.	0.	0.	0.	0.	0.	0.	0.
2	0.	0.	0.	0.	0.	0.	0.	0.
3	0.	0.	0.	0.	0.	0.	0.	0.
4	0.	0.	0.	0.	0.	0.	0.	0.
5	0.	0.	0.	0.	0.	0.	0.	0.
6	0.	0.	0.	0.	0.	0.	0.	0.
7	0.	0.	0.	0.	0.	0.	0.	0.
8	0.	0.	0.	0.	0.	0.	0.	0.
9	0.	0.	0.	0.	0.	0.	0.	0.
10	1.35107E-01	0.	0.	0.	0.	0.	0.	0.
11	4.51930E-02	1.05886E-01	0.	0.	0.	0.	0.	0.
12	3.34210E-02	5.33020E-02	1.20488E-01	0.	0.	0.	0.	0.
13	2.47340E-02	3.94210E-02	6.27540E-02	2.01975E-01	0.	0.	0.	0.
14	1.83230E-02	2.91970E-02	4.63690E-02	7.39550E-02	1.70345E-01	0.	0.	0.
15	1.35760E-02	2.16260E-02	3.43200E-02	5.47710E-02	8.51990E-02	1.82301E-01	0.	0.
16	1.00550E-02	1.60180E-02	2.54270E-02	4.04290E-02	6.30180E-02	9.81900E-02	1.96908E-01	0.
17	1.13050E-02	1.80150E-02	2.85950E-02	4.54170E-02	7.07210E-02	1.10220E-01	1.66602E-01	3.05605E-01
18	1.10130E-02	1.75540E-02	2.78620E-02	4.42530E-02	6.88150E-02	1.06997E-01	1.62496E-01	2.51066E-01
19	4.05100E-03	6.45800E-03	1.02490E-02	1.62800E-02	2.53090E-02	3.93560E-02	5.96670E-02	9.24330E-02
20	1.49000E-03	2.37600E-03	3.77100E-03	5.98900E-03	9.31100E-03	1.44780E-02	2.19500E-02	3.39930E-02
21	5.48000E-04	8.74000E-04	1.38700E-03	2.20300E-03	3.42500E-03	5.32600E-03	8.07500E-03	1.25030E-02
22	2.02000E-04	3.22000E-04	5.10000E-04	8.11000E-04	1.26000E-03	1.95900E-03	2.97100E-03	4.60000E-03
23	7.40000E-05	1.18000E-04	1.88000E-04	2.98000E-04	4.64000E-04	7.21000E-04	1.09300E-03	1.69200E-03
24	2.70000E-05	4.40000E-05	6.90000E-05	1.10000E-04	1.71000E-04	2.65000E-04	4.02000E-04	6.22000E-04
25	1.00000E-05	1.60000E-05	2.50000E-05	4.00000E-05	6.30000E-05	9.80000E-05	1.48000E-04	2.29000E-04
26	4.00000E-06	6.00000E-06	9.00000E-06	1.50000E-05	2.30000E-05	3.60000E-05	5.40000E-05	8.40000E-05
27	1.00000E-06	2.00000E-06	3.00000E-06	5.00000E-06	8.00000E-06	1.30000E-05	2.00000E-05	3.10000E-05
28	0.	1.00000E-06	1.00000E-06	2.00000E-06	3.00000E-06	5.00000E-06	7.00000E-06	1.10000E-05
29	0.	0.	0.	1.00000E-06	1.00000E-06	2.00000E-06	3.00000E-06	4.00000E-06
30	0.	0.	0.	0.	1.00000E-06	1.00000E-06	2.00000E-06	2.00000E-06

TABLE V. - Continued. CROSS-SECTION DATA FOR ALUMINUM, CADMIUM, BORON 10, AND URANYL FLUORIDE SALT IN WATER FUEL SOLUTION

[Atom ratio of hydrogen to uranium 235; 500.]

(a) Continued. Group split A

TO \ FROM	17	18	19	20	21	22	23	24
1	0.	0.	0.	0.	0.	0.	0.	0.
2	0.	0.	0.	0.	0.	0.	0.	0.
3	0.	0.	0.	0.	0.	0.	0.	0.
4	0.	0.	0.	0.	0.	0.	0.	0.
5	0.	0.	0.	0.	0.	0.	0.	0.
6	0.	0.	0.	0.	0.	0.	0.	0.
7	0.	0.	0.	0.	0.	0.	0.	0.
8	0.	0.	0.	0.	0.	0.	0.	0.
9	0.	0.	0.	0.	0.	0.	0.	0.
10	0.	0.	0.	0.	0.	0.	0.	0.
11	0.	0.	0.	0.	0.	0.	0.	0.
12	0.	0.	0.	0.	0.	0.	0.	0.
13	0.	0.	0.	0.	0.	0.	0.	0.
14	0.	0.	0.	0.	0.	0.	0.	0.
15	0.	0.	0.	0.	0.	0.	0.	0.
16	0.	0.	0.	0.	0.	0.	0.	0.
17	0.	0.	0.	0.	0.	0.	0.	0.
18	4.61854E-01	0.	0.	0.	0.	0.	0.	0.
19	1.59708E-01	4.35614E-01	0.	0.	0.	0.	0.	0.
20	5.87520E-02	1.55291E-01	5.00164E-01	0.	0.	0.	0.	0.
21	2.16130E-02	5.71280E-02	1.78951E-01	5.28622E-01	0.	0.	0.	0.
22	7.95100E-03	2.10160E-02	6.58320E-02	1.89097E-01	5.36812E-01	0.	0.	0.
23	2.92500E-03	7.73100E-03	2.42180E-02	6.95650E-02	1.92047E-01	5.43935E-01	0.	0.
24	1.07600E-03	2.84400E-03	8.90900E-03	2.55920E-02	7.06500E-02	1.94629E-01	5.48147E-01	0.
25	3.96000E-04	1.04600E-03	3.27800E-03	9.41500E-03	2.59910E-02	7.16000E-02	1.96166E-01	5.50283E-01
26	1.46000E-04	3.85000E-04	1.20600E-03	3.46300E-03	9.56100E-03	2.63400E-02	7.21650E-02	1.96958E-01
27	5.40000E-05	1.42000E-04	4.44000E-04	1.27400E-03	3.51700E-03	9.69000E-03	2.65480E-02	7.24570E-02
28	2.00000E-05	5.20000E-05	1.63000E-04	4.69030E-04	1.29400E-03	3.56500E-03	9.76700E-03	2.66550E-02
29	7.00000E-06	1.90000E-05	6.00000E-05	1.72000E-04	4.76000E-04	1.31100E-03	3.59300E-03	9.80600E-03
30	4.00000E-06	1.10000E-05	3.50000E-05	1.00000E-04	2.77000E-04	7.63000E-04	2.09100E-03	5.70700E-03

TO \ FROM	25	26	27	28	29	30
1	0.	0.	0.	0.	0.	0.
2	0.	0.	0.	0.	0.	0.
3	0.	0.	0.	0.	0.	0.
4	0.	0.	0.	0.	0.	0.
5	0.	0.	0.	0.	0.	0.
6	0.	0.	0.	0.	0.	0.
7	0.	0.	0.	0.	0.	0.
8	0.	0.	0.	0.	0.	0.
9	0.	0.	0.	0.	0.	0.
10	0.	0.	0.	0.	0.	0.
11	0.	0.	0.	0.	0.	0.
12	0.	0.	0.	0.	0.	0.
13	0.	0.	0.	0.	0.	0.
14	0.	0.	0.	0.	0.	0.
15	0.	0.	0.	0.	0.	0.
16	0.	0.	0.	0.	0.	0.
17	0.	0.	0.	0.	0.	0.
18	0.	0.	0.	0.	0.	0.
19	0.	0.	0.	0.	0.	0.
20	0.	0.	0.	0.	0.	0.
21	0.	0.	0.	0.	0.	0.
22	0.	0.	0.	0.	0.	0.
23	0.	0.	0.	0.	0.	0.
24	0.	0.	0.	0.	0.	0.
25	0.	0.	0.	0.	0.	0.
26	5.53196E-01	0.	0.	0.	0.	0.
27	1.98033E-01	5.54484E-01	0.	0.	0.	0.
28	7.28520E-02	1.98543E-01	5.63532E-01	0.	0.	0.
29	2.68010E-02	7.30400E-02	2.01854E-01	5.69060E-01	0.	9.11000E-04
30	1.55970E-02	4.25060E-02	1.17471E-01	3.22528E-01	9.15858E-01	0.

TABLE V. - Continued. CROSS-SECTION DATA FOR ALUMINUM, CADMIUM, BORON 10, AND URANYL FLUORIDE SALT IN WATER FUEL SOLUTION

[Atom ratio of hydrogen to uranium 235; 500.]

(a) Continued. Group split A

P(0) TRANSFER MATRIX B-10

FROM / TO	1	2	3	4	5	6	7	8
1	0.	0.	0.	0.	0.	0.	0.	0.
2	3.34741E-01	0.	0.	0.	0.	0.	0.	0.
3	1.09145E-01	3.49756E-01	0.	0.	0.	0.	0.	0.
4	9.02500E-02	8.19760E-02	3.80423E-01	0.	0.	0.	0.	0.
5	7.12030E-02	5.71440E-02	6.97120E-02	4.95253E-01	0.	0.	0.	0.
6	5.11720E-02	4.28270E-02	3.73170E-02	6.86810E-02	6.95450E-01	0.	0.	0.
7	3.43080E-02	2.96230E-02	2.67410E-02	1.99790E-02	1.17471E-01	9.53768E-01	0.	0.
8	2.18430E-02	1.93030E-02	1.78890E-02	1.37710E-02	7.31400E-03	1.00871E-01	9.05520E-01	0.
9	1.33840E-02	1.20330E-02	1.13710E-02	8.95000E-03	4.90100E-03	4.41100E-03	7.48370E-02	9.85032E-01
10	7.97000E-03	7.25800E-03	6.95900E-03	5.56900E-03	3.11900E-03	2.86500E-03	2.40200E-03	8.67040E-02
11	4.64700E-03	4.27200E-03	4.14000E-03	3.35400E-03	1.91100E-03	1.78200E-03	1.52500E-03	1.14300E-03
12	2.66800E-03	2.47000E-03	2.41300E-03	1.97200E-03	1.13800E-03	1.07300E-03	9.33000E-04	7.11000E-04
13	1.51300E-03	1.40800E-03	1.38400E-03	1.13900E-03	6.63000E-04	6.31000E-04	5.55000E-04	4.28000E-04
14	8.51000E-04	7.95000E-04	7.85000E-04	6.49300E-04	3.81000E-04	3.64000E-04	3.23000E-04	2.52000E-04
15	4.76000E-04	4.46000E-04	4.41000E-04	3.66000E-04	2.16000E-04	2.08000E-04	1.85000E-04	1.45000E-04
16	2.65000E-04	2.49000E-04	2.47000E-04	2.05000E-04	1.21000E-04	1.17000E-04	1.05000E-04	8.30000E-05
17	2.06000E-04	1.94000E-04	1.93000E-04	1.61000E-04	9.50000E-05	9.20000E-05	8.30000E-05	6.60000E-05
18	1.05000E-04	9.90000E-05	9.90000E-05	8.20000E-05	4.90000E-05	4.80000E-05	4.30000E-05	3.40000E-05
19	1.40000E-05	1.40000E-05	1.40000E-05	1.10000E-05	7.00000E-06	7.00000E-06	6.00000E-06	5.00000E-06
20	2.00000E-06	2.00000E-06	2.00000E-06	2.00000E-06	1.00000E-06	1.00000E-06	1.00000E-06	1.00000E-06
21	0.	0.	0.	0.	0.	0.	0.	0.
22	0.	0.	0.	0.	0.	0.	0.	0.
23	0.	0.	0.	0.	0.	0.	0.	0.
24	0.	0.	0.	0.	0.	0.	0.	0.
25	0.	0.	0.	0.	0.	0.	0.	0.
26	0.	0.	0.	0.	0.	0.	0.	0.
27	0.	0.	0.	0.	0.	0.	0.	0.
28	0.	0.	0.	0.	0.	0.	0.	0.
29	0.	0.	0.	0.	0.	0.	0.	0.
30	0.	0.	0.	0.	0.	0.	0.	0.

FROM / TO	9	10	11	12	13	14	15	16
1	0.	0.	0.	0.	0.	0.	0.	0.
2	0.	0.	0.	0.	0.	0.	0.	0.
3	0.	0.	0.	0.	0.	0.	0.	0.
4	0.	0.	0.	0.	0.	0.	0.	0.
5	0.	0.	0.	0.	0.	0.	0.	0.
6	0.	0.	0.	0.	0.	0.	0.	0.
7	0.	0.	0.	0.	0.	0.	0.	0.
8	0.	0.	0.	0.	0.	0.	0.	0.
9	0.	0.	0.	0.	0.	0.	0.	0.
10	1.15972E 00	0.	0.	0.	0.	0.	0.	0.
11	8.64800E-02	1.51868E 00	0.	0.	0.	0.	0.	0.
12	1.00000E-05	7.94520E-02	1.78207E 00	0.	0.	0.	0.	0.
13	6.00000E-06	0.	8.65150E-02	1.94795E 00	0.	0.	0.	0.
14	4.00000E-06	0.	0.	1.33739E-01	1.96548E 00	0.	0.	0.
15	2.00000E-06	0.	0.	0.	1.28687E-01	2.06910E 00	0.	0.
16	1.00000E-06	0.	0.	0.	0.	1.29702E-01	1.92670E 00	0.
17	1.00000E-06	0.	0.	0.	0.	0.	1.17398E-01	1.73424E 00
18	0.	0.	0.	0.	0.	0.	0.	0.
19	0.	0.	0.	0.	0.	0.	0.	0.
20	0.	0.	0.	0.	0.	0.	0.	0.
21	0.	0.	0.	0.	0.	0.	0.	0.
22	0.	0.	0.	0.	0.	0.	0.	0.
23	0.	0.	0.	0.	0.	0.	0.	0.
24	0.	0.	0.	0.	0.	0.	0.	0.
25	0.	0.	0.	0.	0.	0.	0.	0.
26	0.	0.	0.	0.	0.	0.	0.	0.
27	0.	0.	0.	0.	0.	0.	0.	0.
28	0.	0.	0.	0.	0.	0.	0.	0.
29	0.	0.	0.	0.	0.	0.	0.	0.
30	0.	0.	0.	0.	0.	0.	0.	0.

TABLE V. - Continued. CROSS-SECTION DATA FOR ALUMINUM, CADMIUM, BORON 10, AND URANYL FLUORIDE SALT IN WATER FUEL SOLUTION

[Atom ratio of hydrogen to uranium 235; 500.]

(a) Continued. Group split A

TO \ FROM	17	18	19	20	21	22	23	24
1	0.	0.	0.	0.	0.	0.	0.	0.
2	0.	0.	0.	0.	0.	0.	0.	0.
3	0.	0.	0.	0.	0.	0.	0.	0.
4	0.	0.	0.	0.	0.	0.	0.	0.
5	0.	0.	0.	0.	0.	0.	0.	0.
6	0.	0.	0.	0.	0.	0.	0.	0.
7	0.	0.	0.	0.	0.	0.	0.	0.
8	0.	0.	0.	0.	0.	0.	0.	0.
9	0.	0.	0.	0.	0.	0.	0.	0.
10	0.	0.	0.	0.	0.	0.	0.	0.
11	0.	0.	0.	0.	0.	0.	0.	0.
12	0.	0.	0.	0.	0.	0.	0.	0.
13	0.	0.	0.	0.	0.	0.	0.	0.
14	0.	0.	0.	0.	0.	0.	0.	0.
15	0.	0.	0.	0.	0.	0.	0.	0.
16	0.	0.	0.	0.	0.	0.	0.	0.
17	0.	0.	0.	0.	0.	0.	0.	0.
18	8.80784E-01	0.	0.	0.	0.	0.	0.	0.
19	0.	3.11207E-01	0.	0.	0.	0.	0.	0.
20	0.	0.	6.10653E-01	0.	0.	0.	0.	0.
21	0.	0.	0.	7.61892E-01	0.	0.	0.	0.
22	0.	0.	0.	0.	7.63742E-01	0.	0.	0.
23	0.	0.	0.	0.	0.	7.64173E-01	0.	0.
24	0.	0.	0.	0.	0.	0.	7.65693E-01	0.
25	0.	0.	0.	0.	0.	0.	0.	7.65352E-01
26	0.	0.	0.	0.	0.	0.	0.	0.
27	0.	0.	0.	0.	0.	0.	0.	0.
28	0.	0.	0.	0.	0.	0.	0.	0.
29	0.	0.	0.	0.	0.	0.	0.	0.
30	0.	0.	0.	0.	0.	0.	0.	0.

TO \ FROM	25	26	27	28	29	30
1	0.	0.	0.	0.	0.	0.
2	0.	0.	0.	0.	0.	0.
3	0.	0.	0.	0.	0.	0.
4	0.	0.	0.	0.	0.	0.
5	0.	0.	0.	0.	0.	0.
6	0.	0.	0.	0.	0.	0.
7	0.	0.	0.	0.	0.	0.
8	0.	0.	0.	0.	0.	0.
9	0.	0.	0.	0.	0.	0.
10	0.	0.	0.	0.	0.	0.
11	0.	0.	0.	0.	0.	0.
12	0.	0.	0.	0.	0.	0.
13	0.	0.	0.	0.	0.	0.
14	0.	0.	0.	0.	0.	0.
15	0.	0.	0.	0.	0.	0.
16	0.	0.	0.	0.	0.	0.
17	0.	0.	0.	0.	0.	0.
18	0.	0.	0.	0.	0.	0.
19	0.	0.	0.	0.	0.	0.
20	0.	0.	0.	0.	0.	0.
21	0.	0.	0.	0.	0.	0.
22	0.	0.	0.	0.	0.	0.
23	0.	0.	0.	0.	0.	0.
24	0.	0.	0.	0.	0.	0.
25	0.	0.	0.	0.	0.	0.
26	7.64917E-01	0.	0.	0.	0.	0.
27	0.	7.60940E-01	0.	0.	0.	0.
28	0.	0.	7.62974E-01	0.	0.	0.
29	0.	0.	0.	7.63467E-01	0.	0.
30	0.	0.	0.	0.	7.47149E-01	0.

TABLE V. - Continued. CROSS-SECTION DATA FOR ALUMINUM, CADMIUM, BORON 10, AND URANYL FLUORIDE SALT IN WATER FUEL SOLUTION

[Atom ratio of hydrogen to uranium 235; 500.]

(a) Continued. Group split A

P(1) TRANSFER MATRIX AL

TO \ FROM	1	2	3	4	5	6	7	8
1	0.	0.	0.	0.	0.	0.	0.	0.
2	-1.63580E-02	0.	0.	0.	0.	0.	0.	0.
3	0.	-2.36560E-02	0.	0.	0.	0.	0.	0.
4	0.	0.	-4.38590E-02	0.	0.	0.	0.	0.
5	0.	0.	0.	-4.36720E-02	0.	0.	0.	0.
6	0.	0.	0.	0.	-7.83300E-02	0.	0.	0.
7	0.	0.	0.	0.	0.	-1.37149E-01	0.	0.
8	0.	0.	0.	0.	0.	0.	-1.81900E-01	0.
9	0.	0.	0.	0.	0.	0.	0.	-1.98004E-01
10	0.	0.	0.	0.	0.	0.	0.	0.
11	0.	0.	0.	0.	0.	0.	0.	0.
12	0.	0.	0.	0.	0.	0.	0.	0.
13	0.	0.	0.	0.	0.	0.	0.	0.
14	0.	0.	0.	0.	0.	0.	0.	0.
15	0.	0.	0.	0.	0.	0.	0.	0.
16	0.	0.	0.	0.	0.	0.	0.	0.
17	0.	0.	0.	0.	0.	0.	0.	0.
18	0.	0.	0.	0.	0.	0.	0.	0.
19	0.	0.	0.	0.	0.	0.	0.	0.
20	0.	0.	0.	0.	0.	0.	0.	0.
21	0.	0.	0.	0.	0.	0.	0.	0.
22	0.	0.	0.	0.	0.	0.	0.	0.
23	0.	0.	0.	0.	0.	0.	0.	0.
24	0.	0.	0.	0.	0.	0.	0.	0.
25	0.	0.	0.	0.	0.	0.	0.	0.
26	0.	0.	0.	0.	0.	0.	0.	0.
27	0.	0.	0.	0.	0.	0.	0.	0.
28	0.	0.	0.	0.	0.	0.	0.	0.
29	0.	0.	0.	0.	0.	0.	0.	0.
30	0.	0.	0.	0.	0.	0.	0.	0.

TO \ FROM	9	10	11	12	13	14	15	16
1	0.	0.	0.	0.	0.	0.	0.	0.
2	0.	0.	0.	0.	0.	0.	0.	0.
3	0.	0.	0.	0.	0.	0.	0.	0.
4	0.	0.	0.	0.	0.	0.	0.	0.
5	0.	0.	0.	0.	0.	0.	0.	0.
6	0.	0.	0.	0.	0.	0.	0.	0.
7	0.	0.	0.	0.	0.	0.	0.	0.
8	0.	0.	0.	0.	0.	0.	0.	0.
9	0.	0.	0.	0.	0.	0.	0.	0.
10	-2.34720E-01	0.	0.	0.	0.	0.	0.	0.
11	0.	-4.23014E-01	0.	0.	0.	0.	0.	0.
12	0.	0.	-5.42407E-01	0.	0.	0.	0.	0.
13	0.	0.	0.	-5.83042E-01	0.	0.	0.	0.
14	0.	0.	0.	0.	-9.63334E-01	0.	0.	0.
15	0.	0.	0.	0.	0.	-8.24149E-01	0.	0.
16	0.	0.	0.	0.	0.	0.	-1.73827E 00	0.
17	0.	0.	0.	0.	0.	0.	0.	-9.27291E-01
18	0.	0.	0.	0.	0.	0.	0.	0.
19	0.	0.	0.	0.	0.	0.	0.	0.
20	0.	0.	0.	0.	0.	0.	0.	0.
21	0.	0.	0.	0.	0.	0.	0.	0.
22	0.	0.	0.	0.	0.	0.	0.	0.
23	0.	0.	0.	0.	0.	0.	0.	0.
24	0.	0.	0.	0.	0.	0.	0.	0.
25	0.	0.	0.	0.	0.	0.	0.	0.
26	0.	0.	0.	0.	0.	0.	0.	0.
27	0.	0.	0.	0.	0.	0.	0.	0.
28	0.	0.	0.	0.	0.	0.	0.	0.
29	0.	0.	0.	0.	0.	0.	0.	0.
30	0.	0.	0.	0.	0.	0.	0.	0.

TABLE V. - Continued. CROSS-SECTION DATA FOR ALUMINUM, CADMIUM, BORON 10, AND URANYL FLUORIDE SALT IN WATER FUEL SOLUTION

[Atom ratio of hydrogen to uranium 235; 500.]

(a) Continued. Group split A

TO \ FROM	17	18	19	20	21	22	23	24
1	0.	0.	0.	0.	0.	0.	0.	0.
2	0.	0.	0.	0.	0.	0.	0.	0.
3	0.	0.	0.	0.	0.	0.	0.	0.
4	0.	0.	0.	0.	0.	0.	0.	0.
5	0.	0.	0.	0.	0.	0.	0.	0.
6	0.	0.	0.	0.	0.	0.	0.	0.
7	0.	0.	0.	0.	0.	0.	0.	0.
8	0.	0.	0.	0.	0.	0.	0.	0.
9	0.	0.	0.	0.	0.	0.	0.	0.
10	0.	0.	0.	0.	0.	0.	0.	0.
11	0.	0.	0.	0.	0.	0.	0.	0.
12	0.	0.	0.	0.	0.	0.	0.	0.
13	0.	0.	0.	0.	0.	0.	0.	0.
14	0.	0.	0.	0.	0.	0.	0.	0.
15	0.	0.	0.	0.	0.	0.	0.	0.
16	0.	0.	0.	0.	0.	0.	0.	0.
17	0.	0.	0.	0.	0.	0.	0.	0.
18	-2.54553E-01	0.	0.	0.	0.	0.	0.	0.
19	0.	-3.71260E-07	0.	0.	0.	0.	0.	0.
20	0.	0.	-6.98990E-02	0.	0.	0.	0.	0.
21	0.	0.	0.	-9.30530E-02	0.	0.	0.	0.
22	0.	0.	0.	0.	-9.41690E-02	0.	0.	0.
23	0.	0.	0.	0.	0.	-9.47850E-02	0.	0.
24	0.	0.	0.	0.	0.	0.	-9.54000E-02	0.
25	0.	0.	0.	0.	0.	0.	0.	-9.55790E-02
26	0.	0.	0.	0.	0.	0.	0.	0.
27	0.	0.	0.	0.	0.	0.	0.	0.
28	0.	0.	0.	0.	0.	0.	0.	0.
29	0.	0.	0.	0.	0.	0.	0.	0.
30	0.	0.	0.	0.	0.	0.	0.	0.

TO \ FROM	25	26	27	28	29	30
1	0.	0.	0.	0.	0.	0.
2	0.	0.	0.	0.	0.	0.
3	0.	0.	0.	0.	0.	0.
4	0.	0.	0.	0.	0.	0.
5	0.	0.	0.	0.	0.	0.
6	0.	0.	0.	0.	0.	0.
7	0.	0.	0.	0.	0.	0.
8	0.	0.	0.	0.	0.	0.
9	0.	0.	0.	0.	0.	0.
10	0.	0.	0.	0.	0.	0.
11	0.	0.	0.	0.	0.	0.
12	0.	0.	0.	0.	0.	0.
13	0.	0.	0.	0.	0.	0.
14	0.	0.	0.	0.	0.	0.
15	0.	0.	0.	0.	0.	0.
16	0.	0.	0.	0.	0.	0.
17	0.	0.	0.	0.	0.	0.
18	0.	0.	0.	0.	0.	0.
19	0.	0.	0.	0.	0.	0.
20	0.	0.	0.	0.	0.	0.
21	0.	0.	0.	0.	0.	0.
22	0.	0.	0.	0.	0.	0.
23	0.	0.	0.	0.	0.	0.
24	0.	0.	0.	0.	0.	0.
25	0.	0.	0.	0.	0.	0.
26	-9.57190E-02	0.	0.	0.	0.	0.
27	0.	-9.49650E-02	0.	0.	0.	0.
28	0.	0.	-9.53680E-02	0.	0.	0.
29	0.	0.	0.	-9.54450E-02	0.	-0.
30	0.	0.	0.	0.	-9.23300E-02	0.

TABLE V. - Continued. CROSS-SECTION DATA FOR ALUMINUM, CADMIUM, BORON 10, AND URANYL FLUORIDE SALT IN WATER FUEL SOLUTION

[Atom ratio of hydrogen to uranium 235; 500.]

(a) Continued. Group split A

P(1) TRANSFER MATRIX CD

FROM / TO	1	2	3	4	5	6	7	8
1	0.	0.	0.	0.	0.	0.	0.	0.
2	5.43960E-02	0.	0.	0.	0.	0.	0.	0.
3	0.	3.17400E-02	0.	0.	0.	0.	0.	0.
4	0.	0.	1.42000E-04	0.	0.	0.	0.	0.
5	0.	0.	0.	-1.45720E-02	0.	0.	0.	0.
6	0.	0.	0.	0.	-3.53130E-02	0.	0.	0.
7	0.	0.	0.	0.	0.	-3.85700E-02	0.	0.
8	0.	0.	0.	0.	0.	0.	-4.35830E-02	0.
9	0.	0.	0.	0.	0.	0.	0.	-4.62220E-02
10	0.	0.	0.	0.	0.	0.	0.	0.
11	0.	0.	0.	0.	0.	0.	0.	0.
12	0.	0.	0.	0.	0.	0.	0.	0.
13	0.	0.	0.	0.	0.	0.	0.	0.
14	0.	0.	0.	0.	0.	0.	0.	0.
15	0.	0.	0.	0.	0.	0.	0.	0.
16	0.	0.	0.	0.	0.	0.	0.	0.
17	0.	0.	0.	0.	0.	0.	0.	0.
18	0.	0.	0.	0.	0.	0.	0.	0.
19	0.	0.	0.	0.	0.	0.	0.	0.
20	0.	0.	0.	0.	0.	0.	0.	0.
21	0.	0.	0.	0.	0.	0.	0.	0.
22	0.	0.	0.	0.	0.	0.	0.	0.
23	0.	0.	0.	0.	0.	0.	0.	0.
24	0.	0.	0.	0.	0.	0.	0.	0.
25	0.	0.	0.	0.	0.	0.	0.	0.
26	0.	0.	0.	0.	0.	0.	0.	0.
27	0.	0.	0.	0.	0.	0.	0.	0.
28	0.	0.	0.	0.	0.	0.	0.	0.
29	0.	0.	0.	0.	0.	0.	0.	0.
30	0.	0.	0.	0.	0.	0.	0.	0.

FROM / TO	9	10	11	12	13	14	15	16
1	0.	0.	0.	0.	0.	0.	0.	0.
2	0.	0.	0.	0.	0.	0.	0.	0.
3	0.	0.	0.	0.	0.	0.	0.	0.
4	0.	0.	0.	0.	0.	0.	0.	0.
5	0.	0.	0.	0.	0.	0.	0.	0.
6	0.	0.	0.	0.	0.	0.	0.	0.
7	0.	0.	0.	0.	0.	0.	0.	0.
8	0.	0.	0.	0.	0.	0.	0.	0.
9	0.	0.	0.	0.	0.	0.	0.	0.
10	-4.71330E-02	0.	0.	0.	0.	0.	0.	0.
11	0.	-8.24310E-02	0.	0.	0.	0.	0.	0.
12	0.	0.	-1.05307E-01	0.	0.	0.	0.	0.
13	0.	0.	0.	-1.35722E-01	0.	0.	0.	0.
14	0.	0.	0.	0.	-2.01034E-01	0.	0.	0.
15	0.	0.	0.	0.	0.	-2.46655E-01	0.	0.
16	0.	0.	0.	0.	0.	0.	-2.86664E-01	0.
17	0.	0.	0.	0.	0.	0.	0.	-3.18714E-01
18	0.	0.	0.	0.	0.	0.	0.	0.
19	0.	0.	0.	0.	0.	0.	0.	0.
20	0.	0.	0.	0.	0.	0.	0.	0.
21	0.	0.	0.	0.	0.	0.	0.	0.
22	0.	0.	0.	0.	0.	0.	0.	0.
23	0.	0.	0.	0.	0.	0.	0.	0.
24	0.	0.	0.	0.	0.	0.	0.	0.
25	0.	0.	0.	0.	0.	0.	0.	0.
26	0.	0.	0.	0.	0.	0.	0.	0.
27	0.	0.	0.	0.	0.	0.	0.	0.
28	0.	0.	0.	0.	0.	0.	0.	0.
29	0.	0.	0.	0.	0.	0.	0.	0.
30	0.	0.	0.	0.	0.	0.	0.	0.

TABLE V. - Continued. CROSS-SECTION DATA FOR ALUMINUM, CADMIUM, BORON 10, AND URANYL FLUORIDE SALT IN WATER FUEL SOLUTION

[Atom ratio of hydrogen to uranium 235; 500.]

(a) Continued. Group split A

TO \ FROM	17	18	19	20	21	22	23	24
1	0.	0.	0.	0.	0.	0.	0.	0.
2	0.	0.	0.	0.	0.	0.	0.	0.
3	0.	0.	0.	0.	0.	0.	0.	0.
4	0.	0.	0.	0.	0.	0.	0.	0.
5	0.	0.	0.	0.	0.	0.	0.	0.
6	0.	0.	0.	0.	0.	0.	0.	0.
7	0.	0.	0.	0.	0.	0.	0.	0.
8	0.	0.	0.	0.	0.	0.	0.	0.
9	0.	0.	0.	0.	0.	0.	0.	0.
10	0.	0.	0.	0.	0.	0.	0.	0.
11	0.	0.	0.	0.	0.	0.	0.	0.
12	0.	0.	0.	0.	0.	0.	0.	0.
13	0.	0.	0.	0.	0.	0.	0.	0.
14	0.	0.	0.	0.	0.	0.	0.	0.
15	0.	0.	0.	0.	0.	0.	0.	0.
16	0.	0.	0.	0.	0.	0.	0.	0.
17	0.	0.	0.	0.	0.	0.	0.	0.
18	-2.07160E-01	0.	0.	0.	0.	0.	0.	0.
19	0.	-9.78830E-02	0.	0.	0.	0.	0.	0.
20	0.	0.	-7.76010E-02	0.	0.	0.	0.	0.
21	0.	0.	0.	-7.53610E-02	0.	0.	0.	0.
22	0.	0.	0.	0.	-5.63700E-02	0.	0.	0.
23	0.	0.	0.	0.	0.	-1.60202E-01	0.	0.
24	0.	0.	0.	0.	0.	0.	-8.23020E-02	0.
25	0.	0.	0.	0.	0.	0.	0.	-7.23580E-02
26	0.	0.	0.	0.	0.	0.	0.	0.
27	0.	0.	0.	0.	0.	0.	0.	0.
28	0.	0.	0.	0.	0.	0.	0.	0.
29	0.	0.	0.	0.	0.	0.	0.	0.
30	0.	0.	0.	0.	0.	0.	0.	0.

TO \ FROM	25	26	27	28	29	30
1	0.	0.	0.	0.	0.	0.
2	0.	0.	0.	0.	0.	0.
3	0.	0.	0.	0.	0.	0.
4	0.	0.	0.	0.	0.	0.
5	0.	0.	0.	0.	0.	0.
6	0.	0.	0.	0.	0.	0.
7	0.	0.	0.	0.	0.	0.
8	0.	0.	0.	0.	0.	0.
9	0.	0.	0.	0.	0.	0.
10	0.	0.	0.	0.	0.	0.
11	0.	0.	0.	0.	0.	0.
12	0.	0.	0.	0.	0.	0.
13	0.	0.	0.	0.	0.	0.
14	0.	0.	0.	0.	0.	0.
15	0.	0.	0.	0.	0.	0.
16	0.	0.	0.	0.	0.	0.
17	0.	0.	0.	0.	0.	0.
18	0.	0.	0.	0.	0.	0.
19	0.	0.	0.	0.	0.	0.
20	0.	0.	0.	0.	0.	0.
21	0.	0.	0.	0.	0.	0.
22	0.	0.	0.	0.	0.	0.
23	0.	0.	0.	0.	0.	0.
24	0.	0.	0.	0.	0.	0.
25	0.	0.	0.	0.	0.	0.
26	-7.24660E-02	0.	0.	0.	0.	0.
27	0.	-6.68790E-02	0.	0.	0.	0.
28	0.	0.	-6.71610E-02	0.	0.	0.
29	0.	0.	0.	-8.48610E-02	0.	-0.
30	0.	0.	0.	0.	-1.46300E-01	0.

TABLE V. - Continued. CROSS-SECTION DATA FOR ALUMINUM, CADMIUM, BORON 10, AND URANYL FLUORIDE SALT IN WATER FUEL SOLUTION

[Atom ratio of hydrogen to uranium 235; 500.]

(a) Continued Group split A

P(1) TRANSFER MATRIX UO2F2

FROM / TO	1	2	3	4	5	6	7	8
1	0.	0.	0.	0.	0.	0.	0.	0.
2	3.66340E-02	0.	0.	0.	0.	0.	0.	0.
3	2.24150E-02	4.75840E-02	0.	0.	0.	0.	0.	0.
4	1.42920E-02	2.84770E-02	5.14820E-02	0.	0.	0.	0.	0.
5	9.11300E-03	1.81580E-02	3.49710E-02	5.66480E-02	0.	0.	0.	0.
6	5.81100E-03	1.15780E-02	2.22990E-02	4.24340E-02	4.95090E-02	0.	0.	0.
7	3.70500E-03	7.38200E-03	1.42180E-02	2.70570E-02	5.22580E-02	9.25860E-02	0.	0.
8	2.36200E-03	4.70700E-03	9.06600E-03	1.72520E-02	3.33210E-02	6.21050E-02	8.48780E-02	0.
9	1.50600E-03	3.00100E-03	5.78100E-03	1.10010E-02	2.12470E-02	3.96000E-02	7.30490E-02	9.93400E-02
10	9.61000E-04	1.91400E-03	3.68600E-03	7.01400E-03	1.35470E-02	2.52500E-02	4.65780E-02	8.60040E-02
11	6.12000E-04	1.22000E-03	2.35000E-03	4.47300E-03	8.63800E-03	1.61000E-02	2.97000E-02	5.48380E-02
12	3.91000E-04	7.78000E-04	1.49900E-03	2.85200E-03	5.50800E-03	1.02660E-02	1.89370E-02	3.49660E-02
13	2.49000E-04	4.96000E-04	9.56000E-04	1.81800E-03	3.51200E-03	6.54600E-03	1.20750E-02	2.22960E-02
14	1.59000E-04	3.16000E-04	6.09000E-04	1.15900E-03	2.23900E-03	4.17400E-03	7.69900E-03	1.42160E-02
15	1.01000E-04	2.02000E-04	3.88000E-04	7.39000E-04	1.42800E-03	2.66100E-03	4.90900E-03	9.06500E-03
16	6.50000E-05	1.29000E-04	2.48000E-04	4.71000E-04	9.10000E-04	1.69700E-03	3.13000E-03	5.78000E-03
17	6.00000E-05	1.19000E-04	2.30000E-04	4.38000E-04	8.45000E-04	1.57500E-03	2.90600E-03	5.36600E-03
18	4.20000E-05	8.30000E-05	1.60000E-04	3.04000E-04	5.88000E-04	1.09600E-03	2.02100E-03	3.73200E-03
19	9.00000E-06	1.90000E-05	3.60000E-05	6.80000E-05	1.31000E-04	2.44000E-04	4.51000E-04	8.33000E-04
20	2.00000E-06	4.00000E-06	8.00000E-06	1.50000E-05	2.90000E-05	5.50000E-05	1.01000E-04	1.86000E-04
21	0.	1.00000E-06	2.00000E-06	3.00000E-06	7.00000E-06	1.20000E-05	2.20000E-05	4.10000E-05
22	0.	0.	0.	1.00000E-06	1.00000E-06	3.00000E-06	5.00000E-06	9.00000E-06
23	0.	0.	0.	0.	0.	1.00000E-06	1.00000E-06	2.00000E-06
24	0.	0.	0.	0.	0.	0.	0.	0.
25	0.	0.	0.	0.	0.	0.	0.	0.
26	0.	0.	0.	0.	0.	0.	0.	0.
27	0.	0.	0.	0.	0.	0.	0.	0.
28	0.	0.	0.	0.	0.	0.	0.	0.
29	0.	0.	0.	0.	0.	0.	0.	0.
30	0.	0.	0.	0.	0.	0.	0.	0.

FROM / TO	9	10	11	12	13	14	15	16
1	0.	0.	0.	0.	0.	0.	0.	0.
2	0.	0.	0.	0.	0.	0.	0.	0.
3	0.	0.	0.	0.	0.	0.	0.	0.
4	0.	0.	0.	0.	0.	0.	0.	0.
5	0.	0.	0.	0.	0.	0.	0.	0.
6	0.	0.	0.	0.	0.	0.	0.	0.
7	0.	0.	0.	0.	0.	0.	0.	0.
8	0.	0.	0.	0.	0.	0.	0.	0.
9	0.	0.	0.	0.	0.	0.	0.	0.
10	5.67650E-02	0.	0.	0.	0.	0.	0.	0.
11	9.92890E-02	1.67390E-01	0.	0.	0.	0.	0.	0.
12	6.33090E-02	1.20000E-01	2.20879E-01	0.	0.	0.	0.	0.
13	4.03680E-02	7.65160E-02	1.39931E-01	1.10390E-01	0.	0.	0.	0.
14	2.57400E-02	4.87890E-02	8.92240E-02	1.64841E-01	2.32288E-01	0.	0.	0.
15	1.64120E-02	3.11090E-02	5.68920E-02	1.05107E-01	1.90662E-01	2.88981E-01	0.	0.
16	1.04650E-02	1.98360E-02	3.62760E-02	6.70190E-02	1.21572E-01	2.18783E-01	3.36322E-01	0.
17	9.71600E-03	1.84160E-02	3.36790E-02	6.22220E-02	1.12870E-01	2.03123E-01	3.57761E-01	5.96032E-01
18	6.75700E-03	1.28080E-02	2.34240E-02	4.32750E-02	7.85000E-02	1.41271E-01	2.48822E-01	4.46968E-01
19	1.50800E-03	2.85800E-03	5.22700E-03	9.65600E-03	1.75160E-02	3.15220E-02	5.55200E-02	9.97320E-02
20	3.36000E-04	6.38000E-04	1.16600E-03	2.15500E-03	3.90800E-03	7.03300E-03	1.23880E-02	2.22530E-02
21	7.50000E-05	1.42000E-04	2.60000E-04	4.81000E-04	8.72000E-04	1.56900E-03	2.76400E-03	4.96500E-03
22	1.70000E-05	3.20000E-05	5.80000E-05	1.07000E-04	1.95000E-04	3.50000E-04	6.17000E-04	1.10800E-03
23	4.00000E-06	7.00000E-06	1.30000E-05	2.40000E-05	4.30000E-05	7.80000E-05	1.38000E-04	2.47000E-04
24	1.00000E-06	2.00000E-06	3.00000E-06	5.00000E-06	1.00000E-05	1.70000E-05	3.10000E-05	5.50000E-05
25	0.	0.	1.00000E-06	1.00000E-06	2.00000E-06	4.00000E-06	7.00000E-06	1.20000E-05
26	0.	0.	0.	0.	0.	1.00000E-06	2.00000E-06	3.00000E-06
27	0.	0.	0.	0.	0.	0.	0.	1.00000E-06
28	0.	0.	0.	0.	0.	0.	0.	0.
29	0.	0.	0.	0.	0.	0.	0.	0.
30	0.	0.	0.	0.	0.	0.	0.	0.

TABLE V. - Continued. CROSS-SECTION DATA FOR ALUMINUM, CADMIUM, BORON 10, AND URANYL FLUORIDE SALT IN WATER FUEL SOLUTION

[Atom ratio of hydrogen to uranium 235; 500.]

(a) Continued. Group split A

FROM / TO	17	18	19	20	21	22	23	24
1	0.	0.	0.	0.	0.	0.	0.	0.
2	0.	0.	0.	0.	0.	0.	0.	0.
3	0.	0.	0.	0.	0.	0.	0.	0.
4	0.	0.	0.	0.	0.	0.	0.	0.
5	0.	0.	0.	0.	0.	0.	0.	0.
6	0.	0.	0.	0.	0.	0.	0.	0.
7	0.	0.	0.	0.	0.	0.	0.	0.
8	0.	0.	0.	0.	0.	0.	0.	0.
9	0.	0.	0.	0.	0.	0.	0.	0.
10	0.	0.	0.	0.	0.	0.	0.	0.
11	0.	0.	0.	0.	0.	0.	0.	0.
12	0.	0.	0.	0.	0.	0.	0.	0.
13	0.	0.	0.	0.	0.	0.	0.	0.
14	0.	0.	0.	0.	0.	0.	0.	0.
15	0.	0.	0.	0.	0.	0.	0.	0.
16	0.	0.	0.	0.	0.	0.	0.	0.
17	0.	0.	0.	0.	0.	0.	0.	0.
18	9.25050E-01	0.	0.	0.	0.	0.	0.	0.
19	2.12105E-01	8.22309E-01	0.	0.	0.	0.	0.	0.
20	4.73270E-02	1.86123E-01	9.55187E-01	0.	0.	0.	0.	0.
21	1.05600E-02	4.15300E-02	2.15816E-01	1.01338E 00	0.	0.	0.	0.
22	2.35600E-03	9.26700E-03	4.81550E-02	2.29013E-01	1.03232E 00	0.	0.	0.
23	5.26000E-04	2.06800E-03	1.07450E-02	5.11000E-02	2.33303E-01	1.04803E 00	0.	0.
24	1.17000E-04	4.61000E-04	2.39700E-03	1.14020E-02	5.20570E-02	2.36848E-01	1.05767E 00	0.
25	2.60000E-05	1.03000E-04	5.35000E-04	2.54400E-03	1.16150E-02	5.28480E-02	2.39018E-01	1.06291E 00
26	6.00000E-06	2.30000E-05	1.19000E-04	5.68000E-04	2.59200E-03	1.17920E-02	5.33320E-02	2.40192E-01
27	1.00000E-06	5.00000E-06	2.70000E-05	1.27000E-04	5.78000E-04	2.63100E-03	1.19000E-02	5.35940E-02
28	0.	1.00000E-06	6.00000E-06	2.80000E-05	1.29000E-04	5.87000E-04	2.65500E-03	1.19580E-02
29	0.	0.	1.00000E-06	6.00000E-06	2.90000E-05	1.31000E-04	5.92000E-04	2.66800E-03
30	0.	0.	0.	2.00000E-06	8.00000E-06	3.80000E-05	1.70000E-04	7.65000E-04

FROM / TO	25	26	27	28	29	30
1	0.	0.	0.	0.	0.	0.
2	0.	0.	0.	0.	0.	0.
3	0.	0.	0.	0.	0.	0.
4	0.	0.	0.	0.	0.	0.
5	0.	0.	0.	0.	0.	0.
6	0.	0.	0.	0.	0.	0.
7	0.	0.	0.	0.	0.	0.
8	0.	0.	0.	0.	0.	0.
9	0.	0.	0.	0.	0.	0.
10	0.	0.	0.	0.	0.	0.
11	0.	0.	0.	0.	0.	0.
12	0.	0.	0.	0.	0.	0.
13	0.	0.	0.	0.	0.	0.
14	0.	0.	0.	0.	0.	0.
15	0.	0.	0.	0.	0.	0.
16	0.	0.	0.	0.	0.	0.
17	0.	0.	0.	0.	0.	0.
18	0.	0.	0.	0.	0.	0.
19	0.	0.	0.	0.	0.	0.
20	0.	0.	0.	0.	0.	0.
21	0.	0.	0.	0.	0.	0.
22	0.	0.	0.	0.	0.	0.
23	0.	0.	0.	0.	0.	0.
24	0.	0.	0.	0.	0.	0.
25	0.	0.	0.	0.	0.	0.
26	1.06883E 00	0.	0.	0.	0.	0.
27	2.41514E-01	1.07147E 00	0.	0.	0.	0.
28	5.38890E-02	2.42080E-01	1.09032E 00	0.	0.	0.
29	1.20240E-02	5.40150E-02	2.46299E-01	1.10111E 00	0.	4.95400E-03
30	3.44800E-03	1.54880E-02	7.06200E-02	3.19596E-01	1.45509E 00	0.

TABLE V. - Continued. CROSS-SECTION DATA FOR ALUMINUM, CADMIUM, BORON 10, AND URANYL FLUORIDE SALT IN WATER FUEL SOLUTIONS

[Atom ratio of hydrogen to uranium 235; 500.]

(a) Continued. Group split A

P(1) TRANSFER MATRIX B-10

TO \ FROM	1	2	3	4	5	6	7	8
1	0.	0.	0.	0.	0.	0.	0.	0.
2	2.63418E-01	0.	0.	0.	0.	0.	0.	0.
3	-1.99760E-02	2.32552E-01	0.	0.	0.	0.	0.	0.
4	0.	-3.25480E-02	1.18680E-01	0.	0.	0.	0.	0.
5	0.	0.	-5.22330E-02	-7.29520E-02	0.	0.	0.	0.
6	0.	0.	0.	-9.58400E-02	-3.76575E-01	0.	0.	0.
7	0.	0.	0.	0.	-2.68623E-01	-1.04837E 00	0.	0.
8	0.	0.	0.	0.	0.	-2.50751E-01	-6.47246E-01	0.
9	0.	0.	0.	0.	0.	0.	-1.68875E-01	-8.09462E-01
10	0.	0.	0.	0.	0.	0.	0.	-1.97298E-01
11	0.	0.	0.	0.	0.	0.	0.	0.
12	0.	0.	0.	0.	0.	0.	0.	0.
13	0.	0.	0.	0.	0.	0.	0.	0.
14	0.	0.	0.	0.	0.	0.	0.	0.
15	0.	0.	0.	0.	0.	0.	0.	0.
16	0.	0.	0.	0.	0.	0.	0.	0.
17	0.	0.	0.	0.	0.	0.	0.	0.
18	0.	0.	0.	0.	0.	0.	0.	0.
19	0.	0.	0.	0.	0.	0.	0.	0.
20	0.	0.	0.	0.	0.	0.	0.	0.
21	0.	0.	0.	0.	0.	0.	0.	0.
22	0.	0.	0.	0.	0.	0.	0.	0.
23	0.	0.	0.	0.	0.	0.	0.	0.
24	0.	0.	0.	0.	0.	0.	0.	0.
25	0.	0.	0.	0.	0.	0.	0.	0.
26	0.	0.	0.	0.	0.	0.	0.	0.
27	0.	0.	0.	0.	0.	0.	0.	0.
28	0.	0.	0.	0.	0.	0.	0.	0.
29	0.	0.	0.	0.	0.	0.	0.	0.
30	0.	0.	0.	0.	0.	0.	0.	0.

TO \ FROM	9	10	11	12	13	14	15	16
1	0.	0.	0.	0.	0.	0.	0.	0.
2	0.	0.	0.	0.	0.	0.	0.	0.
3	0.	0.	0.	0.	0.	0.	0.	0.
4	0.	0.	0.	0.	0.	0.	0.	0.
5	0.	0.	0.	0.	0.	0.	0.	0.
6	0.	0.	0.	0.	0.	0.	0.	0.
7	0.	0.	0.	0.	0.	0.	0.	0.
8	0.	0.	0.	0.	0.	0.	0.	0.
9	0.	0.	0.	0.	0.	0.	0.	0.
10	-7.98059E-01	0.	0.	0.	0.	0.	0.	0.
11	-1.97013E-01	-6.93568E-01	0.	0.	0.	0.	0.	0.
12	0.	-2.08509E-01	-6.87140E-01	0.	0.	0.	0.	0.
13	0.	0.	-2.10711E-01	-8.87616E-01	0.	0.	0.	0.
14	0.	0.	0.	-3.30623E-01	-1.14651E 00	0.	0.	0.
15	0.	0.	0.	0.	-3.31991E-01	-1.33235E 00	0.	0.
16	0.	0.	0.	0.	0.	-3.20541E-01	-1.29742E 00	0.
17	0.	0.	0.	0.	0.	0.	-2.89566E-01	-1.38916E 00
18	0.	0.	0.	0.	0.	0.	0.	0.
19	0.	0.	0.	0.	0.	0.	0.	0.
20	0.	0.	0.	0.	0.	0.	0.	0.
21	0.	0.	0.	0.	0.	0.	0.	0.
22	0.	0.	0.	0.	0.	0.	0.	0.
23	0.	0.	0.	0.	0.	0.	0.	0.
24	0.	0.	0.	0.	0.	0.	0.	0.
25	0.	0.	0.	0.	0.	0.	0.	0.
26	0.	0.	0.	0.	0.	0.	0.	0.
27	0.	0.	0.	0.	0.	0.	0.	0.
28	0.	0.	0.	0.	0.	0.	0.	0.
29	0.	0.	0.	0.	0.	0.	0.	0.
30	0.	0.	0.	0.	0.	0.	0.	0.

TABLE V. - Continued. CROSS-SECTION DATA FOR ALUMINUM, CADMIUM, BORON 10, AND URANYL FLUORIDE SALT IN WATER FUEL SOLUTIONS

[Atom ratio of hydrogen to uranium 235; 500.]

(a) Concluded. Group split A

FROM TO	17	18	19	20	21	22	23	24
1	0.	0.	0.	0.	0.	0.	0.	0.
2	0.	0.	0.	0.	0.	0.	0.	0.
3	0.	0.	0.	0.	0.	0.	0.	0.
4	0.	0.	0.	0.	0.	0.	0.	0.
5	0.	0.	0.	0.	0.	0.	0.	0.
6	0.	0.	0.	0.	0.	0.	0.	0.
7	0.	0.	0.	0.	0.	0.	0.	0.
8	0.	0.	0.	0.	0.	0.	0.	0.
9	0.	0.	0.	0.	0.	0.	0.	0.
10	0.	0.	0.	0.	0.	0.	0.	0.
11	0.	0.	0.	0.	0.	0.	0.	0.
12	0.	0.	0.	0.	0.	0.	0.	0.
13	0.	0.	0.	0.	0.	0.	0.	0.
14	0.	0.	0.	0.	0.	0.	0.	0.
15	0.	0.	0.	0.	0.	0.	0.	0.
16	0.	0.	0.	0.	0.	0.	0.	0.
17	0.	0.	0.	0.	0.	0.	0.	0.
18	-7.75699E-01	0.	0.	0.	0.	0.	0.	0.
19	0.	-2.62523E-01	0.	0.	0.	0.	0.	0.
20	0.	0.	-4.81639E-01	0.	0.	0.	0.	0.
21	0.	0.	0.	-6.42895E-01	0.	0.	0.	0.
22	0.	0.	0.	0.	-6.49626E-01	0.	0.	0.
23	0.	0.	0.	0.	0.	-6.52842E-01	0.	0.
24	0.	0.	0.	0.	0.	0.	-6.56099E-01	0.
25	0.	0.	0.	0.	0.	0.	0.	-6.57465E-01
26	0.	0.	0.	0.	0.	0.	0.	0.
27	0.	0.	0.	0.	0.	0.	0.	0.
28	0.	0.	0.	0.	0.	0.	0.	0.
29	0.	0.	0.	0.	0.	0.	0.	0.
30	0.	0.	0.	0.	0.	0.	0.	0.

FROM TO	25	26	27	28	29	30
1	0.	0.	0.	0.	0.	0.
2	0.	0.	0.	0.	0.	0.
3	0.	0.	0.	0.	0.	0.
4	0.	0.	0.	0.	0.	0.
5	0.	0.	0.	0.	0.	0.
6	0.	0.	0.	0.	0.	0.
7	0.	0.	0.	0.	0.	0.
8	0.	0.	0.	0.	0.	0.
9	0.	0.	0.	0.	0.	0.
10	0.	0.	0.	0.	0.	0.
11	0.	0.	0.	0.	0.	0.
12	0.	0.	0.	0.	0.	0.
13	0.	0.	0.	0.	0.	0.
14	0.	0.	0.	0.	0.	0.
15	0.	0.	0.	0.	0.	0.
16	0.	0.	0.	0.	0.	0.
17	0.	0.	0.	0.	0.	0.
18	0.	0.	0.	0.	0.	0.
19	0.	0.	0.	0.	0.	0.
20	0.	0.	0.	0.	0.	0.
21	0.	0.	0.	0.	0.	0.
22	0.	0.	0.	0.	0.	0.
23	0.	0.	0.	0.	0.	0.
24	0.	0.	0.	0.	0.	0.
25	0.	0.	0.	0.	0.	0.
26	-6.56978E-01	0.	0.	0.	0.	0.
27	0.	-6.54951E-01	0.	0.	0.	0.
28	0.	0.	-6.56756E-01	0.	0.	0.
29	0.	0.	0.	-6.57161E-01	0.	0.
30	0.	0.	0.	0.	-6.39973E-01	0.

TABLE V. - Continued. CROSS-SECTION DATA FOR ALUMINUM, CADMIUM, BORON 10, AND URANYL FLUORIDE SALT IN WATER FUEL SOLUTIONS

[Atom ratio of hydrogen to uranium 235; 500.]

(b) Group split B.

ELEMENT 1 AL NGDS 12 NGF 5 NGOST 1 NGDSPI 1 NGUS 1 VSTART 29

GROUP	SIG	SIGSO(G-G)	SIGSI(G-G)	SIGA	ANUSIG	ALPHA	SIGTR
1	1.9179790	0.9268170	1.7458070	0.0945410	0.	-0.	1.3310170
2	2.2684980	1.3222190	2.0739650	0.0192160	0.	-0.	1.5686210
3	2.7516480	2.0502860	2.8498530	0.0023920	0.	-0.	1.8120380
4	3.0464330	2.4494070	2.8824420	0.0004420	0.	-0.	2.1270360
5	3.3209170	2.6628740	2.6638480	0.0004030	0.	-0.	2.5017200
6	3.8545400	3.4707900	2.5941260	0.0006150	0.	-0.	3.0435570
7	3.8818540	3.6667400	1.4078830	0.0011770	0.	-0.	3.5104610
8	6.0826020	5.9715390	0.5819210	0.0034100	0.	-0.	6.0217560
9	5.5118000	5.4677730	0.4398210	0.0070780	0.	-0.	5.3564660
10	0.8633550	0.7827630	0.1331620	0.0030380	0.	-0.	0.8293250
11	2.1692990	2.0628290	0.2536580	0.0052620	0.	-0.	2.1163510
12	1.4110220	1.3085820	0.1985690	0.0009980	0.	-0.	1.3783430
13	1.4113900	1.3085110	0.1991850	0.0013670	0.	-0.	1.3781940
14	1.4121340	1.2743170	0.2319240	0.0021100	0.	-0.	1.3784150
15	1.4131000	1.2741860	0.2322380	0.0030760	0.	-0.	1.3790480
16	1.4144950	1.2746950	0.2317560	0.0044710	0.	-0.	1.3806550
17	1.4165280	1.2742780	0.2324130	0.0065050	0.	-0.	1.3824360
18	1.4188900	1.2055350	0.2977420	0.0088660	0.	-0.	1.3846580
19	1.4214050	1.2069250	0.2958820	0.0113810	0.	-0.	1.3882760
20	1.4246410	1.2065690	0.2963370	0.0146170	0.	-0.	1.3906500
21	1.4287900	1.2065820	0.2963020	0.0187660	0.	-0.	1.3947820
22	1.4326240	1.0017470	0.4901470	0.0226000	0.	-0.	1.3980600
23	1.4356340	1.0017470	0.4901470	0.0256100	0.	-0.	1.4016450
24	1.4390340	1.0017470	0.4901480	0.0290100	0.	-0.	1.4046500
25	1.4429040	1.0017470	0.4901490	0.0328800	0.	-0.	1.4093300
26	1.4472840	1.0017460	0.4901470	0.0372600	0.	-0.	1.4139530
27	1.4522440	1.0017470	0.4901480	0.0422200	0.	-0.	1.4198750
28	1.4578630	1.0017470	0.4901470	0.0478400	0.	-0.	1.4274230
29	1.4642340	1.0017470	0.4901480	0.0542100	0.	-0.	1.4332060
30	1.5946260	1.4100000	0.2041380	0.1846260	-0.	-0.	1.5265800

ELEMENT 2 CD NGDS 12 NGF 8 NGOST 1 NGDSPI 1 NGUS 1 VSTART 29

GROUP	SIG	SIGSO(G-G)	SIGSI(G-G)	SIGA	ANUSIG	ALPHA	SIGTR
1	4.4554850	2.2227690	4.9920610	0.0134830	0.	-0.	2.8065080
2	4.1772110	2.0475330	3.6341830	0.0154250	0.	-0.	2.9613560
3	4.8055870	2.8784090	3.8969430	0.0207030	0.	-0.	3.5206700
4	5.9735520	4.4764890	5.6752050	0.0338630	0.	-0.	4.0588290
5	6.5989820	5.5274410	6.7084450	0.0582140	0.	-0.	4.3853210
6	7.1455250	6.3965760	6.5304110	0.0895590	0.	-0.	4.9837940
7	7.0323050	6.7399590	4.4948210	0.1123320	0.	-0.	5.5516590
8	7.0012380	6.7594940	1.6110870	0.1384470	0.	-0.	6.5014460
9	7.0107100	6.6110390	0.3221800	0.2917460	0.	-0.	6.9497210
10	6.9455700	5.9805990	0.1864480	0.8804170	0.	-0.	6.9339410
11	6.4421660	4.1409120	0.1502980	2.2202350	0.	-0.	6.4137000
12	6.5519190	3.9918970	0.1284360	2.5000000	0.	-0.	6.5419420
13	7.5672790	4.8976890	0.2499010	2.5000000	0.	-0.	7.4873800
14	6.9638240	4.3815180	0.2218000	2.4335220	0.	-0.	6.9579020
15	15.4519980	10.1706510	0.6205030	4.8274710	0.	-0.	15.2625390
16	13.9007510	4.2992010	0.1745740	9.5002820	0.	-0.	14.0171061
17	8.4574450	4.4645080	0.1780030	3.8913580	0.	-0.	8.4240050
18	4.6497700	3.8576820	0.2071960	0.6497430	0.	-0.	4.6298180
19	4.6995170	3.8586510	0.2058860	0.6994900	0.	-0.	4.6768040
20	4.9996920	3.8584040	0.2062140	0.9996650	0.	-0.	4.9764300
21	5.4495160	3.8584110	0.2061940	1.4494880	0.	-0.	5.4261470
22	6.3000280	3.8087200	0.3512650	2.2000000	0.	-0.	6.2736580
23	7.5000300	3.9945130	0.3683940	3.2000000	0.	-0.	7.4706340
24	9.7000310	4.2732020	0.3941120	5.1000000	0.	-0.	9.6663190
25	13.9500340	4.6912320	0.4326430	8.9000000	0.	-0.	13.9109470
26	23.4000421	5.5737340	0.5139590	17.4000001	0.	-0.	23.3443520
27	43.2000480	6.6884870	0.6168700	36.0000000	0.	-0.	43.1328211
28	81.8000622	8.3606020	0.7710510	72.7999983	0.	-0.	81.7115660
29	180.0000591	8.3606040	0.7710960	170.9999981	0.	-0.	179.9527493
30	3055.5466003	17.2365999	-259.9602890	3038.3099976	-0.	-0.	3142.2000122

TABLE V. - Continued. CROSS-SECTION DATA FOR ALUMINUM, CADMIUM, BORON 10, AND URANYL FLUORIDE SALT IN WATER FUEL SOLUTIONS

[Atom ratio of hydrogen to uranium 235; 500.]

(b) Continued. Group split B

ELEMENT 3 UO2F2 NGDS 29 NGF 30 NGDST 0 NGDSPI 29 NGUS 1 NSTART 29

GROUP	SIG	SIGSO(G-G)	SIGSI(G-G)	SIGA	ANUSIG	ALPHA	SIGTR
1	0.1265830	0.0429240	0.0946410	0.0061190	0.0007330	0.0232161	0.0965500
2	0.1770980	0.0628740	0.1286330	0.0020560	0.0004820	0.1082540	0.1253620
3	0.2079710	0.0743240	0.1182300	0.0001850	0.0004840	0.2104590	0.1510210
4	0.2854520	0.0982710	0.1599510	0.0001830	0.0004550	0.2314061	0.1722870
5	0.4210760	0.1688940	0.2237070	0.0001760	0.0004100	0.1804860	0.2290330
6	0.4654510	0.1671800	0.2927530	0.0001790	0.0003890	0.1148379	0.2375860
7	0.6989410	0.3518380	0.5289280	0.0002110	0.0004360	0.0988324	0.2959270
8	0.9094550	0.3979500	0.7860300	0.0002880	0.0005460	0.0255601	0.3305130
9	1.1771330	0.4954560	1.0566000	0.0003970	0.0007120	0.0060194	0.3880960
10	1.3374690	0.5536730	1.2139830	0.0005360	0.0009140	0.0009289	0.4420850
11	1.4099930	0.5813810	1.2793190	0.0009430	0.0013350	-0.	0.4849630
12	1.4331240	0.5911970	1.2956770	0.0013020	0.0020720	-0.	0.5150930
13	1.4529680	0.5988590	1.3110660	0.0022750	0.0034910	-0.	0.5362640
14	1.4643150	0.5023210	1.1028150	0.0036480	0.0055280	-0.	0.5490430
15	1.4694280	0.5038370	1.1051390	0.0045780	0.0066170	-0.	0.5566440
16	1.4762200	0.5053240	1.1100530	0.0064830	0.0089230	-0.	0.5623920
17	1.4858610	0.5073600	1.1139290	0.0100720	0.0117910	-0.	0.5679660
18	1.4903640	0.3843040	0.8431480	0.0125260	0.0137540	-0.	0.5715810
19	1.4982180	0.3852680	0.8471740	0.0184440	0.0235790	-0.	0.5745860
20	1.5043510	0.3878400	0.8541290	0.0104610	0.0066310	-0.	0.5773150
21	1.5115360	0.3904310	0.8614470	0.0062940	0.0056770	-0.	0.5796420
22	1.5151490	0.2260050	0.5299630	0.0042120	0.0041800	-0.	0.5810820
23	1.5196690	0.2264010	0.5308810	0.0060030	0.0047980	-0.	0.5823870
24	1.5208640	0.2267190	0.5315980	0.0050640	0.0049140	-0.	0.5831400
25	1.5280950	0.2269750	0.5321560	0.0106240	0.0138180	-0.	0.5849480
26	1.5358100	0.2272000	0.5328480	0.0150430	0.0234850	-0.	0.5869990
27	1.5509040	0.2289000	0.5376840	0.0122560	0.0178530	-0.	0.5903160
28	1.5822490	0.2324060	0.5476410	0.0144150	0.0214150	-0.	0.5961930
29	1.6076000	0.2350490	0.5550890	0.0186820	0.0287700	-0.	0.6015650
30	2.9997590	2.9120210	2.0854400	0.0868270	0.1434560	-0.	1.9185340

ELEMENT 4 B-10 NGDS 12 NGF 5 NGDST 2 NGDSPI 2 NGUS 1 NSTART 29

GROUP	SIG	SIGSO(G-G)	SIGSI(G-G)	SIGA	ANUSIG	ALPHA	SIGTR
1	1.4543090	0.8672760	1.9628700	0.0822720	0.	-0.	0.7998850
2	1.6641340	1.0411740	2.1828060	0.1435620	0.	-0.	0.9208460
3	2.0651260	1.0941400	1.7204940	0.1980910	0.	-0.	1.5451770
4	2.0585040	1.0911710	1.0896600	0.3127350	0.	-0.	2.0868140
5	2.4997270	1.4083640	1.4322320	0.2139890	0.	-0.	2.3133110
6	3.8222820	2.3081140	2.4810600	0.4378460	0.	-0.	3.2545310
7	4.8329510	3.3784470	2.2444890	0.8493530	0.	-0.	4.2943490
8	4.8205720	2.5798060	1.1100220	1.8436680	0.	-0.	4.7432240
9	5.2833690	1.7106240	0.6918390	3.2615380	0.	-0.	5.2205580
10	7.6387080	1.7861400	0.9571100	5.2419150	0.	-0.	7.3942750
11	12.6616091	3.2353840	1.4415770	8.6643341	0.	-0.	12.3398030
12	18.3887119	3.3363060	1.4693830	14.2886640	0.	-0.	18.1036780
13	27.6613960	3.3358750	1.4726000	23.5613480	0.	-0.	27.3697920
14	40.4416580	3.0785190	1.6974000	36.3416090	0.	-0.	40.1594920
15	56.9785819	3.0776740	1.6989310	52.8785338	0.	-0.	56.6939321
16	81.0211754	3.0808420	1.6970650	76.9211283	0.	-0.	80.7293692
17	116.0363550	3.0785870	1.6983800	111.9363079	0.	-0.	115.7429037
18	156.6763935	2.5620510	2.1445350	152.5763474	0.	-0.	156.4146214
19	199.9076958	2.5697840	2.1403580	195.8076477	0.	-0.	199.6171417
20	255.5474529	2.5678000	2.1413800	251.4474049	0.	-0.	255.2568016
21	326.9812775	2.5678710	2.1413030	322.8812294	0.	-0.	326.6806488
22	392.9000435	1.4285600	2.5761380	388.7999916	0.	-0.	392.6308746
23	444.6000404	1.4285600	2.5761370	440.4999924	0.	-0.	444.3310280
24	503.3000412	1.4285600	2.5761390	499.1999893	0.	-0.	503.0305595
25	569.8000336	1.4285590	2.5761370	565.6999893	0.	-0.	569.5333328
26	645.1000366	1.4285590	2.5761360	640.9999924	0.	-0.	644.8363342
27	730.4000320	1.4285600	2.5761380	726.2999878	0.	-0.	730.1413040
28	827.1000366	1.4285600	2.5761380	822.9999847	0.	-0.	826.8524323
29	936.7000275	1.4285600	2.5761380	932.5999908	0.	-0.	936.4543076
30	2749.0000000	4.0000000	0.7200000	2745.0000000	-0.	-0.	2748.7600098

TABLE V. - Continued. CROSS-SECTION DATA FOR ALUMINUM, CADMIUM, BORON 10, AND URANYL FLUORIDE SALT IN WATER FUEL SOLUTIONS

[Atom ratio of hydrogen to uranium 235; 500.]

(b) Continued. Group split B

P(0) TRANSFER MATRIX AL

FROM / TO	1	2	3	4	5	6	7	8
1	0.	0.	0.	0.	0.	0.	0.	0.
2	3.44180E-01	0.	0.	0.	0.	0.	0.	0.
3	2.21430E-01	3.90258E-01	0.	0.	0.	0.	0.	0.
4	1.63315E-01	2.39735E-01	4.47145E-01	0.	0.	0.	0.	0.
5	9.21420E-02	1.72324E-01	9.71110E-02	4.04270E-01	0.	0.	0.	0.
6	4.40280E-02	8.32510E-02	6.56400E-02	1.25182E-01	5.31051E-01	0.	0.	0.
7	2.66950E-02	3.32840E-02	7.06300E-02	6.71320E-02	7.02510E-02	3.83135E-01	0.	0.
8	4.15000E-03	6.77700E-03	1.41990E-02	0.	4.67650E-02	0.	2.13937E-01	0.
9	5.91000E-04	1.11400E-03	3.03100E-03	0.	7.98500E-03	0.	0.	1.07653E-01
10	8.20000E-05	2.34000E-04	8.22000E-04	0.	1.19300E-03	0.	0.	0.
11	1.10000E-05	6.50000E-05	2.72000E-04	0.	2.58000E-04	0.	0.	0.
12	2.00000E-06	1.70000E-05	1.02000E-04	0.	1.00000E-04	0.	0.	0.
13	0.	3.00000E-06	1.50000E-05	0.	2.80000E-05	0.	0.	0.
14	0.	0.	3.00000E-06	0.	7.00000E-06	0.	0.	0.
15	0.	0.	1.00000E-06	0.	1.00000E-06	0.	0.	0.
16	0.	0.	0.	0.	0.	0.	0.	0.
17	0.	0.	0.	0.	0.	0.	0.	0.
18	0.	0.	0.	0.	0.	0.	0.	0.
19	0.	0.	0.	0.	0.	0.	0.	0.
20	0.	0.	0.	0.	0.	0.	0.	0.
21	0.	0.	0.	0.	0.	0.	0.	0.
22	0.	0.	0.	0.	0.	0.	0.	0.
23	0.	0.	0.	0.	0.	0.	0.	0.
24	0.	0.	0.	0.	0.	0.	0.	0.
25	0.	0.	0.	0.	0.	0.	0.	0.
26	0.	0.	0.	0.	0.	0.	0.	0.
27	0.	0.	0.	0.	0.	0.	0.	0.
28	0.	0.	0.	0.	0.	0.	0.	0.
29	0.	0.	0.	0.	0.	0.	0.	0.
30	0.	0.	0.	0.	0.	0.	0.	0.

FROM / TO	9	10	11	12	13	14	15	16
1	0.	0.	0.	0.	0.	0.	0.	0.
2	0.	0.	0.	0.	0.	0.	0.	0.
3	0.	0.	0.	0.	0.	0.	0.	0.
4	0.	0.	0.	0.	0.	0.	0.	0.
5	0.	0.	0.	0.	0.	0.	0.	0.
6	0.	0.	0.	0.	0.	0.	0.	0.
7	0.	0.	0.	0.	0.	0.	0.	0.
8	0.	0.	0.	0.	0.	0.	0.	0.
9	0.	0.	0.	0.	0.	0.	0.	0.
10	3.69480E-02	0.	0.	0.	0.	0.	0.	0.
11	0.	7.75540E-02	0.	0.	0.	0.	0.	0.
12	0.	0.	1.01208E-01	0.	0.	0.	0.	0.
13	0.	0.	0.	1.01442E-01	0.	0.	0.	0.
14	0.	0.	0.	0.	1.01512E-01	0.	0.	0.
15	0.	0.	0.	0.	0.	1.35707E-01	0.	0.
16	0.	0.	0.	0.	0.	0.	1.35837E-01	0.
17	0.	0.	0.	0.	0.	0.	0.	1.35329E-01
18	0.	0.	0.	0.	0.	0.	0.	0.
19	0.	0.	0.	0.	0.	0.	0.	0.
20	0.	0.	0.	0.	0.	0.	0.	0.
21	0.	0.	0.	0.	0.	0.	0.	0.
22	0.	0.	0.	0.	0.	0.	0.	0.
23	0.	0.	0.	0.	0.	0.	0.	0.
24	0.	0.	0.	0.	0.	0.	0.	0.
25	0.	0.	0.	0.	0.	0.	0.	0.
26	0.	0.	0.	0.	0.	0.	0.	0.
27	0.	0.	0.	0.	0.	0.	0.	0.
28	0.	0.	0.	0.	0.	0.	0.	0.
29	0.	0.	0.	0.	0.	0.	0.	0.
30	0.	0.	0.	0.	0.	0.	0.	0.

TABLE V. - Continued. CROSS-SECTION DATA FOR ALUMINUM, CADMIUM, BORON 10, AND URANYL FLUORIDE SALT IN WATER FUEL SOLUTIONS

[Atom ratio of hydrogen to uranium 235; 500.]

(b) Continued. Group split B.

TO \ FROM	17	18	19	20	21	22	23	24
1	0.	0.	0.	0.	0.	0.	0.	0.
2	0.	0.	0.	0.	0.	0.	0.	0.
3	0.	0.	0.	0.	0.	0.	0.	0.
4	0.	0.	0.	0.	0.	0.	0.	0.
5	0.	0.	0.	0.	0.	0.	0.	0.
6	0.	0.	0.	0.	0.	0.	0.	0.
7	0.	0.	0.	0.	0.	0.	0.	0.
8	0.	0.	0.	0.	0.	0.	0.	0.
9	0.	0.	0.	0.	0.	0.	0.	0.
10	0.	0.	0.	0.	0.	0.	0.	0.
11	0.	0.	0.	0.	0.	0.	0.	0.
12	0.	0.	0.	0.	0.	0.	0.	0.
13	0.	0.	0.	0.	0.	0.	0.	0.
14	0.	0.	0.	0.	0.	0.	0.	0.
15	0.	0.	0.	0.	0.	0.	0.	0.
16	0.	0.	0.	0.	0.	0.	0.	0.
17	0.	0.	0.	0.	0.	0.	0.	0.
18	1.35746E-01	0.	0.	0.	0.	0.	0.	0.
19	0.	2.04488E-01	0.	0.	0.	0.	0.	0.
20	0.	0.	2.03098E-01	0.	0.	0.	0.	0.
21	0.	0.	0.	2.03455E-01	0.	0.	0.	0.
22	0.	0.	0.	0.	2.03442E-01	0.	0.	0.
23	0.	0.	0.	0.	0.	4.08277E-01	0.	0.
24	0.	0.	0.	0.	0.	0.	4.08277E-01	0.
25	0.	0.	0.	0.	0.	0.	0.	4.08277E-01
26	0.	0.	0.	0.	0.	0.	0.	0.
27	0.	0.	0.	0.	0.	0.	0.	0.
28	0.	0.	0.	0.	0.	0.	0.	0.
29	0.	0.	0.	0.	0.	0.	0.	0.
30	0.	0.	0.	0.	0.	0.	0.	0.

TO \ FROM	25	26	27	28	29	30
1	0.	0.	0.	0.	0.	0.
2	0.	0.	0.	0.	0.	0.
3	0.	0.	0.	0.	0.	0.
4	0.	0.	0.	0.	0.	0.
5	0.	0.	0.	0.	0.	0.
6	0.	0.	0.	0.	0.	0.
7	0.	0.	0.	0.	0.	0.
8	0.	0.	0.	0.	0.	0.
9	0.	0.	0.	0.	0.	0.
10	0.	0.	0.	0.	0.	0.
11	0.	0.	0.	0.	0.	0.
12	0.	0.	0.	0.	0.	0.
13	0.	0.	0.	0.	0.	0.
14	0.	0.	0.	0.	0.	0.
15	0.	0.	0.	0.	0.	0.
16	0.	0.	0.	0.	0.	0.
17	0.	0.	0.	0.	0.	0.
18	0.	0.	0.	0.	0.	0.
19	0.	0.	0.	0.	0.	0.
20	0.	0.	0.	0.	0.	0.
21	0.	0.	0.	0.	0.	0.
22	0.	0.	0.	0.	0.	0.
23	0.	0.	0.	0.	0.	0.
24	0.	0.	0.	0.	0.	0.
25	0.	0.	0.	0.	0.	0.
26	4.08277E-01	0.	0.	0.	0.	0.
27	0.	4.08278E-01	0.	0.	0.	0.
28	0.	0.	4.08277E-01	0.	0.	0.
29	0.	0.	0.	4.08276E-01	0.	-0.
30	0.	0.	0.	0.	4.08277E-01	0.

TABLE V. - Continued. CROSS-SECTION DATA FOR ALUMINUM, CADMIUM, BORON 10, AND URANYL FLUORIDE SALT IN WATER FUEL SOLUTIONS

[Atom ratio of hydrogen to uranium 235; 500.]

(b) Continued. Group split B

P(0) TRANSFER MATRIX 00

FROM / TO	1	2	3	4	5	6	7	8
1	0.	0.	0.	0.	0.	0.	0.	0.
2	2.07399E-01	0.	0.	0.	0.	0.	0.	0.
3	4.75908E-01	3.04411E-01	0.	0.	0.	0.	0.	0.
4	6.63851E-01	5.08612E-01	4.53323E-01	0.	0.	0.	0.	0.
5	5.61408E-01	5.39404E-01	5.16850E-01	5.01976E-01	0.	0.	0.	0.
6	3.45297E-01	3.82322E-01	4.35204E-01	4.02635E-01	4.52246E-01	0.	0.	0.
7	2.51703E-01	3.09452E-01	4.00940E-01	4.35695E-01	4.21668E-01	5.09729E-01	0.	0.
8	4.47870E-02	5.93870E-02	8.44230E-02	1.02814E-01	1.15436E-01	1.22302E-01	1.61216E-01	0.
9	6.71200E-03	9.15800E-03	1.34870E-02	1.71640E-02	2.04250E-02	2.32090E-02	1.58120E-02	1.03202E-01
10	9.43000E-04	1.30100E-03	1.94100E-03	2.51100E-03	3.05400E-03	3.56400E-03	2.55600E-03	8.10000E-05
11	1.29000E-04	1.79000E-04	2.69000E-04	3.50000E-04	4.29000E-04	5.05000E-04	3.69000E-04	1.20000E-05
12	1.80000E-05	2.40000E-05	3.70000E-05	4.80000E-05	5.90000E-05	7.00000E-05	5.10000E-05	2.00000E-06
13	2.00000E-06	3.00000E-06	5.00000E-05	6.00000E-06	8.00000E-06	9.00000E-06	7.00000E-06	0.
14	0.	0.	1.00000E-06	1.00000E-06	1.00000E-06	1.00000E-06	1.00000E-06	0.
15	0.	0.	0.	0.	0.	0.	0.	0.
16	0.	0.	0.	0.	0.	0.	0.	0.
17	0.	0.	0.	0.	0.	0.	0.	0.
18	0.	0.	0.	0.	0.	0.	0.	0.
19	0.	0.	0.	0.	0.	0.	0.	0.
20	0.	0.	0.	0.	0.	0.	0.	0.
21	0.	0.	0.	0.	0.	0.	0.	0.
22	0.	0.	0.	0.	0.	0.	0.	0.
23	0.	0.	0.	0.	0.	0.	0.	0.
24	0.	0.	0.	0.	0.	0.	0.	0.
25	0.	0.	0.	0.	0.	0.	0.	0.
26	0.	0.	0.	0.	0.	0.	0.	0.
27	0.	0.	0.	0.	0.	0.	0.	0.
28	0.	0.	0.	0.	0.	0.	0.	0.
29	0.	0.	0.	0.	0.	0.	0.	0.
30	0.	0.	0.	0.	0.	0.	0.	0.

FROM / TO	9	10	11	12	13	14	15	16
1	0.	0.	0.	0.	0.	0.	0.	0.
2	0.	0.	0.	0.	0.	0.	0.	0.
3	0.	0.	0.	0.	0.	0.	0.	0.
4	0.	0.	0.	0.	0.	0.	0.	0.
5	0.	0.	0.	0.	0.	0.	0.	0.
6	0.	0.	0.	0.	0.	0.	0.	0.
7	0.	0.	0.	0.	0.	0.	0.	0.
8	0.	0.	0.	0.	0.	0.	0.	0.
9	0.	0.	0.	0.	0.	0.	0.	0.
10	1.07924E-01	0.	0.	0.	0.	0.	0.	0.
11	0.	8.45540E-02	0.	0.	0.	0.	0.	0.
12	0.	0.	8.10190E-02	0.	0.	0.	0.	0.
13	0.	0.	0.	6.00220E-02	0.	0.	0.	0.
14	0.	0.	0.	0.	1.69590E-01	0.	0.	0.
15	0.	0.	0.	0.	0.	1.48784E-01	0.	0.
16	0.	0.	0.	0.	0.	0.	4.53875E-01	0.
17	0.	0.	0.	0.	0.	0.	0.	1.01268E-01
18	0.	0.	0.	0.	0.	0.	0.	0.
19	0.	0.	0.	0.	0.	0.	0.	0.
20	0.	0.	0.	0.	0.	0.	0.	0.
21	0.	0.	0.	0.	0.	0.	0.	0.
22	0.	0.	0.	0.	0.	0.	0.	0.
23	0.	0.	0.	0.	0.	0.	0.	0.
24	0.	0.	0.	0.	0.	0.	0.	0.
25	0.	0.	0.	0.	0.	0.	0.	0.
26	0.	0.	0.	0.	0.	0.	0.	0.
27	0.	0.	0.	0.	0.	0.	0.	0.
28	0.	0.	0.	0.	0.	0.	0.	0.
29	0.	0.	0.	0.	0.	0.	0.	0.
30	0.	0.	0.	0.	0.	0.	0.	0.

TABLE V. - Continued. CROSS-SECTION DATA FOR ALUMINUM, CADMIUM, BORON 10, AND URANYL FLUORIDE SALT IN WATER FUEL SOLUTIONS

[Atom ratio of hydrogen to uranium 235; 500.]

(b) Continued. Group split B

TO \ FROM	17	18	19	20	21	22	23	24
1	0.	0.	0.	0.	0.	0.	0.	0.
2	0.	0.	0.	0.	0.	0.	0.	0.
3	0.	0.	0.	0.	0.	0.	0.	0.
4	0.	0.	0.	0.	0.	0.	0.	0.
5	0.	0.	0.	0.	0.	0.	0.	0.
6	0.	0.	0.	0.	0.	0.	0.	0.
7	0.	0.	0.	0.	0.	0.	0.	0.
8	0.	0.	0.	0.	0.	0.	0.	0.
9	0.	0.	0.	0.	0.	0.	0.	0.
10	0.	0.	0.	0.	0.	0.	0.	0.
11	0.	0.	0.	0.	0.	0.	0.	0.
12	0.	0.	0.	0.	0.	0.	0.	0.
13	0.	0.	0.	0.	0.	0.	0.	0.
14	0.	0.	0.	0.	0.	0.	0.	0.
15	0.	0.	0.	0.	0.	0.	0.	0.
16	0.	0.	0.	0.	0.	0.	0.	0.
17	0.	0.	0.	0.	0.	0.	0.	0.
18	1.01579E-01	0.	0.	0.	0.	0.	0.	0.
19	0.	1.42345E-01	0.	0.	0.	0.	0.	0.
20	0.	0.	1.41376E-01	0.	0.	0.	0.	0.
21	0.	0.	0.	1.41623E-01	0.	0.	0.	0.
22	0.	0.	0.	0.	1.41616E-01	0.	0.	0.
23	0.	0.	0.	0.	0.	2.91308E-01	0.	0.
24	0.	0.	0.	0.	0.	0.	3.05517E-01	0.
25	0.	0.	0.	0.	0.	0.	0.	3.26829E-01
26	0.	0.	0.	0.	0.	0.	0.	0.
27	0.	0.	0.	0.	0.	0.	0.	0.
28	0.	0.	0.	0.	0.	0.	0.	0.
29	0.	0.	0.	0.	0.	0.	0.	0.
30	0.	0.	0.	0.	0.	0.	0.	0.

TO \ FROM	25	26	27	28	29	30
1	0.	0.	0.	0.	0.	0.
2	0.	0.	0.	0.	0.	0.
3	0.	0.	0.	0.	0.	0.
4	0.	0.	0.	0.	0.	0.
5	0.	0.	0.	0.	0.	0.
6	0.	0.	0.	0.	0.	0.
7	0.	0.	0.	0.	0.	0.
8	0.	0.	0.	0.	0.	0.
9	0.	0.	0.	0.	0.	0.
10	0.	0.	0.	0.	0.	0.
11	0.	0.	0.	0.	0.	0.
12	0.	0.	0.	0.	0.	0.
13	0.	0.	0.	0.	0.	0.
14	0.	0.	0.	0.	0.	0.
15	0.	0.	0.	0.	0.	0.
16	0.	0.	0.	0.	0.	0.
17	0.	0.	0.	0.	0.	0.
18	0.	0.	0.	0.	0.	0.
19	0.	0.	0.	0.	0.	0.
20	0.	0.	0.	0.	0.	0.
21	0.	0.	0.	0.	0.	0.
22	0.	0.	0.	0.	0.	0.
23	0.	0.	0.	0.	0.	0.
24	0.	0.	0.	0.	0.	0.
25	0.	0.	0.	0.	0.	0.
26	3.58802E-01	0.	0.	0.	0.	0.
27	0.	4.26308E-01	0.	0.	0.	0.
28	0.	0.	5.11562E-01	0.	0.	0.
29	0.	0.	0.	6.39463E-01	0.	-0.
30	0.	0.	0.	0.	6.39458E-01	0.

TABLE V. - Continued. CROSS-SECTION DATA FOR ALUMINUM, CADMIUM, BORON 10, AND URANYL FLUORIDE SALT IN WATER FUEL SOLUTIONS

[Atom ratio of hydrogen to uranium 235; 500.]

(b) Continued. Group split B

P(0) TRANSFER MATRIX UO2F2

TO \ FROM	1	2	3	4	5	6	7	8
1	0.	0.	0.	0.	0.	0.	0.	0.
2	3.52400E-02	0.	0.	0.	0.	0.	0.	0.
3	1.66180E-02	5.49000E-02	0.	0.	0.	0.	0.	0.
4	1.01190E-02	2.24880E-02	5.59370E-02	0.	0.	0.	0.	0.
5	6.16000E-03	1.36820E-02	3.04950E-02	8.60050E-02	0.	0.	0.	0.
6	3.73900E-03	8.31600E-03	1.85260E-02	3.97680E-02	1.20413E-01	0.	0.	0.
7	3.62700E-03	8.09700E-03	1.80400E-02	3.87280E-02	8.32120E-02	1.95767E-01	0.	0.
8	1.32400E-03	2.96700E-03	6.62000E-03	1.42250E-02	3.05880E-02	6.46840E-02	2.24233E-01	0.
9	4.84000E-04	1.08800E-03	2.43100E-03	5.22900E-03	1.12490E-02	2.37950E-02	7.75440E-02	3.27764E-01
10	1.78000E-04	4.00000E-04	8.94000E-04	1.92300E-03	4.13800E-03	8.75300E-03	2.85180E-02	1.15970E-01
11	6.50000E-05	1.47000E-04	3.29000E-04	7.07000E-04	1.52200E-03	3.22000E-03	1.04910E-02	4.26580E-02
12	2.40000E-05	5.40000E-05	1.21000E-04	2.60000E-04	5.60000E-04	1.18500E-03	3.85900E-03	1.56930E-02
13	9.00000E-06	2.00000E-05	4.40000E-05	9.60000E-05	2.06000E-04	4.36000E-04	1.42000E-03	5.77300E-03
14	3.00000E-06	6.00000E-06	1.40000E-05	2.90000E-05	6.30000E-05	1.34000E-04	4.36000E-04	1.77300E-03
15	1.00000E-06	3.00000E-06	6.00000E-06	1.40000E-05	3.00000E-05	6.30000E-05	2.06000E-04	8.37000E-04
16	1.00000E-06	1.00000E-06	3.00000E-06	7.00000E-06	1.40000E-05	3.00000E-05	9.70000E-05	3.96000E-04
17	0.	1.00000E-06	1.00000E-06	3.00000E-06	7.00000E-06	1.40000E-05	4.60000E-05	1.87000E-04
18	0.	0.	1.00000E-06	1.00000E-06	2.00000E-06	5.00000E-06	1.60000E-05	6.60000E-05
19	0.	0.	0.	1.00000E-06	1.00000E-06	3.00000E-06	1.00000E-05	4.00000E-05
20	0.	0.	0.	0.	1.00000E-06	2.00000E-06	6.00000E-06	2.40000E-05
21	0.	0.	0.	0.	1.00000E-06	1.00000E-06	4.00000E-06	1.50000E-05
22	0.	0.	0.	0.	0.	0.	1.00000E-06	5.00000E-06
23	0.	0.	0.	0.	0.	0.	1.00000E-06	4.00000E-06
24	0.	0.	0.	0.	0.	0.	1.00000E-06	3.00000E-06
25	0.	0.	0.	0.	0.	0.	1.00000E-06	2.00000E-06
26	0.	0.	0.	0.	0.	0.	0.	2.00000E-06
27	0.	0.	0.	0.	0.	0.	0.	1.00000E-06
28	0.	0.	0.	0.	0.	0.	0.	1.00000E-06
29	0.	0.	0.	0.	0.	0.	0.	1.00000E-06
30	0.	0.	0.	0.	0.	0.	1.00000E-06	3.00000E-06

TO \ FROM	9	10	11	12	13	14	15	16
1	0.	0.	0.	0.	0.	0.	0.	0.
2	0.	0.	0.	0.	0.	0.	0.	0.
3	0.	0.	0.	0.	0.	0.	0.	0.
4	0.	0.	0.	0.	0.	0.	0.	0.
5	0.	0.	0.	0.	0.	0.	0.	0.
6	0.	0.	0.	0.	0.	0.	0.	0.
7	0.	0.	0.	0.	0.	0.	0.	0.
8	0.	0.	0.	0.	0.	0.	0.	0.
9	0.	0.	0.	0.	0.	0.	0.	0.
10	4.35614E-01	0.	0.	0.	0.	0.	0.	0.
11	1.55291E-01	5.00164E-01	0.	0.	0.	0.	0.	0.
12	5.71280E-02	1.78951E-01	5.28622E-01	0.	0.	0.	0.	0.
13	2.10160E-02	6.58320E-02	1.89097E-01	5.36812E-01	0.	0.	0.	0.
14	6.45300E-03	2.02150E-02	5.80660E-02	1.60302E-01	4.56484E-01	0.	0.	0.
15	3.04800E-03	9.54900E-03	2.74290E-02	7.57210E-02	2.08600E-01	5.15050E-01	0.	0.
16	1.44000E-03	4.51100E-03	1.29560E-02	3.57680E-02	9.85360E-02	2.33898E-01	5.16468E-01	0.
17	6.80000E-04	2.13100E-03	6.12000E-03	1.68960E-02	4.65450E-02	1.10486E-01	2.34557E-01	5.18219E-01
18	2.40000E-04	7.51000E-04	2.15600E-03	5.95200E-03	1.63960E-02	3.89190E-02	8.26240E-02	1.75564E-01
19	1.45000E-04	4.55000E-04	1.30800E-03	3.61000E-03	9.94400E-03	2.36060E-02	5.01140E-02	1.06485E-01
20	8.80000E-05	2.76000E-04	7.93000E-04	2.18900E-03	6.03200E-03	1.43180E-02	3.03960E-02	6.45860E-02
21	5.30000E-05	1.67000E-04	4.81000E-04	1.32800E-03	3.65800E-03	8.68400E-03	1.84360E-02	3.91740E-02
22	1.80000E-05	5.70000E-05	1.64000E-04	4.53000E-04	1.24700E-03	2.96100E-03	6.28600E-03	1.33570E-02
23	1.40000E-05	4.40000E-05	1.28000E-04	3.53000E-04	9.71000E-04	2.30600E-03	4.89600E-03	1.04030E-02
24	1.10000E-05	3.50000E-05	9.90000E-05	2.75000E-04	7.57000E-04	1.79600E-03	3.81300E-03	8.10200E-03
25	9.00000E-06	2.70000E-05	7.70000E-05	2.14000E-04	5.89000E-04	1.39900E-03	2.96900E-03	6.31000E-03
26	7.00000E-06	2.10000E-05	6.00000E-05	1.67000E-04	4.59000E-04	1.08900E-03	2.31300E-03	4.91400E-03
27	5.00000E-06	1.60000E-05	4.70000E-05	1.30000E-04	3.57000E-04	8.48000E-04	1.80100E-03	3.82700E-03
28	4.00000E-06	1.30000E-05	3.70000E-05	1.01000E-04	2.78000E-04	6.61000E-04	1.40300E-03	2.98000E-03
29	3.00000E-06	1.00000E-05	2.80000E-05	7.90000E-05	2.17000E-04	5.15000E-04	1.09200E-03	2.32100E-03
30	1.10000E-05	3.50000E-05	1.00000E-04	2.77000E-04	7.63000E-04	1.81200E-03	3.84600E-03	8.17200E-03

TABLE V. - Continued. CROSS-SECTION DATA FOR ALUMINUM, CADMIUM, BORON 10, AND URANYL FLUORIDE SALT IN WATER FUEL SOLUTIONS

[Atom ratio of hydrogen to uranium 235; 500.]

(b) Continued. Group split B

FROM / TO	17	18	19	20	21	22	23	24
1	0.	0.	0.	0.	0.	0.	0.	0.
2	0.	0.	0.	0.	0.	0.	0.	0.
3	0.	0.	0.	0.	0.	0.	0.	0.
4	0.	0.	0.	0.	0.	0.	0.	0.
5	0.	0.	0.	0.	0.	0.	0.	0.
6	0.	0.	0.	0.	0.	0.	0.	0.
7	0.	0.	0.	0.	0.	0.	0.	0.
8	0.	0.	0.	0.	0.	0.	0.	0.
9	0.	0.	0.	0.	0.	0.	0.	0.
10	0.	0.	0.	0.	0.	0.	0.	0.
11	0.	0.	0.	0.	0.	0.	0.	0.
12	0.	0.	0.	0.	0.	0.	0.	0.
13	0.	0.	0.	0.	0.	0.	0.	0.
14	0.	0.	0.	0.	0.	0.	0.	0.
15	0.	0.	0.	0.	0.	0.	0.	0.
16	0.	0.	0.	0.	0.	0.	0.	0.
17	0.	0.	0.	0.	0.	0.	0.	0.
18	3.93104E-01	0.	0.	0.	0.	0.	0.	0.
19	2.26373E-01	4.48433E-01	0.	0.	0.	0.	0.	0.
20	1.37302E-01	2.53828E-01	4.48693E-01	0.	0.	0.	0.	0.
21	8.32780E-02	1.53955E-01	2.54108E-01	4.53268E-01	0.	0.	0.	0.
22	2.83960E-02	5.24950E-02	8.66450E-02	1.44395E-01	2.69799E-01	0.	0.	0.
23	2.21150E-02	4.08830E-02	6.74790E-02	1.12455E-01	1.86918E-01	3.30793E-01	0.	0.
24	1.72230E-02	3.18400E-02	5.25530E-02	8.75800E-02	1.45571E-01	2.11057E-01	3.31314E-01	0.
25	1.34130E-02	2.47970E-02	4.09280E-02	6.82080E-02	1.13371E-01	1.64370E-01	2.11458E-01	3.31720E-01
26	1.04460E-02	1.93120E-02	3.18750E-02	5.31200E-02	8.82930E-02	1.28012E-01	1.64683E-01	2.11771E-01
27	8.13600E-03	1.50400E-02	2.48240E-02	4.13700E-02	6.87630E-02	9.96960E-02	1.28255E-01	1.64926E-01
28	6.33600E-03	1.17130E-02	1.93330E-02	3.22190E-02	5.35530E-02	7.76430E-02	9.98850E-02	1.28444E-01
29	4.93400E-03	9.12200E-03	1.50570E-02	2.50920E-02	4.17070E-02	6.04680E-02	7.77910E-02	1.00033E-01
30	1.73730E-02	3.21170E-02	5.30100E-02	8.83430E-02	1.46838E-01	2.12893E-01	2.73879E-01	3.52188E-01

FROM / TO	25	26	27	28	29	30
1	0.	0.	0.	0.	0.	0.
2	0.	0.	0.	0.	0.	0.
3	0.	0.	0.	0.	0.	0.
4	0.	0.	0.	0.	0.	0.
5	0.	0.	0.	0.	0.	0.
6	0.	0.	0.	0.	0.	0.
7	0.	0.	0.	0.	0.	0.
8	0.	0.	0.	0.	0.	0.
9	0.	0.	0.	0.	0.	0.
10	0.	0.	0.	0.	0.	0.
11	0.	0.	0.	0.	0.	0.
12	0.	0.	0.	0.	0.	0.
13	0.	0.	0.	0.	0.	0.
14	0.	0.	0.	0.	0.	0.
15	0.	0.	0.	0.	0.	0.
16	0.	0.	0.	0.	0.	0.
17	0.	0.	0.	0.	0.	0.
18	0.	0.	0.	0.	0.	0.
19	0.	0.	0.	0.	0.	0.
20	0.	0.	0.	0.	0.	0.
21	0.	0.	0.	0.	0.	0.
22	0.	0.	0.	0.	0.	0.
23	0.	0.	0.	0.	0.	0.
24	0.	0.	0.	0.	0.	0.
25	0.	0.	0.	0.	0.	0.
26	3.32037E-01	0.	0.	0.	0.	0.
27	2.12014E-01	3.32717E-01	0.	0.	0.	0.
28	1.65116E-01	2.12544E-01	3.36298E-01	0.	0.	0.
29	1.28592E-01	1.65528E-01	2.15332E-01	3.41982E-01	0.	9.11000E-04
30	4.52738E-01	5.82779E-01	7.58118E-01	9.93446E-01	1.35387E 00	0.

TABLE V. - Continued. CROSS-SECTION DATA FOR ALUMINUM, CADMIUM, BORON 10, AND URANYL FLUORIDE SALT IN WATER FUEL SOLUTIONS

[Atom ratio of hydrogen to uranium 235; 500.]

(b) Continued. Group split B

P(0) TRANSFER MATRIX 8-10

TO \ FROM	1	2	3	4	5	6	7	8
1	0.	0.	0.	0.	0.	0.	0.	0.
2	3.63280E-01	0.	0.	0.	0.	0.	0.	0.
3	7.49010E-02	4.31722E-01	0.	0.	0.	0.	0.	0.
4	4.20210E-02	2.53030E-02	7.58010E-01	0.	0.	0.	0.	0.
5	2.00120E-02	1.27890E-02	8.23000E-03	6.49835E-01	0.	0.	0.	0.
6	8.61700E-03	5.71100E-03	3.89100E-03	2.72200E-03	8.77002E-01	0.	0.	0.
7	4.84900E-03	3.29800E-03	2.34200E-03	1.72000E-03	3.12000E-04	1.07632E 00	0.	0.
8	7.13000E-04	4.95000E-04	3.62000E-04	2.76000E-04	5.10000E-05	0.	6.05152E-01	0.
9	1.00000E-04	7.00000E-05	5.10000E-05	4.00000E-05	7.00000E-06	0.	0.	3.97098E-01
10	1.40000E-05	1.00000E-05	7.00000E-06	5.00000E-06	1.00000E-06	0.	0.	0.
11	2.00000E-06	1.00000E-06	1.00000E-06	1.00000E-06	0.	0.	0.	0.
12	0.	0.	0.	0.	0.	0.	0.	0.
13	0.	0.	0.	0.	0.	0.	0.	0.
14	0.	0.	0.	0.	0.	0.	0.	0.
15	0.	0.	0.	0.	0.	0.	0.	0.
16	0.	0.	0.	0.	0.	0.	0.	0.
17	0.	0.	0.	0.	0.	0.	0.	0.
18	0.	0.	0.	0.	0.	0.	0.	0.
19	0.	0.	0.	0.	0.	0.	0.	0.
20	0.	0.	0.	0.	0.	0.	0.	0.
21	0.	0.	0.	0.	0.	0.	0.	0.
22	0.	0.	0.	0.	0.	0.	0.	0.
23	0.	0.	0.	0.	0.	0.	0.	0.
24	0.	0.	0.	0.	0.	0.	0.	0.
25	0.	0.	0.	0.	0.	0.	0.	0.
26	0.	0.	0.	0.	0.	0.	0.	0.
27	0.	0.	0.	0.	0.	0.	0.	0.
28	0.	0.	0.	0.	0.	0.	0.	0.
29	0.	0.	0.	0.	0.	0.	0.	0.
30	0.	0.	0.	0.	0.	0.	0.	0.

TO \ FROM	9	10	11	12	13	14	15	16
1	0.	0.	0.	0.	0.	0.	0.	0.
2	0.	0.	0.	0.	0.	0.	0.	0.
3	0.	0.	0.	0.	0.	0.	0.	0.
4	0.	0.	0.	0.	0.	0.	0.	0.
5	0.	0.	0.	0.	0.	0.	0.	0.
6	0.	0.	0.	0.	0.	0.	0.	0.
7	0.	0.	0.	0.	0.	0.	0.	0.
8	0.	0.	0.	0.	0.	0.	0.	0.
9	0.	0.	0.	0.	0.	0.	0.	0.
10	3.11207E-01	0.	0.	0.	0.	0.	0.	0.
11	0.	6.10653E-01	0.	0.	0.	0.	0.	0.
12	0.	0.	7.61892E-01	0.	0.	0.	0.	0.
13	0.	0.	0.	7.63742E-01	0.	0.	0.	0.
14	0.	0.	0.	0.	7.64173E-01	0.	0.	0.
15	0.	0.	0.	0.	0.	1.02153E 00	0.	0.
16	0.	0.	0.	0.	0.	0.	1.02237E 00	0.
17	0.	0.	0.	0.	0.	0.	0.	1.01921E 00
18	0.	0.	0.	0.	0.	0.	0.	0.
19	0.	0.	0.	0.	0.	0.	0.	0.
20	0.	0.	0.	0.	0.	0.	0.	0.
21	0.	0.	0.	0.	0.	0.	0.	0.
22	0.	0.	0.	0.	0.	0.	0.	0.
23	0.	0.	0.	0.	0.	0.	0.	0.
24	0.	0.	0.	0.	0.	0.	0.	0.
25	0.	0.	0.	0.	0.	0.	0.	0.
26	0.	0.	0.	0.	0.	0.	0.	0.
27	0.	0.	0.	0.	0.	0.	0.	0.
28	0.	0.	0.	0.	0.	0.	0.	0.
29	0.	0.	0.	0.	0.	0.	0.	0.
30	0.	0.	0.	0.	0.	0.	0.	0.

TABLE V. - Continued. CROSS-SECTION DATA FOR ALUMINUM, CADMIUM, BORON 10, AND URANYL FLUORIDE SALT IN WATER FUEL SOLUTIONS

[Atom ratio of hydrogen to uranium 235; 500.]

(b) Continued. Group split B

TO \ FROM	17	18	19	20	21	22	23	24
1	0.	0.	0.	0.	0.	0.	0.	0.
2	0.	0.	0.	0.	0.	0.	0.	0.
3	0.	0.	0.	0.	0.	0.	0.	0.
4	0.	0.	0.	0.	0.	0.	0.	0.
5	0.	0.	0.	0.	0.	0.	0.	0.
6	0.	0.	0.	0.	0.	0.	0.	0.
7	0.	0.	0.	0.	0.	0.	0.	0.
8	0.	0.	0.	0.	0.	0.	0.	0.
9	0.	0.	0.	0.	0.	0.	0.	0.
10	0.	0.	0.	0.	0.	0.	0.	0.
11	0.	0.	0.	0.	0.	0.	0.	0.
12	0.	0.	0.	0.	0.	0.	0.	0.
13	0.	0.	0.	0.	0.	0.	0.	0.
14	0.	0.	0.	0.	0.	0.	0.	0.
15	0.	0.	0.	0.	0.	0.	0.	0.
16	0.	0.	0.	0.	0.	0.	0.	0.
17	0.	0.	0.	0.	0.	0.	0.	0.
18	1.02146E 00	0.	0.	0.	0.	0.	0.	0.
19	0.	1.53800E 00	0.	0.	0.	0.	0.	0.
20	0.	0.	1.53026E 00	0.	0.	0.	0.	0.
21	0.	0.	0.	1.53225E 00	0.	0.	0.	0.
22	0.	0.	0.	0.	1.33255E 00	0.	0.	0.
23	0.	0.	0.	0.	1.99624E-01	2.27087E 00	0.	0.
24	0.	0.	0.	0.	0.	4.00616E-01	2.27087E 00	0.
25	0.	0.	0.	0.	0.	0.	4.00616E-01	2.27087E 00
26	0.	0.	0.	0.	0.	0.	0.	4.00616E-01
27	0.	0.	0.	0.	0.	0.	0.	0.
28	0.	0.	0.	0.	0.	0.	0.	0.
29	0.	0.	0.	0.	0.	0.	0.	0.
30	0.	0.	0.	0.	0.	0.	0.	0.

TO \ FROM	25	26	27	28	29	30
1	0.	0.	0.	0.	0.	0.
2	0.	0.	0.	0.	0.	0.
3	0.	0.	0.	0.	0.	0.
4	0.	0.	0.	0.	0.	0.
5	0.	0.	0.	0.	0.	0.
6	0.	0.	0.	0.	0.	0.
7	0.	0.	0.	0.	0.	0.
8	0.	0.	0.	0.	0.	0.
9	0.	0.	0.	0.	0.	0.
10	0.	0.	0.	0.	0.	0.
11	0.	0.	0.	0.	0.	0.
12	0.	0.	0.	0.	0.	0.
13	0.	0.	0.	0.	0.	0.
14	0.	0.	0.	0.	0.	0.
15	0.	0.	0.	0.	0.	0.
16	0.	0.	0.	0.	0.	0.
17	0.	0.	0.	0.	0.	0.
18	0.	0.	0.	0.	0.	0.
19	0.	0.	0.	0.	0.	0.
20	0.	0.	0.	0.	0.	0.
21	0.	0.	0.	0.	0.	0.
22	0.	0.	0.	0.	0.	0.
23	0.	0.	0.	0.	0.	0.
24	0.	0.	0.	0.	0.	0.
25	0.	0.	0.	0.	0.	0.
26	2.27087E 00	0.	0.	0.	0.	0.
27	4.00617E-01	2.27087E 00	0.	0.	0.	0.
28	0.	4.00617E-01	2.27087E 00	0.	0.	0.
29	0.	0.	4.00616E-01	2.27087E 00	0.	-0.
30	0.	0.	0.	4.00616E-01	2.67149E 00	0.

TABLE V. - Continued. CROSS-SECTION DATA FOR ALUMINUM, CADMIUM, BORON 10, AND URANYL FLUORIDE SALT IN WATER FUEL SOLUTIONS

[Atom ratio of hydrogen to uranium 235; 500.]

(b) Continued. Group split B

P(L) TRANSFER MATRIX AL

FROM / TO	1	2	3	4	5	6	7	8
1	0.	0.	0.	0.	0.	0.	0.	0.
2	-2.17710E-02	0.	0.	0.	0.	0.	0.	0.
3	0.	-3.87590E-02	0.	0.	0.	0.	0.	0.
4	0.	0.	-9.35690E-02	0.	0.	0.	0.	0.
5	0.	0.	0.	-1.28772E-01	0.	0.	0.	0.
6	0.	0.	0.	0.	-1.78120E-01	0.	0.	0.
7	0.	0.	0.	0.	0.	-3.04229E-01	0.	0.
8	0.	0.	0.	0.	0.	0.	-2.32774E-01	0.
9	0.	0.	0.	0.	0.	0.	0.	-1.09474E-01
10	0.	0.	0.	0.	0.	0.	0.	0.
11	0.	0.	0.	0.	0.	0.	0.	0.
12	0.	0.	0.	0.	0.	0.	0.	0.
13	0.	0.	0.	0.	0.	0.	0.	0.
14	0.	0.	0.	0.	0.	0.	0.	0.
15	0.	0.	0.	0.	0.	0.	0.	0.
16	0.	0.	0.	0.	0.	0.	0.	0.
17	0.	0.	0.	0.	0.	0.	0.	0.
18	0.	0.	0.	0.	0.	0.	0.	0.
19	0.	0.	0.	0.	0.	0.	0.	0.
20	0.	0.	0.	0.	0.	0.	0.	0.
21	0.	0.	0.	0.	0.	0.	0.	0.
22	0.	0.	0.	0.	0.	0.	0.	0.
23	0.	0.	0.	0.	0.	0.	0.	0.
24	0.	0.	0.	0.	0.	0.	0.	0.
25	0.	0.	0.	0.	0.	0.	0.	0.
26	0.	0.	0.	0.	0.	0.	0.	0.
27	0.	0.	0.	0.	0.	0.	0.	0.
28	0.	0.	0.	0.	0.	0.	0.	0.
29	0.	0.	0.	0.	0.	0.	0.	0.
30	0.	0.	0.	0.	0.	0.	0.	0.

FROM / TO	9	10	11	12	13	14	15	16
1	0.	0.	0.	0.	0.	0.	0.	0.
2	0.	0.	0.	0.	0.	0.	0.	0.
3	0.	0.	0.	0.	0.	0.	0.	0.
4	0.	0.	0.	0.	0.	0.	0.	0.
5	0.	0.	0.	0.	0.	0.	0.	0.
6	0.	0.	0.	0.	0.	0.	0.	0.
7	0.	0.	0.	0.	0.	0.	0.	0.
8	0.	0.	0.	0.	0.	0.	0.	0.
9	0.	0.	0.	0.	0.	0.	0.	0.
10	-3.71260E-02	0.	0.	0.	0.	0.	0.	0.
11	0.	-6.98990E-02	0.	0.	0.	0.	0.	0.
12	0.	0.	-9.30530E-02	0.	0.	0.	0.	0.
13	0.	0.	0.	-9.41690E-02	0.	0.	0.	0.
14	0.	0.	0.	0.	-9.47850E-02	0.	0.	0.
15	0.	0.	0.	0.	0.	-1.27523E-01	0.	0.
16	0.	0.	0.	0.	0.	0.	-1.27838E-01	0.
17	0.	0.	0.	0.	0.	0.	0.	-1.27355E-01
18	0.	0.	0.	0.	0.	0.	0.	0.
19	0.	0.	0.	0.	0.	0.	0.	0.
20	0.	0.	0.	0.	0.	0.	0.	0.
21	0.	0.	0.	0.	0.	0.	0.	0.
22	0.	0.	0.	0.	0.	0.	0.	0.
23	0.	0.	0.	0.	0.	0.	0.	0.
24	0.	0.	0.	0.	0.	0.	0.	0.
25	0.	0.	0.	0.	0.	0.	0.	0.
26	0.	0.	0.	0.	0.	0.	0.	0.
27	0.	0.	0.	0.	0.	0.	0.	0.
28	0.	0.	0.	0.	0.	0.	0.	0.
29	0.	0.	0.	0.	0.	0.	0.	0.
30	0.	0.	0.	0.	0.	0.	0.	0.

TABLE V. - Continued. CROSS-SECTION DATA FOR ALUMINUM, CADMIUM, BORON 10, AND URANYL FLUORIDE SALT IN WATER FUEL SOLUTIONS

[Atom ratio of hydrogen to uranium 235; 500.]

(b) Continued. Group split B

FROM / TO	17	18	19	20	21	22	23	24
1	0.	0.	0.	0.	0.	0.	0.	0.
2	0.	0.	0.	0.	0.	0.	0.	0.
3	0.	0.	0.	0.	0.	0.	0.	0.
4	0.	0.	0.	0.	0.	0.	0.	0.
5	0.	0.	0.	0.	0.	0.	0.	0.
6	0.	0.	0.	0.	0.	0.	0.	0.
7	0.	0.	0.	0.	0.	0.	0.	0.
8	0.	0.	0.	0.	0.	0.	0.	0.
9	0.	0.	0.	0.	0.	0.	0.	0.
10	0.	0.	0.	0.	0.	0.	0.	0.
11	0.	0.	0.	0.	0.	0.	0.	0.
12	0.	0.	0.	0.	0.	0.	0.	0.
13	0.	0.	0.	0.	0.	0.	0.	0.
14	0.	0.	0.	0.	0.	0.	0.	0.
15	0.	0.	0.	0.	0.	0.	0.	0.
16	0.	0.	0.	0.	0.	0.	0.	0.
17	0.	0.	0.	0.	0.	0.	0.	0.
18	-1.28012E-01	0.	0.	0.	0.	0.	0.	0.
19	0.	-1.93342E-01	0.	0.	0.	0.	0.	0.
20	0.	0.	-1.91482E-01	0.	0.	0.	0.	0.
21	0.	0.	0.	-1.91937E-01	0.	0.	0.	0.
22	0.	0.	0.	0.	-1.91902E-01	0.	0.	0.
23	0.	0.	0.	0.	0.	-3.85747E-01	0.	0.
24	0.	0.	0.	0.	0.	0.	-3.85747E-01	0.
25	0.	0.	0.	0.	0.	0.	0.	-3.85747E-01
26	0.	0.	0.	0.	0.	0.	0.	0.
27	0.	0.	0.	0.	0.	0.	0.	0.
28	0.	0.	0.	0.	0.	0.	0.	0.
29	0.	0.	0.	0.	0.	0.	0.	0.
30	0.	0.	0.	0.	0.	0.	0.	0.

FROM / TO	25	26	27	28	29	30
1	0.	0.	0.	0.	0.	0.
2	0.	0.	0.	0.	0.	0.
3	0.	0.	0.	0.	0.	0.
4	0.	0.	0.	0.	0.	0.
5	0.	0.	0.	0.	0.	0.
6	0.	0.	0.	0.	0.	0.
7	0.	0.	0.	0.	0.	0.
8	0.	0.	0.	0.	0.	0.
9	0.	0.	0.	0.	0.	0.
10	0.	0.	0.	0.	0.	0.
11	0.	0.	0.	0.	0.	0.
12	0.	0.	0.	0.	0.	0.
13	0.	0.	0.	0.	0.	0.
14	0.	0.	0.	0.	0.	0.
15	0.	0.	0.	0.	0.	0.
16	0.	0.	0.	0.	0.	0.
17	0.	0.	0.	0.	0.	0.
18	0.	0.	0.	0.	0.	0.
19	0.	0.	0.	0.	0.	0.
20	0.	0.	0.	0.	0.	0.
21	0.	0.	0.	0.	0.	0.
22	0.	0.	0.	0.	0.	0.
23	0.	0.	0.	0.	0.	0.
24	0.	0.	0.	0.	0.	0.
25	0.	0.	0.	0.	0.	0.
26	-3.85747E-01	0.	0.	0.	0.	0.
27	0.	-3.85747E-01	0.	0.	0.	0.
28	0.	0.	-3.85747E-01	0.	0.	0.
29	0.	0.	0.	-3.85747E-01	0.	-0.
30	0.	0.	0.	0.	-3.85747E-01	0.

TABLE V. - Continued. CROSS-SECTION DATA FOR ALUMINUM, CADMIUM, BORON 10, AND URANYL FLUORIDE SALT IN WATER FUEL SOLUTIONS

[Atom ratio of hydrogen to uranium 235; 500.]

(b) Continued. Group split B

P(1) TRANSFER MATRIX CD

TO \ FROM	1	2	3	4	5	6	7	8
1	0.	0.	0.	0.	0.	0.	0.	0.
2	9.30000E-03	0.	0.	0.	0.	0.	0.	0.
3	0.	-1.20460E-02	0.	0.	0.	0.	0.	0.
4	0.	0.	-2.63140E-02	0.	0.	0.	0.	0.
5	0.	0.	0.	-2.79910E-02	0.	0.	0.	0.
6	0.	0.	0.	0.	-3.43910E-02	0.	0.	0.
7	0.	0.	0.	0.	0.	-5.90650E-02	0.	0.
8	0.	0.	0.	0.	0.	0.	-6.61470E-02	0.
9	0.	0.	0.	0.	0.	0.	0.	-8.90920E-02
10	0.	0.	0.	0.	0.	0.	0.	0.
11	0.	0.	0.	0.	0.	0.	0.	0.
12	0.	0.	0.	0.	0.	0.	0.	0.
13	0.	0.	0.	0.	0.	0.	0.	0.
14	0.	0.	0.	0.	0.	0.	0.	0.
15	0.	0.	0.	0.	0.	0.	0.	0.
16	0.	0.	0.	0.	0.	0.	0.	0.
17	0.	0.	0.	0.	0.	0.	0.	0.
18	0.	0.	0.	0.	0.	0.	0.	0.
19	0.	0.	0.	0.	0.	0.	0.	0.
20	0.	0.	0.	0.	0.	0.	0.	0.
21	0.	0.	0.	0.	0.	0.	0.	0.
22	0.	0.	0.	0.	0.	0.	0.	0.
23	0.	0.	0.	0.	0.	0.	0.	0.
24	0.	0.	0.	0.	0.	0.	0.	0.
25	0.	0.	0.	0.	0.	0.	0.	0.
26	0.	0.	0.	0.	0.	0.	0.	0.
27	0.	0.	0.	0.	0.	0.	0.	0.
28	0.	0.	0.	0.	0.	0.	0.	0.
29	0.	0.	0.	0.	0.	0.	0.	0.
30	0.	0.	0.	0.	0.	0.	0.	0.

TO \ FROM	9	10	11	12	13	14	15	16
1	0.	0.	0.	0.	0.	0.	0.	0.
2	0.	0.	0.	0.	0.	0.	0.	0.
3	0.	0.	0.	0.	0.	0.	0.	0.
4	0.	0.	0.	0.	0.	0.	0.	0.
5	0.	0.	0.	0.	0.	0.	0.	0.
6	0.	0.	0.	0.	0.	0.	0.	0.
7	0.	0.	0.	0.	0.	0.	0.	0.
8	0.	0.	0.	0.	0.	0.	0.	0.
9	0.	0.	0.	0.	0.	0.	0.	0.
10	-9.78830E-02	0.	0.	0.	0.	0.	0.	0.
11	0.	-7.76010E-02	0.	0.	0.	0.	0.	0.
12	0.	0.	-7.53610E-02	0.	0.	0.	0.	0.
13	0.	0.	0.	-5.63700E-02	0.	0.	0.	0.
14	0.	0.	0.	0.	-1.60202E-01	0.	0.	0.
15	0.	0.	0.	0.	0.	-1.41445E-01	0.	0.
16	0.	0.	0.	0.	0.	0.	-4.32138E-01	0.
17	0.	0.	0.	0.	0.	0.	0.	-9.64150E-02
18	0.	0.	0.	0.	0.	0.	0.	0.
19	0.	0.	0.	0.	0.	0.	0.	0.
20	0.	0.	0.	0.	0.	0.	0.	0.
21	0.	0.	0.	0.	0.	0.	0.	0.
22	0.	0.	0.	0.	0.	0.	0.	0.
23	0.	0.	0.	0.	0.	0.	0.	0.
24	0.	0.	0.	0.	0.	0.	0.	0.
25	0.	0.	0.	0.	0.	0.	0.	0.
26	0.	0.	0.	0.	0.	0.	0.	0.
27	0.	0.	0.	0.	0.	0.	0.	0.
28	0.	0.	0.	0.	0.	0.	0.	0.
29	0.	0.	0.	0.	0.	0.	0.	0.
30	0.	0.	0.	0.	0.	0.	0.	0.

TABLE V. - Continued. CROSS-SECTION DATA FOR ALUMINUM, CADMIUM, BORON 10, AND URANYL FLUORIDE SALT IN WATER FUEL SOLUTIONS

[Atom ratio of hydrogen to uranium 235; 500.]

(b) Continued. Group split B

FROM / TO	17	18	19	20	21	22	23	24
1	0.	0.	0.	0.	0.	0.	0.	0.
2	0.	0.	0.	0.	0.	0.	0.	0.
3	0.	0.	0.	0.	0.	0.	0.	0.
4	0.	0.	0.	0.	0.	0.	0.	0.
5	0.	0.	0.	0.	0.	0.	0.	0.
6	0.	0.	0.	0.	0.	0.	0.	0.
7	0.	0.	0.	0.	0.	0.	0.	0.
8	0.	0.	0.	0.	0.	0.	0.	0.
9	0.	0.	0.	0.	0.	0.	0.	0.
10	0.	0.	0.	0.	0.	0.	0.	0.
11	0.	0.	0.	0.	0.	0.	0.	0.
12	0.	0.	0.	0.	0.	0.	0.	0.
13	0.	0.	0.	0.	0.	0.	0.	0.
14	0.	0.	0.	0.	0.	0.	0.	0.
15	0.	0.	0.	0.	0.	0.	0.	0.
16	0.	0.	0.	0.	0.	0.	0.	0.
17	0.	0.	0.	0.	0.	0.	0.	0.
18	-9.69130E-02	0.	0.	0.	0.	0.	0.	0.
19	0.	-1.36158E-01	0.	0.	0.	0.	0.	0.
20	0.	0.	-1.34850E-01	0.	0.	0.	0.	0.
21	0.	0.	0.	-1.35158E-01	0.	0.	0.	0.
22	0.	0.	0.	0.	-1.35144E-01	0.	0.	0.
23	0.	0.	0.	0.	0.	-2.78450E-01	0.	0.
24	0.	0.	0.	0.	0.	0.	-2.92031E-01	0.
25	0.	0.	0.	0.	0.	0.	0.	-3.12404E-01
26	0.	0.	0.	0.	0.	0.	0.	0.
27	0.	0.	0.	0.	0.	0.	0.	0.
28	0.	0.	0.	0.	0.	0.	0.	0.
29	0.	0.	0.	0.	0.	0.	0.	0.
30	0.	0.	0.	0.	0.	0.	0.	0.

FROM / TO	25	26	27	28	29	30
1	0.	0.	0.	0.	0.	0.
2	0.	0.	0.	0.	0.	0.
3	0.	0.	0.	0.	0.	0.
4	0.	0.	0.	0.	0.	0.
5	0.	0.	0.	0.	0.	0.
6	0.	0.	0.	0.	0.	0.
7	0.	0.	0.	0.	0.	0.
8	0.	0.	0.	0.	0.	0.
9	0.	0.	0.	0.	0.	0.
10	0.	0.	0.	0.	0.	0.
11	0.	0.	0.	0.	0.	0.
12	0.	0.	0.	0.	0.	0.
13	0.	0.	0.	0.	0.	0.
14	0.	0.	0.	0.	0.	0.
15	0.	0.	0.	0.	0.	0.
16	0.	0.	0.	0.	0.	0.
17	0.	0.	0.	0.	0.	0.
18	0.	0.	0.	0.	0.	0.
19	0.	0.	0.	0.	0.	0.
20	0.	0.	0.	0.	0.	0.
21	0.	0.	0.	0.	0.	0.
22	0.	0.	0.	0.	0.	0.
23	0.	0.	0.	0.	0.	0.
24	0.	0.	0.	0.	0.	0.
25	0.	0.	0.	0.	0.	0.
26	-3.42971E-01	0.	0.	0.	0.	0.
27	0.	-4.07485E-01	0.	0.	0.	0.
28	0.	0.	-4.88986E-01	0.	0.	0.
29	0.	0.	0.	-6.11240E-01	0.	-0.
30	0.	0.	0.	0.	-6.11231E-01	0.

TABLE V. - Continued. CROSS-SECTION DATA FOR ALUMINUM, CADMIUM, BORON 10, AND URANYL FLUORIDE SALT IN WATER FUEL SOLUTIONS

[Atom ratio of hydrogen to uranium 235; 500.]

(b) Continued. Group split B

P(1) TRANSFER MATRIX UO2F2

TO \ FROM	1	2	3	4	5	6	7	8
1	0.	0.	0.	0.	0.	0.	0.	0.
2	6.62060E-02	0.	0.	0.	0.	0.	0.	0.
3	3.14430E-02	7.91090E-02	0.	0.	0.	0.	0.	0.
4	1.48530E-02	4.13220E-02	1.19814E-01	0.	0.	0.	0.	0.
5	7.01600E-03	1.95190E-02	5.81480E-02	1.38959E-01	0.	0.	0.	0.
6	3.31400E-03	9.22000E-03	2.74670E-02	7.23510E-02	1.61636E-01	0.	0.	0.
7	2.30500E-03	6.41300E-03	1.91030E-02	5.03200E-02	1.39459E-01	3.88824E-01	0.	0.
8	5.14000E-04	1.43100E-03	4.26200E-03	1.12280E-02	3.11180E-02	8.65800E-02	4.06169E-01	0.
9	1.15000E-04	3.19000E-04	9.51000E-04	2.50500E-03	6.94300E-03	1.93190E-02	9.35540E-02	6.08535E-01
10	2.60000E-05	7.10000E-05	2.12000E-04	5.59000E-04	1.54900E-03	4.31100E-03	2.08750E-02	1.38233E-01
11	6.00000E-06	1.60000E-05	4.70000E-05	1.25000E-04	3.46000E-04	9.62000E-04	4.65800E-03	3.08440E-02
12	1.00000E-06	4.00000E-06	1.10000E-05	2.80000E-05	7.70000E-05	2.15000E-04	1.03900E-03	6.88200E-03
13	0.	1.00000E-06	2.00000E-06	6.00000E-06	1.70000E-05	4.80000E-05	2.32000E-04	1.53600E-03
14	0.	0.	0.	1.00000E-06	3.00000E-06	9.00000E-06	4.50000E-05	2.98000E-04
15	0.	0.	0.	0.	1.00000E-06	3.00000E-06	1.50000E-05	9.70000E-05
16	0.	0.	0.	0.	0.	1.00000E-06	5.00000E-06	3.10000E-05
17	0.	0.	0.	0.	0.	0.	2.00000E-06	1.00000E-05
18	0.	0.	0.	0.	0.	0.	0.	3.00000E-06
19	0.	0.	0.	0.	0.	0.	0.	1.00000E-06
20	0.	0.	0.	0.	0.	0.	0.	1.00000E-06
21	0.	0.	0.	0.	0.	0.	0.	0.
22	0.	0.	0.	0.	0.	0.	0.	0.
23	0.	0.	0.	0.	0.	0.	0.	0.
24	0.	0.	0.	0.	0.	0.	0.	0.
25	0.	0.	0.	0.	0.	0.	0.	0.
26	0.	0.	0.	0.	0.	0.	0.	0.
27	0.	0.	0.	0.	0.	0.	0.	0.
28	0.	0.	0.	0.	0.	0.	0.	0.
29	0.	0.	0.	0.	0.	0.	0.	0.
30	0.	0.	0.	0.	0.	0.	0.	0.

TO \ FROM	9	10	11	12	13	14	15	16
1	0.	0.	0.	0.	0.	0.	0.	0.
2	0.	0.	0.	0.	0.	0.	0.	0.
3	0.	0.	0.	0.	0.	0.	0.	0.
4	0.	0.	0.	0.	0.	0.	0.	0.
5	0.	0.	0.	0.	0.	0.	0.	0.
6	0.	0.	0.	0.	0.	0.	0.	0.
7	0.	0.	0.	0.	0.	0.	0.	0.
8	0.	0.	0.	0.	0.	0.	0.	0.
9	0.	0.	0.	0.	0.	0.	0.	0.
10	8.22309E-01	0.	0.	0.	0.	0.	0.	0.
11	1.86123E-01	9.55187E-01	0.	0.	0.	0.	0.	0.
12	4.15300E-02	2.15816E-01	1.01338E 00	0.	0.	0.	0.	0.
13	9.26700E-03	4.81550E-02	2.29013E-01	1.03232E 00	0.	0.	0.	0.
14	1.79700E-03	9.34100E-03	4.44220E-02	2.02815E-01	9.09316E-01	0.	0.	0.
15	5.84000E-04	3.03200E-03	1.44220E-02	6.58440E-02	2.99577E-01	1.06199E 00	0.	0.
16	1.89000E-04	9.84000E-04	4.68200E-03	2.13770E-02	9.72580E-02	3.50648E-01	1.06544E 00	0.
17	6.20300E-05	3.20000E-04	1.52000E-03	6.94300E-03	3.15750E-02	1.13839E-01	3.51784E-01	1.06936E 00
18	1.60000E-05	8.10000E-05	3.86000E-04	1.76000E-03	8.00900E-03	2.88740E-02	8.92280E-02	2.75815E-01
19	7.00000E-06	3.80000E-05	1.82000E-04	8.31000E-04	3.78300E-03	1.36390E-02	4.21480E-02	1.30286E-01
20	3.00000E-06	1.80000E-05	8.60000E-05	3.93000E-04	1.78700E-03	6.44300E-03	1.99090E-02	6.15430E-02
21	2.00000E-06	9.00000E-06	4.10000E-05	1.86000E-04	8.44000E-04	3.04300E-03	9.40500E-03	2.90710E-02
22	0.	2.00000E-06	1.10000E-05	5.20000E-05	2.36000E-04	8.52000E-04	2.63300E-03	8.13900E-03
23	0.	2.00000E-06	8.00000E-06	3.60000E-05	1.62000E-04	5.86000E-04	1.81000E-03	5.59400E-03
24	0.	1.00000E-06	5.00000E-06	2.50000E-05	1.12000E-04	4.02000E-04	1.24400E-03	3.84400E-03
25	0.	1.00000E-06	4.00000E-06	1.70000E-05	7.70000E-05	2.77000E-04	8.55000E-04	2.64200E-03
26	0.	1.00000E-06	3.00000E-06	1.20000E-05	5.30000E-05	1.90000E-04	5.87000E-04	1.81600E-03
27	0.	0.	2.00000E-06	8.00000E-06	3.60000E-05	1.31000E-04	4.04000E-04	1.24800E-03
28	0.	0.	1.00000E-06	5.00000E-06	2.50000E-05	9.00000E-05	2.77000E-04	8.58000E-04
29	0.	0.	1.00000E-06	4.00000E-06	1.70000E-05	6.20000E-05	1.91000E-04	5.90000E-04
30	0.	0.	2.00000E-06	8.00000E-06	3.80000E-05	1.35000E-04	4.18000E-04	1.29400E-03

TABLE V. - Continued. CROSS-SECTION DATA FOR ALUMINUM, CADMIUM, BORON 10, AND URANYL FLUORIDE SALT IN WATER FUEL SOLUTIONS

[Atom ratio of hydrogen to uranium 235; 500.]

(b) Continued. Group split B

TO \ FROM	17	18	19	20	21	22	23	24
1	0.	0.	0.	0.	0.	0.	0.	0.
2	0.	0.	0.	0.	0.	0.	0.	0.
3	0.	0.	0.	0.	0.	0.	0.	0.
4	0.	0.	0.	0.	0.	0.	0.	0.
5	0.	0.	0.	0.	0.	0.	0.	0.
6	0.	0.	0.	0.	0.	0.	0.	0.
7	0.	0.	0.	0.	0.	0.	0.	0.
8	0.	0.	0.	0.	0.	0.	0.	0.
9	0.	0.	0.	0.	0.	0.	0.	0.
10	0.	0.	0.	0.	0.	0.	0.	0.
11	0.	0.	0.	0.	0.	0.	0.	0.
12	0.	0.	0.	0.	0.	0.	0.	0.
13	0.	0.	0.	0.	0.	0.	0.	0.
14	0.	0.	0.	0.	0.	0.	0.	0.
15	0.	0.	0.	0.	0.	0.	0.	0.
16	0.	0.	0.	0.	0.	0.	0.	0.
17	0.	0.	0.	0.	0.	0.	0.	0.
18	8.35286E-01	0.	0.	0.	0.	0.	0.	0.
19	4.03131E-01	9.76260E-01	0.	0.	0.	0.	0.	0.
20	1.90426E-01	4.74095E-01	9.76778E-01	0.	0.	0.	0.	0.
21	8.99510E-02	2.23947E-01	4.74216E-01	9.87868E-01	0.	0.	0.	0.
22	2.51820E-02	6.26950E-02	1.32760E-01	2.84175E-01	5.79232E-01	0.	0.	0.
23	1.73070E-02	4.30900E-02	9.12440E-02	1.95311E-01	4.16791E-01	6.67506E-01	0.	0.
24	1.18950E-02	2.96150E-02	6.27110E-02	1.34235E-01	2.86457E-01	4.96340E-01	6.68871E-01	0.
25	8.17500E-03	2.03540E-02	4.31010E-02	9.22580E-02	1.96879E-01	3.41132E-01	4.97281E-01	6.69933E-01
26	5.61900E-03	1.39890E-02	2.96230E-02	6.34080E-02	1.35313E-01	2.34456E-01	3.41779E-01	4.98013E-01
27	3.86200E-03	9.61500E-03	2.03590E-02	4.35800E-02	9.29990E-02	1.61139E-01	2.34901E-01	3.42283E-01
28	2.65400E-03	6.60800E-03	1.39930E-02	2.99520E-02	6.39170E-02	1.10749E-01	1.61445E-01	2.35247E-01
29	1.82400E-03	4.54200E-03	9.61700E-03	2.05860E-02	4.39300E-02	7.61170E-02	1.10959E-01	1.61683E-01
30	4.00200E-03	9.96500E-03	2.11010E-02	4.51670E-02	9.63860E-02	1.67007E-01	2.43455E-01	3.54747E-01

TO \ FROM	25	26	27	28	29	30
1	0.	0.	0.	0.	0.	0.
2	0.	0.	0.	0.	0.	0.
3	0.	0.	0.	0.	0.	0.
4	0.	0.	0.	0.	0.	0.
5	0.	0.	0.	0.	0.	0.
6	0.	0.	0.	0.	0.	0.
7	0.	0.	0.	0.	0.	0.
8	0.	0.	0.	0.	0.	0.
9	0.	0.	0.	0.	0.	0.
10	0.	0.	0.	0.	0.	0.
11	0.	0.	0.	0.	0.	0.
12	0.	0.	0.	0.	0.	0.
13	0.	0.	0.	0.	0.	0.
14	0.	0.	0.	0.	0.	0.
15	0.	0.	0.	0.	0.	0.
16	0.	0.	0.	0.	0.	0.
17	0.	0.	0.	0.	0.	0.
18	0.	0.	0.	0.	0.	0.
19	0.	0.	0.	0.	0.	0.
20	0.	0.	0.	0.	0.	0.
21	0.	0.	0.	0.	0.	0.
22	0.	0.	0.	0.	0.	0.
23	0.	0.	0.	0.	0.	0.
24	0.	0.	0.	0.	0.	0.
25	0.	0.	0.	0.	0.	0.
26	6.70760E-01	0.	0.	0.	0.	0.
27	4.98584E-01	6.72615E-01	0.	0.	0.	0.
28	3.42675E-01	4.99860E-01	6.82267E-01	0.	0.	0.
29	2.35517E-01	3.43551E-01	5.06494E-01	5.97373E-01	0.	4.95400E-03
30	5.16745E-01	7.53782E-01	1.11130E 00	1.55009E 00	2.38072E 00	0.

TABLE V. - Continued. CROSS-SECTION DATA FOR ALUMINUM, CADMIUM, BORON 10, AND URANYL FLUORIDE SALT IN WATER FUEL SOLUTIONS

[Atom ratio of hydrogen to uranium 235; 500.]

(b) Continued. Group split B

P(1) TRANSFER MATRIX B-10

TO \ FROM	1	2	3	4	5	6	7	8
1	0.	0.	0.	0.	0.	0.	0.	0.
2	9.25340E-02	0.	0.	0.	0.	0.	0.	0.
3	0.	-2.51446E-01	0.	0.	0.	0.	0.	0.
4	0.	0.	-1.00588E 00	0.	0.	0.	0.	0.
5	0.	0.	0.	-6.09412E-01	0.	0.	0.	0.
6	0.	0.	0.	0.	-6.23779E-01	0.	0.	0.
7	0.	0.	0.	0.	0.	-6.42111E-01	0.	0.
8	0.	0.	0.	0.	0.	0.	-5.18119E-01	0.
9	0.	0.	0.	0.	0.	0.	0.	-3.33600E-01
10	0.	0.	0.	0.	0.	0.	0.	0.
11	0.	0.	0.	0.	0.	0.	0.	0.
12	0.	0.	0.	0.	0.	0.	0.	0.
13	0.	0.	0.	0.	0.	0.	0.	0.
14	0.	0.	0.	0.	0.	0.	0.	0.
15	0.	0.	0.	0.	0.	0.	0.	0.
16	0.	0.	0.	0.	0.	0.	0.	0.
17	0.	0.	0.	0.	0.	0.	0.	0.
18	0.	0.	0.	0.	0.	0.	0.	0.
19	0.	0.	0.	0.	0.	0.	0.	0.
20	0.	0.	0.	0.	0.	0.	0.	0.
21	0.	0.	0.	0.	0.	0.	0.	0.
22	0.	0.	0.	0.	0.	0.	0.	0.
23	0.	0.	0.	0.	0.	0.	0.	0.
24	0.	0.	0.	0.	0.	0.	0.	0.
25	0.	0.	0.	0.	0.	0.	0.	0.
26	0.	0.	0.	0.	0.	0.	0.	0.
27	0.	0.	0.	0.	0.	0.	0.	0.
28	0.	0.	0.	0.	0.	0.	0.	0.
29	0.	0.	0.	0.	0.	0.	0.	0.
30	0.	0.	0.	0.	0.	0.	0.	0.

TO \ FROM	9	10	11	12	13	14	15	16
1	0.	0.	0.	0.	0.	0.	0.	0.
2	0.	0.	0.	0.	0.	0.	0.	0.
3	0.	0.	0.	0.	0.	0.	0.	0.
4	0.	0.	0.	0.	0.	0.	0.	0.
5	0.	0.	0.	0.	0.	0.	0.	0.
6	0.	0.	0.	0.	0.	0.	0.	0.
7	0.	0.	0.	0.	0.	0.	0.	0.
8	0.	0.	0.	0.	0.	0.	0.	0.
9	0.	0.	0.	0.	0.	0.	0.	0.
10	-2.62523E-01	0.	0.	0.	0.	0.	0.	0.
11	0.	-4.81639E-01	0.	0.	0.	0.	0.	0.
12	0.	0.	-6.42895E-01	0.	0.	0.	0.	0.
13	0.	0.	0.	-6.49626E-01	0.	0.	0.	0.
14	0.	0.	0.	0.	-6.52842E-01	0.	0.	0.
15	0.	0.	0.	0.	0.	-8.77643E-01	0.	0.
16	0.	0.	0.	0.	0.	0.	-8.79173E-01	0.
17	0.	0.	0.	0.	0.	0.	0.	-8.77308E-01
18	0.	0.	0.	0.	0.	0.	0.	0.
19	0.	0.	0.	0.	0.	0.	0.	0.
20	0.	0.	0.	0.	0.	0.	0.	0.
21	0.	0.	0.	0.	0.	0.	0.	0.
22	0.	0.	0.	0.	0.	0.	0.	0.
23	0.	0.	0.	0.	0.	0.	0.	0.
24	0.	0.	0.	0.	0.	0.	0.	0.
25	0.	0.	0.	0.	0.	0.	0.	0.
26	0.	0.	0.	0.	0.	0.	0.	0.
27	0.	0.	0.	0.	0.	0.	0.	0.
28	0.	0.	0.	0.	0.	0.	0.	0.
29	0.	0.	0.	0.	0.	0.	0.	0.
30	0.	0.	0.	0.	0.	0.	0.	0.

TABLE V. - Concluded. CROSS-SECTION DATA FOR ALUMINUM, CADMIUM, BORON 10, AND URANYL FLUORIDE SALT IN WATER FUEL SOLUTIONS

[Atom ratio of hydrogen to uranium 235; 500.]

(b) Concluded. Group split B

TO \ FROM	17	18	19	20	21	22	23	24
1	0.	0.	0.	0.	0.	0.	0.	0.
2	0.	0.	0.	0.	0.	0.	0.	0.
3	0.	0.	0.	0.	0.	0.	0.	0.
4	0.	0.	0.	0.	0.	0.	0.	0.
5	0.	0.	0.	0.	0.	0.	0.	0.
6	0.	0.	0.	0.	0.	0.	0.	0.
7	0.	0.	0.	0.	0.	0.	0.	0.
8	0.	0.	0.	0.	0.	0.	0.	0.
9	0.	0.	0.	0.	0.	0.	0.	0.
10	0.	0.	0.	0.	0.	0.	0.	0.
11	0.	0.	0.	0.	0.	0.	0.	0.
12	0.	0.	0.	0.	0.	0.	0.	0.
13	0.	0.	0.	0.	0.	0.	0.	0.
14	0.	0.	0.	0.	0.	0.	0.	0.
15	0.	0.	0.	0.	0.	0.	0.	0.
16	0.	0.	0.	0.	0.	0.	0.	0.
17	0.	0.	0.	0.	0.	0.	0.	0.
18	-8.78623E-01	0.	0.	0.	0.	0.	0.	0.
19	0.	-1.32477E 00	0.	0.	0.	0.	0.	0.
20	0.	0.	-1.32060E 00	0.	0.	0.	0.	0.
21	0.	0.	0.	-1.32162E 00	0.	0.	0.	0.
22	0.	0.	0.	0.	-8.78256E-01	0.	0.	0.
23	0.	0.	0.	0.	-4.43288E-01	-8.65313E-01	0.	0.
24	0.	0.	0.	0.	0.	-8.91067E-01	-8.65312E-01	0.
25	0.	0.	0.	0.	0.	0.	-8.91067E-01	-8.65315E-01
26	0.	0.	0.	0.	0.	0.	0.	-8.91067E-01
27	0.	0.	0.	0.	0.	0.	0.	0.
28	0.	0.	0.	0.	0.	0.	0.	0.
29	0.	0.	0.	0.	0.	0.	0.	0.
30	0.	0.	0.	0.	0.	0.	0.	0.

TO \ FROM	25	26	27	28	29	30
1	0.	0.	0.	0.	0.	0.
2	0.	0.	0.	0.	0.	0.
3	0.	0.	0.	0.	0.	0.
4	0.	0.	0.	0.	0.	0.
5	0.	0.	0.	0.	0.	0.
6	0.	0.	0.	0.	0.	0.
7	0.	0.	0.	0.	0.	0.
8	0.	0.	0.	0.	0.	0.
9	0.	0.	0.	0.	0.	0.
10	0.	0.	0.	0.	0.	0.
11	0.	0.	0.	0.	0.	0.
12	0.	0.	0.	0.	0.	0.
13	0.	0.	0.	0.	0.	0.
14	0.	0.	0.	0.	0.	0.
15	0.	0.	0.	0.	0.	0.
16	0.	0.	0.	0.	0.	0.
17	0.	0.	0.	0.	0.	0.
18	0.	0.	0.	0.	0.	0.
19	0.	0.	0.	0.	0.	0.
20	0.	0.	0.	0.	0.	0.
21	0.	0.	0.	0.	0.	0.
22	0.	0.	0.	0.	0.	0.
23	0.	0.	0.	0.	0.	0.
24	0.	0.	0.	0.	0.	0.
25	0.	0.	0.	0.	0.	0.
26	-8.65312E-01	0.	0.	0.	0.	0.
27	-8.91069E-01	-8.65309E-01	0.	0.	0.	0.
28	0.	-8.91069E-01	-8.65313E-01	0.	0.	0.
29	0.	0.	-8.91067E-01	-8.65314E-01	0.	-0.
30	0.	0.	0.	-8.91067E-01	-1.75655E 00	0.